PROPERTIES OF LIGHT AND HEAVY BARYONS IN LIGHT CONE QCD SUM RULES FORMALISM

A THESIS SUBMITTED TO
THE GRADUATE SCHOOL OF NATURAL AND APPLIED SCIENCES
OF
MIDDLE EAST TECHNICAL UNIVERSITY

BY

KAZEM AZIZI

IN PARTIAL FULFILLMENT OF THE REQUIREMENTS
FOR
THE DEGREE OF DOCTOR OF PHILOSOPHY
IN
PHYSICS

MARCH 2009

Approval of the thesis:

PROPERTIES OF LIGHT AND HEAVY BARYONS IN LIGHT CONE QCD SUM RULES FORMALISM

submitted by **KAZEM AZIZI** in partial fulfillment of the requirements for the degree of **Doctor of Philosophy in Physics Department, Middle East Technical University** by,

Prof. Dr. Canan Özgen _____
Dean, Graduate School of **Natural and Applied Sciences**

Prof. Dr. Sinan Bilikmen _____
Head of Department, **Physics**

Assoc. Prof. Dr. Altuğ Özpineci _____
Supervisor, **Physics Department, METU**

Prof. Dr. T. M. Aliev _____
Co-supervisor, **Physics Department, METU**

Examining Committee Members:

Prof. Dr. Namık Kemal Pak
Physics, METU _____

Assoc. Prof. Dr. Altuğ Özpineci
Physics, METU _____

Prof. Dr. Ali Ulvi Yılmazer
Physics Eng., Ankara University _____

Prof. Dr. Mehmet T. Zeyrek
Physics, METU _____

Prof. Dr. Erhan Onur Iltan
Physics, METU _____

Date: _____

I hereby declare that all information in this document has been obtained and presented in accordance with academic rules and ethical conduct. I also declare that, as required by these rules and conduct, I have fully cited and referenced all material and results that are not original to this work.

Name, Last Name: KAZEM AZIZI

Signature :

ABSTRACT

PROPERTIES OF LIGHT AND HEAVY BARYONS IN LIGHT CONE QCD SUM RULES FORMALISM

Azizi, Kazem
Ph.D., Department of Physics
Supervisor : Assoc. Prof. Dr. Altuğ Özpineci
Co-Supervisor : Prof. Dr. T. M. Aliev

March 2009, 102 pages

In this thesis, we investigate the masses, form factors and magnetic dipole moments of some light octet, decuplet and heavy baryons containing a single heavy quark in the framework of the light cone QCD sum rules. The magnetic dipole moments can be measured considering radiative transitions within a multiplet or between multiplets. Analyzing the transitions among the baryons and calculating the above mentioned parameters can give us insight into the structure of those baryons. In analyzing the aforementioned processes, the transition form factors play a crucial role. In this thesis, the form factors for these transitions are calculated using the light cone QCD sum rules approach.

In the limit when the light quark masses are equal, $m_u = m_d = m_s$, QCD has an SU(3) flavour symmetry which can be used to classify the light baryons. This classification results in the light decuplet, octet and singlet baryons. The baryons containing single heavy quark, on the other hand, can be classified according to the spin of the light degrees of freedom in the heavy quark limit, $m_Q \to \infty$. QCD at low energies, when

the baryons are formed, is a non-perturbative theory. Hence, for phenomenology of the baryons, the QCD sum rules as a more powerful non-perturbative approach is used.

Understanding the properties of nucleons is one of the main objectives of QCD. To investigate the properties of the nucleons, the axial $N-\Delta(1232)$ transition form factors are calculated within the light cone QCD sum rules method. A comparison of our results on those form factors with the predictions of lattice QCD and quark model is presented. The nucleon electromagnetic form factors are also calculated in the same framework using the most general form of the nucleon interpolating current. Using two forms of the distribution amplitudes (DA's), predictions for the form factors are presented and compared with existing experimental data. It is shown that our results describe the existing experimental data remarkably well.

Another important property of the baryons is their magnetic moments. The magnetic moments of the heavy Ξ_Q ($Q = b$ or c) baryons containing a single charm or bottom quark are calculated within the light cone QCD sum rules approach. A comparison of our results with the predictions of other approaches, such as relativistic and non-relativistic quark models, hyper central model, Chiral perturbation theory, soliton and skyrmion models is presented. Moreover, inspired by the results of recent experimental discoveries for charm and bottom baryons, the masses and magnetic moments of the heavy baryons with $J^P = 3/2^+$ containing a single heavy quark are studied also within the light cone QCD sum rules method. Our results on the masses of heavy baryons are in good agreement with predictions of other approaches, as well as with the existing experimental values. Our predictions on the masses of the states, which are not experimentally discovered yet, can be tested in the future experiments. A comparison of our results on the magnetic moments of these baryons and the hyper central model predictions is also presented.

Keywords: Non-perturbative approaches, light cone QCD sum rules, form factors, magnetic dipole moments, operator product expansion.

ÖZ

IŞIK KONİSİ QCD TOPLAMA KURALLARI ÇERÇEVESİNDE HAFİF VE AĞIR BARYONLARIN ÖZELLİKLERİ

Azizi, Kazem
Doktora, Fizik Bölümü
Tez Yöneticisi : Doç. Dr. Altuğ Özpineci
Ortak Tez Yöneticisi : Prof. Dr. T. M. Aliev

Mart 2009, 102 sayfa

Bu tezde, ışık konisi QCD toplama kurallarını kullanarak, bazı hafif onlu (decuplet), sekizli (octet) ve ağır baryonların kütle, yapı faktörleri ve manyetik çift kutup (dipol) momentlerini araştırıyoruz. Bir çoklunun içinde ve ya çoklular arasındaki ışınsal geçişlerde manyetik çift kutup momentler ölçülebilir. Baryonlar arasındaki süreçleri analiz etmek ve yukarıda bahsedilen parametreleri hesaplamak, baryonların iç yapıları hakkında bize bilgi verebilir. Bahsedilen süreçlerin analizinde geçiş yapı faktörleri önemli rol oynar. Bu tezde, ışık konisi QCD toplama kurallarını kullanarak bu geçişler için yapı faktörleri hesaplanmıştır.

Hafif kuarkların kütlelerinin eşit olduğu, $m_u = m_d = m_s$, limitinde, QCD'nin bir SU(3) çeşni simetrisi var. Bu simetri hafif baryonların sınıflandırılmasında kullanılabilir. Bu sınıflandırılmadan, hafif onlu, sekizli ve birli baryonlar elde edilebilir. Diğer taraftan, bir ağır quark içeren ağır baryonlar, $m_Q \to \infty$ limitinde, hafif serbestlik derecelerinin spinlerine göre sınıflandırılabilirler. Baryonların oluştuğu düşük enerjilerde QCD tedirgeme yapılamayan bir kuramdır. Bu sebepten, baryonların fenomenolojisi

için tedirgemesiz yaklaşım olan QCD toplama kuralları kullanılmıştır.

Nükleonların özelliklerini anlamak modern QCD teorisinin en büyük amaçlarından biridir. Onların özelliklerini incelemek için, ışık konisi QCD toplama kuralları yöntemi ile sözde (axial) $N - \Delta(1232)$ geçiş yapı faktörleri hesaplanmıştır ve elde edilen sonuçlar kuark model ve örgü (lattice) kuramı öngörüleri ile karşılaştırılmıştır. Nükleon ara kestirim akımının en genel formunu kullanarak nükleon elektromanyetik yapı faktörleri de aynı çerçevede hesaplanmıştır. Dağılım genliklerinin (DA's) iki formunu kullanarak, yapı faktörleri için öngörülerimiz varolan deneysel verilerle karşılaştırılmıştır. Bulunan sonuçların varolan deneysel verilerle uyum içinde oldukları gösterilmiştir.

Baryonların başka bir özelliği de manyetik momentleridir. Tek tılsım (charm) ve ya alt (bottom) kuark içeren ağır Ξ_Q ($Q = b$ ve ya c) baryonlarının manyetik momentleri ışık konisi QCD toplama kuralları yöntemi ile hesaplanmıştır ve elde edilen sonuçlar, göreli ve göreli olmayan kuark modelleri, hiper merkezi model, Chiral tedirgeme kuramı, soliton ve skyrmion modelleri gibi yaklaşımların öngörüleri ile karşılaştırılmıştır. Sonunda, tılsımlı ve alt baryonlar için son deneysel gözlem sonuçlarına dayanarak, tek ağır kuark içeren $J^P = 3/2^+$ kuantum sayılı ağır baryonların kütleleri ve manyetik momentleri de ışık konisi QCD toplama kuralları metodu ile hesaplanmıştır. Ağır baryonların kütleleri için bulduğumuz sonuçlar hem diğer yaklaşımların öngörüleri hemde var olan deneysel değerlerle uyum içindedir. Deneyde henüz gözlenmeyen baryonların kütleleri yakın gelecekte test edilebilir. Bu baryonların manyetik momentlerinin değerleri, hiper merkezi modelin öngörüleri ile karşılaştırılmıştır.

Anahtar Kelimeler: tedirgemesiz yaklaşımlar, ışık konisi QCD toplama kuralları, yapı faktörleri, manyetik çift kutup (dipol) momenti, işlemci çarpım açılımı.

To: SHFAORASFLKFHPNMM

ACKNOWLEDGMENTS

I would like to express my deep sincere feelings to my supervisor Assoc. Prof. Dr. Altuğ Özpineci and my co-supervisor, Prof. Dr. Takhmasib M. Aliev. I am grateful to them for their painstaking care in the course of this project and for their meticulous effort in teaching me numerous very precious concepts. They provided me unflinching encouragement and support in various ways. I am deeply thankful to Prof. Dr. Namık Kemal Pak for his stimulating scientific discussions and motivations during my entire Ph.D. program and also for a very thorough and critical reading of the thesis. I am grateful to the examining committee members for their valuable hints helped and encouraged me to go ahead with my thesis. I also thank to Assoc. Prof. Dr. Vali Bashiry for his help. I would like to thank also TUBITAK, Turkish Scientific and Technical Research Council, for the partial support they granted. Finally, I would like to express my gratitude to my wife and my family for their morale supports.

TABLE OF CONTENTS

LIST OF TABLES

TABLES

LIST OF FIGURES

FIGURES

CHAPTER 1

INTRODUCTION

The Standard Model (SM) of particle physics is a gauge theory of the electroweak and strong interactions with the gauge group $SU(3)_c \otimes SU(2)_L \otimes U(1)_Y$. This model explains all known particles and their interactions except than gravity. These fundamental particles make up all the visible matter in the universe and up to now, the SM describes all experimental results well. Although, the problems of flavour, unification, quantum gravity and origin of the matter in the universe provide reasons to expect physics beyond the Standard Model, the SM is the only minimal model of fundamental particles which is in perfect agreement with all confirmed collider data despite it requires a missing ingredient, the Higgs boson or something else to give masses to the elementary particles.

Theory of the strong interactions, called quantum chromodynamics (QCD), is a framework describing the strong interactions of the quarks and gluons found in hadrons. QCD is a non-abelian SU(3) Yang-Mills gauge theory of color-carrying quarks and has a peculiar property: in very high-energies, quarks and gluons interact very weakly, a property called asymptotic freedom. It is also believed that the QCD is a confining theory. The confinement means that the force between quarks does not diminish as they are separated and it would take an infinite amount of energy to separate two quarks, so they are forever bound into hadrons. At high energies or small distances, due to the asymptotic freedom, the quarks move almost freely. Hence, we can use perturbation theory in this regime. Although limited in scope, the perturbation theory has resulted in the most precise tests of QCD to date. However, in low energies

and hadronic scales, it is difficult to get reliable theoretical results using the perturbation theory since the effective strong coupling constant between quarks and gluons becomes large in such scales and hence perturbation theory fails. Therefore, in large distances (hadronic scales), we need some non-perturbative approaches to describe the non-perturbative phenomena.

Some non-perturbative methods are QCD sum rules, lattice QCD, different relativistic and non-relativistic quark models, bound state approach, potential, hyper central, soliton, and skyrmion models, Chiral perturbation theory, heavy quark effective theory, soft-collinear effective theory and Nambu-Jona-Lasinio model. Among the non-perturbative methods, the QCD sum rules (QSR) and one of its extensions, the light cone QCD sum rules (LCQSR), are more powerful and attractive since they are based on the fundamental QCD Lagrangian. Furthermore, in this method, instead of a model-dependent treatment in terms of constituent quarks, hadrons are represented by their interpolating quark currents. This approach has been successfully applied to various problems (see e.g. [1, 2, 3, 4]). In the present thesis, we use this method to analyze properties of the light and heavy baryons.

Some of the important parameters of the baryons are their masses, form factors and electromagnetic moments. These parameters give valuable information about the internal structures of the baryons. In this thesis, we discuss these properties using the radiative transitions. These transitions can be within a multiplet or between multiplets. The low energy QCD at which the baryons are formed is a non-perturbative theory, so for the phenomenology of the baryons the QCD sum rules [5] method as a non-perturbative approach is used.

The structure of the decuplet, octet and heavy baryons have been of interest for a long time. The experimental studies on the light decuplet and octet baryons have been done in some laboratories such as the MAMI in Mainz and Jeferson Lab (see e.g. [6, 7]) . In the recent years, considerable experimental progress has also been made in the spectroscopy of the heavy baryons. The CDF [8, 9], DO [10] and BaBar [11] Collaborations announced the observation of some heavy baryons. A theoretical analysis of experimental results can give essential information about the structure of

these baryons.

The outline of this thesis is as follows: in chapter 2, classification of the baryons within unitary symmetry is discussed. In this chapter, we classify the light octet, decuplet and singlet baryons as well as the heavy baryons with a single heavy quarks in SU(3) flavor symmetry. In chapter 3, we briefly review the QCD sum rules approach and one of its extensions, the light cone QCD sum rules. The axial $N \to \Delta$ transition form factors, as well as the nucleon electromagnetic form factors are discussed in the framework of the light cone QCD sum rules in chapter 4. It is found that our results on the axial form factors of the $N \to \Delta$ reproduce the existing predictions of the lattice QCD. The results on the electromagnetic form factors of the nucleons, which have been of great interest for physicists more than forty years both experimentally and theoretically, explain the recent experimental data well. In chapter 5, we present the phenomenology of the heavy baryons. In this chapter, the magnetic moments of the heavy Ξ_Q baryons as well as the mass and magnetic moments of the heavy flavored baryons with $J = \frac{3}{2}$ are analyzed in LCQSR. It is shown that the results on the mass of the heavy spin 3/2 baryons are in a good consistency with the predictions of the other non-perturbative approaches and existing experimental data. We predict that the masses of some heavy spin 3/2 particles which have not been discovered yet as well as the magnetic moments of the heavy spin 3/2 particles and also heavy spin 1/2, Ξ_Q baryons can be verified by the future experiments. Finally, chapter 6 includes our conclusions.

CHAPTER 2

CLASSIFICATION OF BARYONS

In this chapter, we review briefly the classification of the light baryons and heavy baryons with single heavy quark in framework of the unitary symmetry along the lines similar to [12]. According to the quark picture, the light baryons are composed of three light quarks. To construct the light baryons, we consider the SU(3) flavor symmetry with quarks $q^1 = u$, $q^2 = d$ and $q^3 = s$. Baryons contain three quarks, so let us make a product of three 3-spinors of SU(3) and search for octet and decuplet baryons in the decomposition of the triple product of the irreducible representations (IR's): $3 \otimes 3 \otimes 3 = 10 \oplus 8 \oplus 8' \oplus 1$. This contains two octet IR's and, so we proceed to construct baryon octet of quarks and symmetrize and antisymmetrize all indices to obtain

$$\begin{aligned} q^i \times q^j \times q^k &= \frac{1}{6}(q^iq^jq^k + q^jq^iq^k + q^iq^kq^j + q^jq^kq^i + q^kq^jq^i + q^kq^iq^j) \\ &+ \frac{1}{6}(2q^iq^jq^k + 2q^jq^iq^k - q^iq^kq^j - q^jq^kq^i - q^kq^jq^i - q^kq^iq^j) \\ &+ \frac{1}{6}(2q^iq^jq^k - 2q^jq^iq^k + q^iq^kq^j - q^jq^kq^i + q^kq^jq^i - q^kq^iq^j) \\ &+ \frac{1}{6}(q^iq^jq^k - q^jq^iq^k - q^iq^kq^j + q^jq^kq^i - q^kq^jq^i + q^kq^iq^j) \\ &= T^{\{ijk\}} + T^{\{ij\}k} + T^{[ij]k} + T^{[ijk]}, \end{aligned} \tag{2.1}$$

where the {...} and [...] denote the symmetric and antisymmetric flavor wave functions and each i, j and k goes from 1 to 3. A symmetrical tensor of the 3rd rank has the dimension $N_n^{SSS} = (n^3 + 3n^2 + 2n)/6$ and for $n = 3$, $N_3^{SSS} = 10$. However, an antisymmetrical tensor of the 3rd rank has the dimension $N_n^{AAA} = (n^3 - 3n^2 + 2n)/6$ and for $n = 3$, $N_3^{AAA} = 1$. Tensors of mixed symmetry of the dimension $N_n^{mix} = n(n^2 - 1)/3$

for $n = 3$, $N_3^{mix} = 8$, could be rewritten in a more suitable form as T^{α}_{β}, by using antisymmetric Levi-Civita tensor of 3rd rank $\epsilon_{\alpha\beta\gamma}$ which transforms as the singlet IR of the SU(3) group. With the help of the Levi-Civita tensor, partly antisymmetric 8-dimensional tensor $T^{[\alpha\beta]\gamma}$ could be written as:

$$B^{\beta}_{\alpha} \mid^{As}_{SU(3)} = \epsilon_{\alpha\gamma\eta} T^{[\gamma\eta]\beta}, \tag{2.2}$$

and for the proton $p = B^1_3$ we would have

$$\sqrt{2} \mid p\rangle^{As}_{SU(3)} = \sqrt{2} B^1_3 \mid^{As}_{SU(3)} = -|udu\rangle + |duu\rangle. \tag{2.3}$$

The baryon octet based on partly symmetric 8-dimensional tensor $T^{\{\alpha\beta\}\gamma}$ could also be written in terms of quark wave functions as

$$\sqrt{6} B^{\alpha}_{\beta} \mid^{Sy}_{SU(3)} = \epsilon_{\beta\delta\eta} \{q^{\alpha}, q^{\delta}\} q^{\eta}, \tag{2.4}$$

where, for the proton B^1_3 we obtain

$$\sqrt{6} \mid p\rangle^{Sy}_{SU(3)} = \sqrt{6} B^1_3 \mid^{Sy}_{SU(3)} = 2 \mid uud\rangle - \mid udu\rangle - \mid duu\rangle \tag{2.5}$$

The complete wave function of a baryon is a product of space, spin, flavor and color wave functions. For the lowest lying baryons, $l = 0$ and hence the space part is symmetric. Due to the fact that baryons have to be color singlet, the color wave function is antisymmetric. Hence, to obtain overall antisymmetric wave function, the spin-flavor wave function has to be symmetric. The spin is described by the unitary group SU(N) for $N = 2$. Hence the previous general derivations can be used with the definitions $n = 2$, $q^1 = |\uparrow\rangle$ and $q^2 = |\downarrow\rangle$. The singlet under SU(2) is the rank, 2 Levi-Civita tensor ϵ_{ij}. Define $t^j_A by$

$$\varepsilon_{ik} T^{[ik]j} = t^j_A, \tag{2.6}$$

where t^j_A is just the IR corresponding to one of two possible constructions of spin $1/2$ state of three $1/2$ states (the two of them being antisymmetrized). The state with the $s_z = +1/2$ is just

$$t^1_A = \frac{1}{\sqrt{2}} (q^1 q^2 - q^2 q^1) q^1 = \frac{1}{\sqrt{2}} (|\uparrow\downarrow\uparrow\rangle - |\downarrow\uparrow\uparrow\rangle), \tag{2.7}$$

The tensor of mixed symmetry describes state of spin $1/2$ made of three spins $1/2$:

$$\varepsilon_{ij}T^{\{ik\}j} = T^k_S, \tag{2.8}$$

where, T^k_S is just the IR corresponding to the 2nd possible construction of spin $1/2$ state of three $1/2$ states (with two of them being symmetrized). The state with the $s_z = +1/2$ is just

$$T^1_S = \frac{1}{\sqrt{6}}[\varepsilon_{12}2q^1q^1q^2 + \varepsilon_{21}(q^2q^1 + q^1q^2)q^1] = \frac{1}{\sqrt{6}}(2\,|\uparrow\uparrow\downarrow\rangle - |\uparrow\downarrow\uparrow\rangle - |\downarrow\uparrow\uparrow\rangle), \tag{2.9}$$

Multiplying spin wave functions of Eqs. (2.7, 2.9) and unitary spin wave functions of Eqs. (2.3, 2.5) one gets

$$\sqrt{18}B^\alpha_\beta\,|\uparrow\rangle = \sqrt{18}(B^\alpha_\beta\,|^{As}_{SU(3)}\,.t^j_A + B^\alpha_\beta\,|^{Sy}_{SU(3)}\,.T^j_s) \tag{2.10}$$

Taking the proton B^1_3 as an example one obtains

$$\begin{aligned}
\sqrt{18}\,|\,p\rangle_\uparrow &= |\,-udu + uud\rangle.\,|-\uparrow\downarrow\uparrow + \uparrow\uparrow\downarrow\rangle \\
&+ |\,2uud - udu - duu\rangle.\,|\,2\uparrow\uparrow\downarrow - \uparrow\downarrow\uparrow - \downarrow\uparrow\uparrow\rangle \\
&= |\,2u_\uparrow u_\uparrow d_\downarrow - u_\uparrow d_\uparrow u_\downarrow - d_\uparrow u_\uparrow u_\downarrow + 2u_\uparrow d_\downarrow u_\uparrow - u_\uparrow u_\downarrow d_\uparrow \\
&- d_\uparrow u_\downarrow u_\uparrow + 2d_\downarrow u_\uparrow u_\uparrow - u_\downarrow u_\uparrow d_\uparrow - u_\downarrow d_\uparrow u_\uparrow\rangle,
\end{aligned} \tag{2.11}$$

where, the following notation has been used

$$|\,uud\rangle.\,|\downarrow\uparrow\uparrow\rangle = |\,u_\downarrow u_\uparrow d_\uparrow\rangle. \tag{2.12}$$

The shorter version of the above equation can be written as the following equation, where we can not change the order of spinors at all

$$\sqrt{6}\,|\,p\rangle = \sqrt{6}\,|\,B^1_3\rangle_\uparrow = |\,2u_\uparrow u_\uparrow d_\downarrow - u_\uparrow d_\uparrow u_\downarrow - d_\uparrow u_\uparrow u_\downarrow\rangle. \tag{2.13}$$

From the same procedure, we obtain the wave function of the isosinglet Λ as the following structure

$$2\,|\,\Lambda\rangle_\uparrow = -\sqrt{6}\,|\,B^3_3\rangle_\uparrow = |\,d_\uparrow s_\uparrow u_\downarrow + s_\uparrow d_\uparrow u_\downarrow - u_\uparrow s_\uparrow d_\downarrow - s_\uparrow u_\uparrow d_\downarrow\rangle \tag{2.14}$$

The decuplet of baryon resonances $T^{\{\alpha\beta\gamma\}}$ with $J^P = 3/2^+$ could be written in the form of a so called weight diagram. This weight diagram gives a convenient graphic image

of the SU(3) IR's on the 2-parameter plane. The y axis shows the strangeness which is -1, 0 and 0 for the s, u and d quarks, respectively. The x axis is characterized by the 3rd projection of the isospin, I_3, which is 0 for s, $\frac{1}{2}$ for u and $-\frac{1}{2}$ for d quark. This diagram for light decuplet baryons has the form of a triangle:

$$\begin{array}{lccccccc} s=0 & & \Delta^- & & \Delta^0 & & \Delta^+ & & \Delta^{++} \\ s=-1 & & & \Sigma^{*-} & & \Sigma^{*0} & & \Sigma^{*0} & \\ s=-2 & & & & \Xi^{*-} & & \Xi^{*0} & & \\ s=-3 & & & & & \Omega^{*-} & & & \\ & I_3=-\frac{3}{2} & -1 & -\frac{1}{2} & 0 & \frac{1}{2} & 1 & \frac{3}{2} & \end{array} \tag{2.15}$$

The quark contents for decuplet baryons are

$$\begin{array}{c} ddd \quad udd \quad uud \quad uuu \\ sdd \quad sud \quad suu \\ ssd \quad ssu \\ sss \end{array} \tag{2.16}$$

In the SU(3) group, all the weight diagrams are either hexagons or triangles. For the octet baryons, the weight diagram is a hexagon with the 2 elements in center

$$\begin{array}{lccccc} s=0 & & n & & p & \\ s=-1 & \Sigma^- & & (\Sigma^0,\Lambda) & & \Sigma^+ \\ s=-2 & & \Xi^- & & \Xi^0 & \\ & I_3=-1 & -\frac{1}{2} & 0 & \frac{1}{2} & 1 \end{array} \tag{2.17}$$

or in terms of the quark contents:

$$\begin{array}{c} udd \quad uud \\ sdd \quad sud \quad suu \\ ssd \quad ssu \end{array} \tag{2.18}$$

Having classified the light octet, decuplet and singlet baryons in SU(3) flavour symmetry representation, now, we construct the heavy baryons containing single heavy quark. The baryons containing single heavy quark can be classified according to the spin of the light degrees of freedom in the heavy quark limit, $m_Q \to \infty$. In this limit, the total angular momentum of the light quarks is a good quantum number. In these baryons, the light degrees of freedom (quarks and gluons) form a diquark which orbits the nearly static heavy charm or bottom quark. This system is the QCD analogue of the familiar hydrogen atom (proton and electron bounded by the electromagnetic interactions) [13]. These baryons have been at the focus of much attention, particularly since the development of the heavy quark effective theory (HQET) and its application to baryons containing a single heavy quark. The heavy quark provides a window that allows us to see somewhat further under the skin of the non-perturbative QCD as compared the light baryons. These states are expected to be somewhat narrow, so that their detection and isolation are relatively easy. The baryons with single heavy quark belong to either antisymmetric $\bar{3}_F$ or symmetric 6_F flavor representation of SU(3) since $3 \otimes 3 = \bar{3}_F \oplus 6_F$. For the S-wave heavy baryons, flavor -spin wave function of the two light quarks must be symmetric, since their color wave function is antisymmetric. The spin of the light diquark is either $S = 1$ for 6_F, or $S = 0$ for $\bar{3}_F$. The ground state will have angular momentum $l = 0$. Therefore, the spin of the ground state is $1/2$ for $\bar{3}_F$ representing the Λ_Q and Ξ_Q baryons, while it can be both $3/2$ or $1/2$ for 6_F, corresponding to Σ_Q, Σ_Q^*, Ξ_Q', Ξ_Q^*, Ω_Q and Ω_Q^* states, where $*$ indicates spin 3/2 states. In the heavy quark limit, the heavy baryons which differ only by the spin of the heavy quark are degenerate, i.e., they can be grouped into degenerate doublets which differ only by the spin. For instance, in the heavy quark limit, the Σ_Q^* and Σ_Q are degenerate.

CHAPTER 3

QCD SUM RULES FORMALISM

3.1 Introduction

In this chapter, we review briefly the QCD sum rules and its extension, light cone QCD sum rules, introducing a simple correlation function for a scalar meson. More complicated correlation functions for baryons and details of the calculations are discussed in sum rules sections of chapters 4 and 5. Our aim in this chapter is to show how this method works and discuss briefly its foundation as well as its accuracy. The full review on this method and some of its applications can be found in [1, 2, 3, 4]. This chapter will follow closely [1, 14]. The QCD or SVZ sum rules approach, developed about thirty years ago by Shifman, Vainshtein and Zakharov [5], has become one of the most applicable tools in the phenomenology of hadrons. In this method, hadrons are represented by their interpolating quark currents. The main object in this approach is the so called correlation function expressed in terms of these interpolating currents. This correlation function is calculated in the framework of the operator product expansion (OPE), where the short- and long-distance quark-gluon interactions are separated. The former is calculated using QCD perturbation theory, whereas the latter are parameterized in terms of the vacuum condensates or light-cone distribution amplitudes. This gives us the QCD or theoretical side of the correlation function. On the other hand, the correlator is calculated in hadronic language by inserting a complete set of hadronic states. The sum rules for the physical quantities is obtained matching these two representations of the correlation function via dispersion relation. The sum rules obtained in this way allows us to calculate the physical quantities

characterizing the hadronic ground state.

3.2 Foundation of the QCD Sum Rules

3.2.1 Correlation Function

The main advantage of the QCD sum rules as a nonperturbative method is that, it is based on the fundamental QCD Lagrangian. The QCD Lagrangian is

$$\mathcal{L}_{QCD} = -\frac{1}{4} G^a_{\mu\nu} G^{a\mu\nu} + \sum_q \bar{\psi}_q (i \not{D} - m_q) \psi_q, \tag{3.1}$$

where $G^a_{\mu\nu}$ is the gluon field-strength tensor and ψ_q are the quark fields with different flavors $q = u, d, c, s, t, b$. In principle, this Lagrangian is responsible for all properties of the hadrons and hadronic processes. However, a direct use of Eq. (3.1) is possible only within the limited framework of the perturbation theory. The condition that guarantees the smallness of the corresponding effective quark-gluon coupling $\alpha_s = g_s^2/4\pi$ and adequacy of the perturbative expansion is that, at least some of the quarks or gluons in a hadronic process have to be highly virtual. Mainly, high virtuality is obtained in a scattering of hadrons at large momentum transfer. However, even for these hard scattering processes, a perturbative calculation of the quark-gluon Feynman diagrams is not sufficient, since the quarks participating in the hard scattering are confined inside hadrons. Therefore, one should combine the perturbative QCD result with certain wave functions or momentum distributions of quarks in hadrons. To calculate these characteristics, we need to know the QCD dynamics at distances of order of the hadron size: $R_{hadr} \sim 1/\Lambda_{QCD}$, the scale at which perturbation theory in α_s fails.

We consider the following correlation function between vacuum states i.e., with no initial and final hadrons:

$$\Pi(q^2) = i \int d^4x \, e^{iq\cdot x} \langle 0 | \, T\{ j(x) \bar{j}(0) \} \, | 0 \rangle, \tag{3.2}$$

where q is the momentum of the quarks, $j(x)$ is the quark current that injects quarks into the QCD vacuum at point x and T is the time ordering operator. The correla-

tion function injects quarks at the origin and analyze the evolution of quarks to the space-time point x. The amplitude $\Pi(q^2)$ in the above equation is called a two-point correlation function. This correlator leads to mass-sum rules. In the case when the four-momentum squared is large, $Q^2 \equiv -q^2 \gg \Lambda^2_{QCD}$, this correlation function receives contributions only from short-distance and short-time effects. This implies that

$$|\vec{x}| \sim x_0 \sim 1/\sqrt{Q^2} \ll R_{hadr}\,. \tag{3.3}$$

Therefore, at large Q^2, due to the asymptotic freedom of QCD, the quark-gluon interactions are then suppressed and, as a first approximation, one can calculate the correlation function (3.2) representing virtual quarks by the free-quark propagators implied directly from the QCD Lagrangian.

3.2.2 Phenomenological Side

In this part, we show how the correlation function is related to the physically observed hadrons. The invariant amplitude $\Pi(q^2)$ is an analytic function of q^2 defined at both negative (spacelike) and positive (timelike) values of q^2. When q^2 is shifted from large and negative to positive values, the correlation function starts receiving contributions from long-distance quark-gluon interactions. In this regime, the quarks start to form hadrons. Inserting a complete set of intermediate hadronic states with the same quantum number as interpolating currents in Eq. (3.2), i.e., inserting

$$1 = |0\rangle\langle 0| + \sum_h \int \frac{d^4p_h}{(2\pi)^4} 2\pi\delta(p_h^2 - m_h^2)|h(p_h)\rangle\langle h(p_h)| + \text{higher Fock states}, \tag{3.4}$$

we get the physical or phenomenological representation of the correlation function as:

$$\begin{aligned} 2\text{Im}\,\Pi(q^2) &= \sum_h \int \langle 0|\, j\,|h\rangle\langle h|\,\bar{j}\,|0\rangle\, d\tau_h (2\pi)^4 \delta^{(4)}(q - p_h) \\ &= 2\pi f_h^2 \delta(q^2 - m_h^2) + 2\pi\rho^h(q^2)\,, \end{aligned} \tag{3.5}$$

where, the summation goes over all possible hadronic states $|h\rangle$ created by the quark current j. The $\rho^h(q^2)$ represents the contributions of the higher states and continuum and $f_h = \langle 0 \mid j(0) \mid h\rangle$ is the leptonic decay constant (for mesons) or residue (for

baryons) of the ground state hadron (hadron with the lowest mass) and $d\tau_h$ denotes the integration measure over the phase space volume of these states.

Now, to link the values of the $\Pi(q^2)$ for positive values of the q^2 to the negative values, we use the Cauchy formula for the analytic function $\Pi(q^2)$ and derive the dispersion relation for the correlation function. Using the Cauchy formula for analytic functions, for the contour shown in Fig. 3.1, we can write:

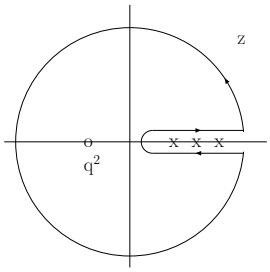

Figure 3.1: The contour in the plane of the complex variable $z = q^2$. The open point represents the $q^2 < 0$ reference point of the QCD calculation and the crosses indicate positions of the hadronic thresholds at $q^2 > 0$.

$$\begin{aligned}\Pi(q^2) &= \frac{1}{2\pi i}\oint_C dz \frac{\Pi(z)}{z-q^2} = \frac{1}{2\pi i}\oint_{|z|=R} dz \frac{\Pi(z)}{z-q^2} \\ &+ \frac{1}{2\pi i}\int_{t_{min}}^{R} dz \frac{\Pi(z+i\epsilon)-\Pi(z-i\epsilon)}{z-q^2}\,. \end{aligned} \tag{3.6}$$

where, t_{min} is the threshold for creation of real states, the radius R of the circular part of the contour is to be sent to infinity. At $|z| \to \infty$, if the function $\Pi(z)$ vanishes fast enough, the first term in the above equation vanishes. If it does not vanish, we can expand the denominator in terms of q^2/z, and eventually, at some order n, $\Pi(z)/z^n$ would vanish sufficiently fast and the remaining terms will not contribute. Therefore, at this limit the first term reduces to a polynomial in q^2 called subtraction terms. Considering the fact that the $\Pi(q^2)$ function is real in the region $q^2 < t_{min}$, Schwartz reflection principle states that $\Pi(z+i\epsilon) - \Pi(z-i\epsilon) = 2iIm\Pi(q^2)$ at $q^2 > t_{min}$. Hence

the following dispersion relation

$$\Pi(q^2) = \frac{1}{\pi}\int_{t_{min}}^{\infty} ds \frac{Im\Pi(s)}{s - q^2 - i\epsilon} + \text{subtraction terms} \tag{3.7}$$

is obtained. The $Im\Pi(s)/\pi = \rho(s)$ is the so called the spectral density. Combining Eqs. (3.5) and (3.7), one gets the following relation for the hadronic side of the correlation function:

$$\Pi(q^2) = \frac{f_h^2}{m_h^2 - q^2} + \int_{s_0^h}^{\infty} ds \frac{\rho^h(s)}{s - q^2} + \text{subtraction terms}, \tag{3.8}$$

where s_0^h is the threshold for the creation of higher mass states.

3.2.3 Theoretical or QCD Side

From the QCD side, on the other hand, the correlation function can also be calculated in the quark-gluon language with the help of the operator product expansion in large Euclidean region $Q^2 = -q^2 \gg \Lambda^2_{QCD}$. The OPE states that for small x, the time order product of two currents at different points in the correlation function can be expanded in terms of local operators with space time dependent coefficients as:

$$T\{j(x)\bar{j}(0)\} = \sum_d C_d(x^2) O_d, \tag{3.9}$$

where, $C_d(x^2)$ are Wilson coefficients which can be calculated using perturbation theory and O_d are a set of local operators ordered according to their dimensions. The lowest-dimension operator with $d = 0$ is the unit operator associated with the perturbative contribution. In QCD, there are no colorless operators with lower dimensions, $d = 1, 2$. The operators with 3, 4, 5 and 6 dimensions are:

$$\begin{aligned}
O_3 &= \bar{\psi}\psi, \\
O_4 &= G^a_{\mu\nu} G^{a\mu\nu}, \\
O_5 &= \bar{\psi}\sigma_{\mu\nu}\frac{\lambda^a}{2} G^{a\mu\nu}\psi\,, \\
O_6^{\psi} &= (\bar{\psi}\Gamma_r\psi)(\bar{\psi}\Gamma_s\psi)\,, \\
O_6^{G} &= f_{abc} G^a_{\mu\nu} G^{b\,\nu}_{\sigma} G^{c\sigma\mu},
\end{aligned} \tag{3.10}$$

and so on. Here, operators with Lorentz indices are ignored because they do not contribute to the vacuum-vacuum correlation function. The $\Gamma_{r,s}$ denote various combinations of Lorentz and color matrices. The correlation function can be written in terms of the OPE as:

$$\Pi(q^2) = \sum_d C_d(x^2)\langle O_d\rangle. \tag{3.11}$$

The $\langle O_d\rangle$ form a set of vacuum condensates which parameterize the non-perturbative effects. The vacuum averages of O_3 and O_4 are so called the quark and gluon condensates, respectively, and the vacuum averages of the remaining operators are, correspondingly the quark-gluon, four-quark and three-gluon condensates. Once the correlation function is calculated using OPE, the spectral density is given as $\rho^{OPE}(q^2) = \frac{1}{\pi} Im\Pi^{OPE}(q^2)$ and

$$\Pi(q^2) = \int_0^\infty ds \frac{\rho^{OPE}(s)}{s - q^2} + \text{subtraction terms}. \tag{3.12}$$

3.2.4 QCD Sum Rules for Physical Quantities

Equating two representations of the correlation function, we obtain

$$\begin{aligned} \frac{f_h^2}{m_h^2 - q^2} + \int_{s_0^h}^\infty ds \frac{\rho^h(s)}{s - q^2} + \text{subtraction terms} &= \int_0^\infty ds \frac{\rho^{OPE}(s)}{s - q^2} \\ &+ \text{subtraction terms}. \end{aligned} \tag{3.13}$$

To eliminate the subtraction terms, the Borel transformation with respect to the $Q^2 = -q^2$ is applied on both sides. This also suppresses the contributions of the higher states and continuum. The Borel transformation is defined as

$$\mathcal{B}_{M^2} f(q^2) = lim_{\substack{Q^2,n\to\infty \\ \frac{Q^2}{n}=M^2}} \frac{(-q^2)^n}{(n-1)!} (\frac{d}{dq^2})^{n-1} f(q^2), \tag{3.14}$$

where, it leads to the following three important examples:

$$\begin{aligned} \mathcal{B}_{M^2}(q^2)^k &= 0, \qquad k \geq 0 \\ \mathcal{B}_{M^2}(\frac{1}{(m^2[s] - q^2)^k}) &= \frac{1}{(k-1)!} \frac{e^{-m^2[s]/M^2}}{(M^2)^(k-1)}, \\ \mathcal{B}_{M^2}(e^{-\alpha q^2}) &= \delta(\frac{1}{M^2} - \alpha). \end{aligned} \tag{3.15}$$

Applying the Borel transformation, Eq. (3.13) is written as:

$$f_h^2 e^{-m_h^2/M^2} + \int_{s_0^h}^{\infty} ds\rho^h(s)e^{-s/M^2} = \int_0^{\infty} ds\rho^{OPE}(s)e^{-s/M^2} \tag{3.16}$$

where, not only the subtraction terms has been eliminated, but the contributions of the higher states and continuum are exponentially suppressed.

3.2.5 Quark-Hadron Duality Assumption

At $Q^2 \to \infty$ limit, the correlation function in QCD side is completely given in terms of the perturbative part. The matching between two representations of the correlation function and writing the QCD side in terms of two integrals, we get:

$$f_h^2 e^{-m_h^2/M^2} + \int_{s_0^h}^{\infty} ds\rho^h(s)e^{-s/M^2} = \int_0^{s_0} ds\rho^{OPE}(s)e^{-s/M^2} + \int_{s_0}^{\infty} ds\rho^{OPE}(s)e^{-s/M^2}.$$

To parameterize the contribution of the higher states and the continuum the following approximation is considered:

$$\int_{s_0^h}^{\infty} ds\rho^h(s)e^{-s/M^2} = \int_{s_0}^{\infty} ds\rho^{OPE}(s)e^{-s/M^2},$$

which is called the local quark hadron duality assumption. The s_0 in the above equation is called the continuum threshold. This threshold is not completely arbitrary and it is related to the energy of the exited states. The result of the physical quantities should be stable with respect to the small variations of this parameter. Applying the quark hadron duality approximation, the final sum rules is obtained as:

$$f_h^2 e^{-m_h^2/M^2} = \int_0^{s_0} ds\rho^{OPE}(s)e^{-s/M^2},$$

where, the Borel mass squared, M^2, is an auxiliary unphysical parameter in this sum rules, hence the physical quantities should be independent of it. However, in sum rules method the operator product expansion (OPE) is truncated and as a result the dependency of the predictions of physical quantities on the auxiliary parameter M^2 appears. For this reason one should look for a region of M^2 such that the predictions

for the physical quantities do not vary with respect to the Borel mass parameter. This region is the so called the "working region" and within this region the truncation is reasonable and meaningful. The upper limit of M^2 is determined from condition that the continuum and higher states contributions should be small than the total dispersion integral. The lower limit is determined by demanding that in the truncated OPE the condensate term with highest dimension remains small than sum of all terms, i.e., convergence of OPE should be under control.

3.3 Three -Point Sum Rules

The two-point correlation function can be used for determination of the mass of hadrons. It can be generalized to study the transition amplitudes, decay rates and branching ratios by calculating the transition form factors. For instance consider $h_1(p) \to h_2(p')l^+l^-$, where h_1 and h_2 are the initial and final hadrons with momentum p and $p' = p - q$. The following three point correlation function can be used to study matrix elements of operators responsible for the above transitions:

$$\Pi(p^2, p'^2) = i^2 \int d^4x d^4y \; e^{-ip\cdot x} e^{ip'\cdot y} \langle 0 | \; T\{j_1(x) j_3(0) \bar{j}_2(y)\} \; | 0 \rangle, \tag{3.17}$$

where, j_1 and j_2 are interpolating currents of the initial and final states, respectively and j_3 is the transition current. Similar to the two-point case, the aforementioned correlator can be calculated by inserting two complete sets of the hadronic states between the currents. As a result, we obtain the following double dispersion relation:

$$\begin{aligned} \Pi(p^2, p'^2) &= \frac{f_1 f_2 \langle h_1 | j_3 | h_2 \rangle}{(m_{h_1}^2 - p^2)(m_{h_2}^2 - p'^2)} + \int_{s_0^h}^{\infty} ds \int_{s_0'^h}^{\infty} ds' \frac{\rho^h(s, s')}{(s - p^2)(s' - p'^2)} \\ &+ \text{subtraction terms}, \end{aligned} \tag{3.18}$$

where, the $\langle h_1 | j_3 | h_2 \rangle$ can be parameterized in terms of some form factors. Calculation of these form factors play crucial role in analyzing the above mentioned transitions. Using the quark hadron duality assumption and applying double Borel transformation with respect to the variables p^2 and p'^2 to suppress the contribution of the higher states

and continuum, the following sum rules is obtained:

$$f_1 f_2 \langle h_1|j_3|h_2\rangle e^{-m_{h_1}^2/M_1^2} e^{-m_{h_2}^2/M_2^2} = \int_0^{s_0} ds \int_0^{s_0'} ds' \rho^{OPE}(s,s') e^{-s/M_1^2} e^{-s'/M_2^2}, \tag{3.19}$$

where, the M_1^2 and M_2^2 are new Borel parameters and s_0 and s_0' are continuum thresholds in the h_1 and h_2 channels, respectively. Here, we should stress that in the three point sum rules with double dispersion relation, the subtraction of the continuum states and the quark-hadron duality is highly nontrivial. For $q^2 > 0$ values, there may be an inconsistency between double dispersion integrals and corresponding coefficients of the structures in the Feynman amplitudes in the bare loop diagram. In this case, the double spectral density receives contributions beyond the contributions coming from the Landau-type singularities. This problem has been discussed in detail in [15].

3.4 Light Cone QCD Sum Rules

The LCQSR sum rules as an extension of the SVZ sum rules is a theory of the hard exclusive processes. The main idea, here, is to expand the matrix elements of the time ordered products of currents in the correlation function near the light cone, $x^2 \simeq 0$. Instead of the expansion of the long-distance effects in terms of operators with different mass dimensions, as in traditional sum rules, in LCQSR , those effects are parameterized in terms of light-cone distribution amplitudes with different twists. Twist is defined as the difference between the mass dimension and the spin of a traceless and totally symmetric local operators. The SVZ sum rules employ vacuum to vacuum correlation functions while in light cone sum rules, we consider T-product of two quark currents between vacuum and an on-shell state such as photon, i.e.,

$$\Pi(p^2, p'^2) = i \int d^4x e^{ipx} \langle \gamma(q)|T\{j_1(x) j_2(0)\}|0\rangle. \tag{3.20}$$

In calculating the above correlation function, matrix elements $\langle \gamma(q) \mid \bar{q}(x_1)\Gamma_i q(x_2) \mid 0\rangle$ are encountered, where $\Gamma_i = \left\{1,\ \gamma_5,\ \gamma_\mu,\ i\gamma_5\gamma_\mu,\ \sigma_{\mu\nu}/\sqrt{2}\right\}$. These matrix elements can be expanded near the light cone, $x^2 = 0$, in terms of the photon distribution amplitudes (see [16]). As an illustration, consider $\langle \gamma(q) \mid \bar{q}(x)\gamma_\mu\gamma_5 q(0) \mid 0\rangle$.

Expanding $q(x)$ using

$$q(x) = q(0) + x_\alpha D_\alpha q(x)|_{x=0} + ..., \tag{3.21}$$

one can write

$$\langle \gamma(q) \mid \bar{q}(x)\gamma_\mu\gamma_5 q(0) \mid 0\rangle = \sum_n \frac{1}{n!} x_{\alpha_1} x_{\alpha_2} ... x_{\alpha_n} \langle \gamma(q) \mid \bar{q}(0)\overleftarrow{D_{\{\alpha_1}}\overleftarrow{D_{\alpha_2}}...\overleftarrow{D_{\alpha_n\}}}\gamma_\mu\gamma_5 q(0) \mid 0\rangle,$$

where, {...} is used to show that the indices in between are completely symmetrized. The matrix elements in the right-hand-side of the above equation have the following general decomposition:

$$\begin{aligned} \langle \gamma(q) \mid \bar{q}(0)\overleftarrow{D_{\{\alpha_1}}\overleftarrow{D_{\alpha_2}}...\overleftarrow{D_{\alpha_n\}}}\gamma_\mu\gamma_5 q(0) \mid 0\rangle &= i^n \epsilon^\nu q^\lambda \varepsilon_{\mu\nu\lambda\{\alpha_1} q_{\alpha_2} q_{\alpha_3} .... q_{\alpha_n\}} M_n \\ &+ i^n \epsilon^\nu q^\lambda \varepsilon_{\mu\nu\lambda\{\alpha_1} g_{\alpha_2\alpha_3} q_{\alpha_4} .... q_{\alpha_n\}} M'_n + ... \end{aligned} \tag{3.22}$$

where, M_n and M'_n are matrix elements of local operators. Using the above equations one gets

$$\begin{aligned} \langle \gamma(q) \mid \bar{q}(x)\gamma_\mu\gamma_5 q(0) \mid 0\rangle &= \varepsilon_{\mu\nu\lambda\alpha}\epsilon^\nu q^\lambda x^\alpha \sum_n \frac{i}{n!}(iqx)^{n-1} M_n \\ &- x^2 \varepsilon_{\mu\nu\lambda\alpha}\epsilon^\nu q^\lambda x^\alpha \sum_n \frac{i}{n!}(iqx)^{n-3} M'_n + ... \end{aligned} \tag{3.23}$$

Using this result in the correlation function in Eq. (3.20) and performing integral over x, the following forms are encountered:

$$\sum_n \frac{(2pq)^n}{(-p^2)^n} M_n q_\mu + \sum_n \frac{(2pq)^n}{(-p^2)^{n+1}} M'_n q_\mu + ..., \tag{3.24}$$

where, each term in the series is multiplied by a dimensionless constant

$$\xi = \frac{2pq}{-p^2} = \frac{(p+q)^2 - p^2 - q^2}{-p^2}. \tag{3.25}$$

The ξ is of order one, generally, and we have to keep all the terms in the above expansion.

In Eq. (3.22), the mass dimension of operator on the left-hand-side is: $n+3$. The spins of the first and second terms in r. h. s. are $n+1$ and $n-1$, respectively because the

operator without derivatives has dimension 3, and the Lorentz spin 1. Therefore, the twists of first and second terms in r. h. s. are 2 and 4, respectively (after multiplying both parts of Eq. (3.22) by $g_{\alpha_1\alpha_2}$ it becomes clear that the matrix elements M'_n receive their contributions from the twist 4 operators). Hence, the expansion in Eq. (3.23) is an expansion in terms of the twist, rather than the mass dimension of the local operators. As an example, we focus on the lowest twist terms M and define a function $\varphi(u)$ such that

$$\frac{i}{n}M_n = \frac{f}{4}ee_q \int_0^1 duu^n\varphi(u). \tag{3.26}$$

The distribution amplitude $\varphi(u)$ is normalized to unity, $\int_0^1 du\varphi(u) = 1$. As a result of this procedure, the Eq. (3.23) can be written as:

$$\langle\gamma(q) \mid \bar{q}(x)\gamma_\mu\gamma_5 q(0) \mid 0\rangle = \frac{f}{4}ee_q\varepsilon_{\mu\nu\lambda\alpha}\epsilon^\nu q^\lambda x^\alpha \int_0^1 due^{iuqx}\varphi(u), \tag{3.27}$$

where, e_q is the quark charge in units of the unit charge e and $\varphi(u)$ is called the twist 2 wave function or distribution amplitude of the photon. The u in the argument of $\varphi(u)$ corresponds to the momentum fraction carried by the photon. The explicit expressions for $\varphi(u)$ and other distribution amplitudes (DA's) of the photon will be given in next chapters.

CHAPTER 4

PROPERTIES OF THE NUCLEONS

A nucleon is a collective name for two members of the octet baryons, namely neutron and proton. Understanding the nucleons' properties is one of the major goals of the modern theory of strong interactions(QCD). Among the baryons, the proton is stable and other baryons decay directly or indirectly to it. For instance, a free neutron decays to a proton via beta decay. The proton is the lightest baryon and its stability is a measure of baryon number conservation. The proton's lifetime impose strong constraints on theories which try to extend the SM of particle physics. The nucleon electromagnetic form factors and transition of the nucleons to their first and well known excited states (Δ baryons) with the help of an axial current can give valuable information about the understanding of the properties of the nucleons. In this chapter, first we discuss the transition of the nucleon to Δ via the axial current. We will show that our predictions on related form factors reproduce the data obtained from the lattice QCD analysis. Then, in the second section, we discuss other properties of the nucleons by calculating their electromagnetic form factors. Since 1965, the analysis of these form factors have been of interest for both experimentalists and theoreticians. But unfortunately, different experimental data are not exactly in good agreement. However, with the help of the general interpolating currents of the nucleons, our predictions for the electromagnetic form factors describe well the predictions of the recent experiments.

4.1 Analysis of the Axial $N \to \Delta$ Transition Form Factors

Form factors have great importance in the investigation of the internal structure of baryons. The inner structure of the nucleon is encoded in several form factors. The electromagnetic form factors of the nucleon, which parameterize the matrix element of the electromagnetic current operator, are measured in a wide range of q^2 values [17, 18, 19]. The interest in nucleon form factor has been renewed by recent progress in experimental physics, where it became possible to get polarized beams and polarized targets. This possibility opened up two new methods [20] to measure the ratio of the electric and magnetic form factors, namely polarization transfer and beam-target asymmetry. New experimental data obtained from $e + p \to e + p$ reaction, which is performed at JLAB [7], gave the result that the ratio $\mu_\rho G_E/G_M$ decreases from unity substantially for high Q^2 values. Not only form factors relevant for the diagonal transitions, but also the electromagnetic transition form factors for electro-production of the Δ have also been the subject of recent experimental [7, 21, 22] and theoretical studies [23].

The main advantage of the nucleon to Δ transition is that, the Δ is a dominant nucleon resonance and its identification is easy. The $N - \Delta$ transition form factors due to the weak axial current can give valuable information about the structure of the baryons, complementary to that obtained from electromagnetic transitions. For example, measurement of axial form factors for $N - \Delta$ transition, allows us to check off diagonal Goldberger-Treiman relation, order of conservation of the axial current and etc. Weak axial $N - \Delta$ transition form factors are investigated in neutrino (or charged lepton) scattering on deuterium or hydrogen in the Δ region experiments. New information on the weak axial form factors is expected from parity-violating electron scattering experiments planned at Jefferson Laboratory [24].

In this section, we calculate the axial $N \to \Delta$ transition form factors in LCQSR by the help of the light cone distribution amplitudes (DA's) of the proton calculated in [25, 26, 27]. Using these DA's, the semileptonic $\Lambda_b \to p\ell\nu$ [28] decay, scalar form factor of the proton [29, 30], axial and induced pseudo scalar form factors of

the nucleon [31, 32], $\Sigma - n$ form factors [33] are studied. In [34], the distribution amplitudes of Λ in leading conformal spin is calculated and the obtained amplitudes are used to study the $\Lambda_c \to \Lambda \ell \nu$ decay. Note that these form factors are calculated in lattice QCD in [35, 36], and in chiral constituent quark model in [37].

4.1.1 Sum Rules for the Axial Nucleon to Delta Transition Form Factors

In the present subsection, light cone QCD sum rules for the axial N to Δ transition form factors are derived. These form factors are defined by the matrix element of the axial current (in our case isovector part of the axial current), i.e.,

$$J_\nu^3(x) = \overline{\psi}(x)\gamma_\nu\gamma_5\frac{\tau^3}{2}\psi(x), \tag{4.1}$$

between the nucleon state with momentum p and the Δ-state with momentum $p' = p - q$, where τ^3 is the third Pauli matrix, and q is the transferred momentum. Hence, the axial $N \to \Delta$ transition form factors are defined by the matrix element $\langle \Delta(p', s') \mid J_\nu^3 \mid N(p, s)\rangle$. This N to Δ weak matrix element can be expressed in terms of four invariant transition form factors as follows [38, 39]:

$$\begin{aligned}\langle \Delta(p', s') \mid J_\nu^3 \mid N(p, s)\rangle &= i\overline{u}^\lambda(p', s')\{(\frac{C_3^A(q^2)}{m_N}\gamma_\mu + \frac{C_4^A(q^2)}{m_N^2}p'_\mu)(g_{\lambda\nu}g_{\rho\mu} \\ &- g_{\lambda\rho}g_{\mu\nu})q^\rho + C_5^A(q^2)g_{\lambda\nu} + \frac{C_6^A(q^2)}{m_N^2}q_\lambda q_\nu\}u(p, s),\end{aligned} \tag{4.2}$$

where $u^\lambda(p', s')$ is the Rarita-Schwinger spinor for Δ and $u(p, s)$ is the nucleon spinor. Note that, the partial conservation of axial current (PCAC) and pion meson dominance leads to the relation [36]

$$C_6^A(Q^2) = \frac{m_N^2}{Q^2 + m_\pi^2}C_5(Q^2). \tag{4.3}$$

For the calculation of the above mentioned form factors within the light cone QCD sum rules method, we consider the matrix element in which one of the hadrons is described by an interpolating current with the quantum numbers of this hadron and another one is represented by the state vector. For the construction of the light cone

sum rules, the distribution amplitudes (DA's) of hadron state vector is needed. The nucleon distribution amplitudes for three quark operators are calculated in [25, 26, 27] and DA's for Δ isobar is not yet calculated. For this reason, we consider the following correlation function where the nucleon is described by the state vector

$$\Pi_{\mu\nu}(p,q) = i \int d^4x e^{iqx} \langle 0 \mid T\{\eta_\mu(0) J^3_\nu(x)\} \mid N(p)\rangle. \tag{4.4}$$

The interpolating current for the Δ^+ isobar is chosen in the form [40]:

$$\eta_\mu(0) = \frac{1}{\sqrt{3}} \varepsilon^{abc} [2(u^{aT}(0) C\gamma_\mu d^b(0)) u^c(0) + (u^{aT}(0) C\gamma_\mu u^b(0)) d^c(0)], \tag{4.5}$$

and the axial current is:

$$J^3_\nu(x) = \frac{1}{2}[\overline{u}(x)\gamma_\nu\gamma_5 u(x) - \overline{d}(x)\gamma_\nu\gamma_5 d(x)].$$

In order to construct the sum rules for the form factors, the correlation function will be represented in two different forms, i.e. in terms of hadron parameters and in terms of the quark-gluon parameters. Let us first consider the representation of the correlation function in terms of hadron parameters (phenomenological part). Phenomenological part of the correlation function can be obtained by inserting a complete set of hadronic states with the same quantum numbers of $\eta_\mu(0)$ inside the correlation function. Saturating the correlator with these hadrons and isolating the contribution coming from the ground state hadron, we get

$$\Pi_{\mu\nu}(p,q) = \sum_{s'} \frac{\langle 0 \mid \eta_\mu \mid \Delta^+(p',s')\rangle \langle \Delta^+(p',s') \mid J_\nu \mid N(p,s)\rangle}{m^2_\Delta - p'^2} + \cdots, \tag{4.6}$$

where m_Δ is Δ^+ mass and $\cdots$ represents contributions from the higher states and the continuum. The matrix element $\langle \Delta^+ \mid J_\nu(x) \mid N\rangle$ entering in Eq. (4.6) is given by Eq. (4.2) and the matrix element $\langle 0 \mid \eta_\mu(0) \mid \Delta^+\rangle$ is determined as

$$\langle 0 \mid \eta_\mu(0) \mid \Delta^+\rangle = \lambda_\Delta u^\mu(p',s'), \tag{4.7}$$

where λ_Δ is the residue of Δ^+ isobar and the value of the residue λ_Δ is determined from the two point sum rules [40, 41, 42, 43, 44]. Performing summation over spin of Rarita-Schwinger spinor using the formula

$$\sum_s u_\mu(p',s)\overline{u_\nu}(p',s) = -(\not{p}' + m_\Delta)\{g_{\mu\nu} - \frac{1}{3}\gamma_\mu\gamma_\nu - \frac{2p'_\mu p'_\nu}{3m^2_\Delta} + \frac{p'_\mu\gamma_\nu - p'_\nu\gamma_\mu}{3m_\Delta}\}, \tag{4.8}$$

and using Eqs. (4.2), (4.6), (4.7) and (4.8) the contribution of Δ^+ to the correlation function can be written as

$$\begin{aligned}\Pi_{\mu\nu}(p,q) &= \frac{-i\lambda_\Delta}{m_\Delta^2-p'^2}(\not{p}'+m_\Delta)\left[g_{\mu\lambda}-\frac{1}{3}\gamma_\mu\gamma_\lambda-\frac{2p'_\mu p'_\lambda}{3m_\Delta^2}+\frac{p'_\mu\gamma_\lambda-p'_\lambda\gamma_\mu}{3m_\Delta}\right]\Bigg\{\\ &\left[\frac{C_3^A(q^2)}{m_N}\gamma_\alpha+\frac{C_4^A(q^2)}{m_N^2}p'_\alpha\right](g_{\lambda\nu}q_\alpha-q_\lambda g_{\nu\alpha})+C_5^A(q^2)g_{\lambda\nu}\\ &+\frac{C_6^A(q^2)}{m_N^2}q_\lambda q_\nu\Bigg\}u(p). \end{aligned} \tag{4.9}$$

From Eq. (4.9) it follows that the correlation function contains numerous tensor structures and not all of them are independent. The dependence can be removed by ordering gamma matrices in a specific order. In this work the ordering $\gamma_\mu\ \not{p}'\gamma_\nu\ \not{q}$ is chosen. With this ordering, the correlation function becomes

$$\begin{aligned}\Pi_{\mu\nu}(p,q) &= \frac{-i\lambda_\Delta}{m_\Delta^2-p'^2}\Bigg\{g_{\mu\nu}\ \not{q}C_3^A(q^2)+g_{\mu\nu}\ \not{p}'\ \not{q}\frac{C_3^A(q^2)}{m_N}+g_{\mu\nu}(\not{p}'+m_\Delta)\\ &\times\left(C_5^A(q^2)+C_4^A(q^2)\frac{p'q}{m_N^2}\right)-q_\mu(\not{p}'+m_\Delta)\gamma_\nu\frac{C_3^A(q^2)}{m_N}\\ &-q_\mu(\not{p}'+m_\Delta)p'_\nu\frac{C_4^A(q^2)}{m_N^2}+q_\mu q_\nu(\not{p}'+m_\Delta)\frac{C_6^A(q^2)}{m_N^2}\Bigg\}u(p)\\ &+\text{other structures with }\gamma_\mu\text{ at the beginning or which are}\\ &\quad\text{proportional to }p'_\mu. \end{aligned} \tag{4.10}$$

The reason why the structures $\sim p'_\mu$ and structures with γ_μ at the beginning is not considered is as follows. The interpolating current η_μ couples not only to spin-parity $(3/2)^+$ states, but also to spin-parity $(1/2)^-$ states. In other words, the η_μ has nonzero overlap with spin $1/2$ states. This coupling can be written in the most general form as:

$$\langle 0\mid\eta_\mu\mid\frac{1}{2}(p')\rangle=(Ap'_\mu+B\gamma_\mu)u(p). \tag{4.11}$$

Using the condition $\gamma^\mu\eta_\mu=0$, which is imposed to decrease the theoric degree of freedom of spin 3/2 particles to physical degree of freedom, one can easily obtain that $B=\frac{-Am_{1/2}}{4}$. Therefore, in the general case, the spin $1/2$ states give also contribution to the considered correlation function, but they contribute only to the structures which contain a γ_μ at the beginning or which are proportional to p'_μ. By choosing the ordering $\gamma_\mu\ \not{p}'\gamma_\nu\ \not{q}$ and ignoring the structures proportional to p'_μ and the structures

that contain a γ_μ at the beginning, the contributions to the correlation function from states that have spin $1/2$ are eliminated.

Now, we turn our attention to the calculation of the correlation function from the QCD side for the large Euclidean virtuality $p'^2 = (p-q)^2 << 0$ in terms of the nucleon distribution amplitudes. Using the explicit expression for the Δ^+ isobar interpolating current in Eq. (4.5) and axial current in Eq. (4.6), and carrying out all contractions for the correlation function in Eq. (4.4), we get the following result in x representation:

$$\begin{aligned}
\Pi_{\mu\nu}(p,q) &= \frac{-1}{16\pi^2\sqrt{3}}\int\frac{d^4x e^{iqx}}{x^4}\Big\{(C\gamma_\mu)_{\alpha\beta}(\gamma_\nu\gamma_5)_{\rho\sigma}\varepsilon^{abc}\langle 0\mid\Big[4u^a_\eta(0)u^b_\theta(x)d^c_\phi(0)\\
&\quad \{2g_{\alpha\eta}g_{\sigma\theta}g_{\beta\phi}(\not{x})_{\lambda\rho}+2g_{\lambda\eta}g_{\sigma\theta}g_{\beta\phi}(\not{x})_{\alpha\rho}+g_{\alpha\eta}g_{\sigma\theta}g_{\lambda\phi}(\not{x})_{\beta\rho}\\
&+ \quad g_{\beta\eta}g_{\sigma\theta}g_{\lambda\phi}(\not{x})_{\alpha\rho}\}-4u^a_\eta(0)u^b_\theta(0)d^c_\phi(x)\{2g_{\alpha\eta}g_{\lambda\theta}g_{\sigma\phi}(\not{x})_{\beta\rho}\\
&+ \quad g_{\alpha\eta}g_{\beta\theta}g_{\sigma\phi}(\not{x})_{\lambda\rho}\}\Big]\mid N(p)\rangle\Big\},
\end{aligned} \tag{4.12}$$

where, we have used the light cone expanded light quark propagator as [43]:

$$\begin{aligned}
S_q(x) &= S_q^{free}(x)-\frac{\langle\bar{q}q\rangle}{12}\Big(1-i\frac{m_q}{4}\not{x}\Big)-\frac{x^2}{192}m_0^2\langle\bar{q}q\rangle\Big(1-i\frac{m_q}{6}\not{x}\Big)\\
&\quad -ig_s\int_0^1 du\Big[\frac{\not{x}}{16\pi^2x^2}G_{\mu\nu}(ux)\sigma_{\mu\nu}-ux^\mu G_{\mu\nu}(ux)\gamma^\nu\frac{i}{4\pi^2x^2}\\
&\quad -i\frac{m_q}{32\pi^2}G_{\mu\nu}\sigma^{\mu\nu}\Big(\ln\Big(\frac{-x^2\Lambda^2}{4}\Big)+2\gamma_E\Big)\Big],
\end{aligned} \tag{4.13}$$

where, Λ is the energy cut off separating perturbative and nonperturbative domains. In order to achieve a factorization of large and small scales in the OPE, all infrared logarithms should be removed from the coefficient functions and absorbed in the matrix elements of operators. In our case, this means that the $ln\Lambda$ must be included in the condensates of different operator or distribution amplitude. A more detailed discussion on this point can be found in [45]. For this reason, we will choose the scale parameter Λ as a factorization scale, i.e., $\Lambda = (0.5-1)\ GeV$. The free part of the peopagator in above equation is defined as:

$$S_q^{free} = \frac{i\not{x}}{2\pi^2x^4}-\frac{m_q}{4\pi^2x^2}, \tag{4.14}$$

The terms proportional to the gluon strength tensor can give contribution to four and five particle distribution functions but they are expected to be small [25, 26, 27] and

for this reason we will neglect these amplitudes in further analysis. The terms proportional to $\langle\bar{q}q\rangle$ can also be omitted because Borel transformation eliminates these terms. The terms proportional to u and d quark masses are also ignored and hence only first term in the free part of the propagator is relevant for our discussion. From Eq. (4.12) it follows that for the calculation of $\Pi_{\mu\nu}(p,q)$ we need to know the matrix element $\langle 0 \mid [4u^a_\eta(0)u^b_\theta(x)d^c_\phi(0) \mid N(p)\rangle$. This three quark matrix element between vacuum and the proton state is given in [25, 26, 27] as:

$$
\begin{aligned}
& 4\langle 0|\epsilon^{abc}u^a_\alpha(a_1x)u^b_\beta(a_2x)d^c_\gamma(a_3x)|P\rangle = \mathcal{S}_1 m_N C_{\alpha\beta}(\gamma_5 N)_\gamma + \mathcal{S}_2 m_N^2 C_{\alpha\beta}(\not{x}\gamma_5 N)_\gamma \\
+ \;& \mathcal{P}_1 m_N(\gamma_5 C)_{\alpha\beta}N_\gamma + \mathcal{P}_2 m_N^2(\gamma_5 C)_{\alpha\beta}(\not{x}N)_\gamma + (\mathcal{V}_1 + \frac{x^2 m_N^2}{4}\mathcal{V}_1^M)(\not{p}C)_{\alpha\beta}(\gamma_5 N)_\gamma \\
+ \;& \mathcal{V}_2 m_N(\not{p}C)_{\alpha\beta}(\not{x}\gamma_5 N)_\gamma + \mathcal{V}_3 m_N(\gamma_\mu C)_{\alpha\beta}(\gamma^\mu\gamma_5 N)_\gamma + \mathcal{V}_4 m_N^2(\not{x}C)_{\alpha\beta}(\gamma_5 N)_\gamma \\
+ \;& \mathcal{V}_5 m_N^2(\gamma_\mu C)_{\alpha\beta}(i\sigma^{\mu\nu}x_\nu\gamma_5 N)_\gamma + \mathcal{V}_6 m_N^3(\not{x}C)_{\alpha\beta}(\not{x}\gamma_5 N)_\gamma + (\mathcal{A}_1 \\
+ \;& \frac{x^2 m_N^2}{4}\mathcal{A}_1^M)(\not{p}\gamma_5 C)_{\alpha\beta}N_\gamma + \mathcal{A}_2 m_N(\not{p}\gamma_5 C)_{\alpha\beta}(\not{x}N)_\gamma + \mathcal{A}_3 m_N(\gamma_\mu\gamma_5 C)_{\alpha\beta}(\gamma^\mu N)_\gamma \\
+ \;& \mathcal{A}_4 m_N^2(\not{x}\gamma_5 C)_{\alpha\beta}N_\gamma + \mathcal{A}_5 m_N^2(\gamma_\mu\gamma_5 C)_{\alpha\beta}(i\sigma^{\mu\nu}x_\nu N)_\gamma + \mathcal{A}_6 m_N^3(\not{x}\gamma_5 C)_{\alpha\beta}(\not{x}N)_\gamma \\
+ \;& (\mathcal{T}_1 + \frac{x^2 m_N^2}{4}\mathcal{T}_1^M)(p^\nu i\sigma_{\mu\nu}C)_{\alpha\beta}(\gamma^\mu\gamma_5 N)_\gamma + \mathcal{T}_2 m_N(x^\mu p^\nu i\sigma_{\mu\nu}C)_{\alpha\beta}(\gamma_5 N)_\gamma \\
+ \;& \mathcal{T}_3 m_N(\sigma_{\mu\nu}C)_{\alpha\beta}(\sigma^{\mu\nu}\gamma_5 N)_\gamma + \mathcal{T}_4 m_N(p^\nu\sigma_{\mu\nu}C)_{\alpha\beta}(\sigma^{\mu\rho}x_\rho\gamma_5 N)_\gamma \\
+ \;& \mathcal{T}_5 m_N^2(x^\nu i\sigma_{\mu\nu}C)_{\alpha\beta}(\gamma^\mu\gamma_5 N)_\gamma + \mathcal{T}_6 m_N^2(x^\mu p^\nu i\sigma_{\mu\nu}C)_{\alpha\beta}(\not{x}\gamma_5 N)_\gamma \\
+ \;& \mathcal{T}_7 m_N^2(\sigma_{\mu\nu}C)_{\alpha\beta}(\sigma^{\mu\nu}\not{x}\gamma_5 N)_\gamma + \mathcal{T}_8 m_N^3(x^\nu\sigma_{\mu\nu}C)_{\alpha\beta}(\sigma^{\mu\rho}x_\rho\gamma_5 N)_\gamma \;, \qquad (4.15)
\end{aligned}
$$

where the calligraphic functions are functions of the scalar product (px) and of the parameters a_i, $i = 1,\ 2,\ 3$. These functions can be expressed in terms of the nucleon distribution amplitudes with increasing twist. Explicit expressions of distribution amplitudes with definite twist are (see also [23, 25, 26, 27]):

$$
\begin{aligned}
\mathcal{S}_1 &= S_1, \\
2px\mathcal{S}_2 &= S_1 - S_2, \\
\mathcal{P}_1 &= P_1, \\
2px\mathcal{P}_2 &= P_1 - P_2, \qquad (4.16)
\end{aligned}
$$

$$
\begin{aligned}
\mathcal{V}_1 &= V_1, \\
2px\mathcal{V}_2 &= V_1 - V_2 - V_3, \\
2\mathcal{V}_3 &= V_3, \\
4px\mathcal{V}_4 &= -2V_1 + V_3 + V_4 + 2V_5, \\
4px\mathcal{V}_5 &= V_4 - V_3, \\
4(px)^2\mathcal{V}_6 &= -V_1 + V_2 + V_3 + V_4 + V_5 - V_6,
\end{aligned} \tag{4.17}
$$

$$
\begin{aligned}
\mathcal{A}_1 &= A_1, \\
2px\mathcal{A}_2 &= -A_1 + A_2 - A_3, \\
2\mathcal{A}_3 &= A_3, \\
4px\mathcal{A}_4 &= -2A_1 - A_3 - A_4 + 2A_5, \\
4px\mathcal{A}_5 &= A_3 - A_4 \\
4(px)^2\mathcal{A}_6 &= A_1 - A_2 + A_3 + A_4 - A_5 + A_6,
\end{aligned} \tag{4.18}
$$

$$
\begin{aligned}
\mathcal{T}_1 &= T_1, \\
2px\mathcal{T}_2 &= T_1 + T_2 - 2T_3, \\
2\mathcal{T}_3 &= T_7, \\
2px\mathcal{T}_4 &= T_1 - T_2 - 2T_7, \\
2px\mathcal{T}_5 &= -T_1 + T_5 + 2T_8, \\
4(px)^2\mathcal{T}_6 &= 2T_2 - 2T_3 - 2T_4 + 2T_5 + 2T_7 + 2T_8, \\
4px\mathcal{T}_7 &= T_7 - T_8, \\
4(px)^2\mathcal{T}_8 &= -T_1 + T_2 + T_5 - T_6 + 2T_7 + 2T_8.
\end{aligned} \tag{4.19}
$$

The Eqs. (4.16), (4.17), (4.18) and (4.19) are for scalar, pseudo scalar, vector, axial vector and tensor distribution amplitudes respectively. The distribution amplitudes $F = S_i, P_i, V_i, A_i, T_i$ can be written as:

$$
F(a_i px) = \int dx_1 dx_2 dx_3 \delta(x_1 + x_2 + x_3 - 1) e^{-ipx\Sigma_i x_i a_i} F(x_i) \,, \tag{4.20}
$$

where, x_i with $i = 1,\ 2,\ 3$ correspond to the longitudinal momentum fractions carried by the quarks. Using Eqs. (4.12)-(4.20) and after carrying out the Fourier transformation, the correlation function is obtained in the momentum representation.

In order to construct sum rules for axial $N - \Delta$ transition form factors we need to choose structures. From Eq. (4.10) it follows that in principle different tensor structures can be used for obtaining sum rules for axial form factors. We have chosen the structures proportional to $g_{\mu\nu}\ \not{p}'\ \not{q}$, $q_\mu p'_\nu\ \not{p}'$, $g_{\mu\nu}\ \not{p}'$, $q_\mu q_\nu\ \not{p}'$ to obtain sum rules for the form factors C_3^A, C_4^A, $C_5^A + C_4^A \frac{p'.q}{m_\Delta^2}$ and C_6^A, respectively. Equating the coefficients of the structures $g_{\mu\nu}\ \not{p}'\ \not{q}$, $q_\mu p'_\nu\ \not{p}'$, $g_{\mu\nu}\ \not{p}'$, $q_\mu q_\nu\ \not{p}'$ from both sides and applying the Borel transformation with respect to the variable $p'^2 = (p - q)^2$ which suppress the contributions of the higher states and continuum, we get desired sum rules for the form factors C_3^A, C_4^A, C_5^A and C_6^A as:

$$
\begin{aligned}
C_3(Q^2) &= \frac{m_N}{\sqrt{3}\lambda_\Delta}\, e^{\frac{m_\Delta^2}{M_B^2}} \Bigg\{ \int_{t_0}^{1} dx_2 \int_0^{1-x_2} dx_1 \frac{e^{-\frac{s(x_2,Q^2)}{M_B^2}}}{x_2} \left[2V_1 - T_1\right](x_i) \\
&+ \int_{t_0}^{1} dx_3 \int_0^{1-x_3} dx_1 \frac{e^{-\frac{s(x_3,Q^2)}{M_B^2}}}{x_3} T_1(x'_i) \\
&+ \int_{t_0}^{1} dx_3 \int_0^{1-x_3} dx_1 \int_{t_0}^{x_3} \frac{dt_1}{t_1^2} e^{-\frac{s(t_1,Q^2)}{M_B^2}} \frac{m_N^2}{M_B^2}(x_3 - t_1)\mathcal{T}_{234578}(x'_i) \\
&+ \int_{t_0}^{1} dx_3 \int_0^{1-x_3} dx_1 e^{-\frac{s_0}{M_B^2}} \frac{m_N^2}{Q^2 + m_N^2 t_0^2}(-t_0 + x_3)\mathcal{T}_{234578}(x'_i) \Bigg\},
\end{aligned}
\tag{4.21}
$$

$$
\begin{aligned}
C_4(Q^2) = \frac{m_N^2}{\sqrt{3}\lambda_\Delta}\, e^{\frac{m_\Delta^2}{M_B^2}} \Bigg\{ & \int_{t_0}^{1} dx_2 \int_0^{1-x_2} dx_1 \int_{t_0}^{x_2} dt_1\, e^{-\frac{s(t_1,Q^2)}{M_B^2}} \Bigg[\\
+ \ & \frac{2m_N}{M_B^2 t_1}(\mathcal{V}_{123} - \mathcal{T}_{123})(x_i) + \frac{2m_N(1 - 2t_1)}{M_B^2 t_1}(-\mathcal{A}_{123} + \mathcal{T}_{127})(x_i) \\
+ \ & \frac{4m_N^3(-1 + t_1)(t_1 - x_2)}{M_B^4 t_1}\mathcal{A}_{123456}(x_i) + \frac{4m_N^3(-1 + t_1)(t_1 - x_2)}{M_B^4 t_1}\mathcal{T}_{125678}(x_i) \Bigg] \\
+ \ & \int_{t_0}^{1} dx_2 \int_0^{1-x_2} dx_1\, e^{-\frac{s_0}{M_B^2}} \Bigg[\left(\frac{2m_N t_0}{Q^2 + m_N^2 t_0^2}\right)(\mathcal{V}_{123} - \mathcal{T}_{123})(x_i) \\
- \ & \frac{2m_N t_0(-1 + 2t_0)}{Q^2 + m_N^2 t_0^2}(-\mathcal{A}_{123} + \mathcal{T}_{127})(x_i)
\end{aligned}
$$

$$
\begin{aligned}
&+ \quad \frac{4m_N^3 t_0}{Q^2+m_N^2 t_0^2}\left\{(-1+t_0)(-x_2+t_0)\left(\frac{2m_N^2 t_0^5}{(Q^2+m_N^2 t_0^2)^2}+\frac{1}{M_B^2}\right)\right.\\
&- \quad \left.\frac{t_0^2(4x_2-5(1+x_2))t_0+6t_0^2)}{(Q^2+m_N^2 t_0^2)}\right\}(\mathcal{A}_{123456}+\mathcal{T}_{125678})(x_i)\Bigg]\\
&+ \quad \int_{t_0}^1 dx_3\int_0^{1-x_3}dx_1\int_{t_0}^{x_3}dt_1 e^{-\frac{s(t_1,Q^2)}{M_B^2}}\left[-\frac{m_N}{M_B^2}(2\mathcal{V}_{123}+\mathcal{A}_{123})(x_i')\right.\\
&- \quad \frac{2m_N(-1+t_1)}{M_B^2 t_1}\mathcal{T}_{127}(x_i')\\
&+ \quad \left.\frac{m_N^3(-1+t_1)(t_1-x_3)}{M_B^4 t_1}(-2\mathcal{V}_{123456}-\mathcal{A}_{123456}+2\mathcal{T}_{125678})(x_i')\right]\\
&+ \quad \int_{t_0}^1 dx_3\int_0^{1-x_3}dx_1 e^{-\frac{s_0}{M_B^2}}\left[-\frac{m_N t_0^2}{Q^2+m_N^2 t_0^2}\,(2\mathcal{V}_{123}+\mathcal{A}_{123})(x_i')\right.\\
&- \quad \frac{2m_N t_0(-1+t_0)}{Q^2+m_N^2 t_0^2}\mathcal{T}_{127}(x_i')\\
&+ \quad \left(\frac{2m_N^5(-1+t_0)t_0^5(-x_3+t_0)}{(Q^2+m_N^2 t_0^2)^3}-\frac{m_N^3 t_0^3(4x_3-5(1+x_3)t_0+6t_0^2)}{(Q^2+m_N^2 t_0^2)^2}\right.\\
&+ \quad \left.\left.\frac{m_N^3(-1+t_0)t_0(-x_3+t_0)}{M_B^2(Q^2+m_N^2 t_0^2)}\right)(2\mathcal{V}_{123456}-\mathcal{A}_{123456}+2\mathcal{T}_{125678})(x_i')\right]\Bigg\},
\end{aligned}
\tag{4.22}
$$

$$
\begin{aligned}
C_5(Q^2) = \frac{1}{\sqrt{3}\lambda_\Delta}e^{\frac{m_\Delta^2}{M_B^2}}\Bigg\{&\\
\times \quad &\int_{t_0}^1 dx_2\int_0^{1-x_2}dx_1 e^{-\frac{s(x_2,Q^2)}{M_B^2}}\,m_N(-S_1+P_1-V_3+A_3)(x_i)\\
+ \quad &\int_{t_0}^1 dx_3\int_0^{1-x_3}dx_1 e^{-\frac{s(x_3,Q^2)}{M_B^2}}\,m_N\left(-V_3+\frac{A_3}{2}\right)(x_i')\\
+ \quad &\int_{t_0}^1 dx_2\int_0^{1-x_2}dx_1\int_{t_0}^{x_2}dt_1 e^{-\frac{s(t_1,Q^2)}{M_B^2}}\,\frac{m_N}{t_1}\\
\times \quad &\left[\left(2-\frac{Q^2+m_N^2(-1+2t_1)+s(t_1,Q^2)}{M_B^2}\right)\mathcal{V}_{123}(x_i)+\frac{m_N^2(t_1-x_2)}{M_B^2}T_{125678}(x_i)\right.\\
+ \quad &\left.\frac{Q^2+m_N^2(-1+2t_1)+s(t_1,Q^2)}{2M_B^2}(-2\mathcal{A}_{123}+\mathcal{T}_{123}+\mathcal{T}_{127})(x_i)\right]\\
+ \quad &\int_{t_0}^1 dx_2\int_0^{1-x_2}dx_1\; e^{-\frac{s_0}{M_B^2}}\,\frac{m_N t_0}{Q^2+m_N^2 t_0^2}\Bigg[+m_N^2 t_0(t_0-x_2)\mathcal{T}_{125678}(x_i)
\end{aligned}
$$

$$
\begin{aligned}
&(-m_N^2 + Q^2 + s(t_0, Q^2) + 2m_N^2 t_0)(-\mathcal{V}_{123} - \mathcal{A}_{123} + \mathcal{T}_{123} + \mathcal{T}_{127})(x_i)\Big] \\
+ &\int_{t_0}^{1} dx_3 \int_0^{1-x_3} dx_1 \int_{t_0}^{x_3} dt_1 e^{-\frac{s(t_1,Q^2)}{M_B^2}} \frac{m_N^3(t_1 - x_3)}{2M_B^2 t_1}(2\mathcal{V}_{123456}(x_i') - \mathcal{A}_{123456}(x_i')) \\
+ &\int_{t_0}^{1} dx_3 \int_0^{1-x_3} dx_1 e^{-\frac{s_0}{M_B^2}} \frac{m_N^3(t_0 - x_3)t_0}{2(Q^2 + M^2 t_0^2)}(2\mathcal{V}_{123456}(x_i') - \mathcal{A}_{123456}(x_i'))\Bigg\} \\
- &\frac{(m_N^2 - m_\Delta^2 + Q^2)}{2m_N^2} C_4(Q^2, M_B^2),
\end{aligned} \tag{4.23}
$$

$$
\begin{aligned}
&C_6(Q^2) = \frac{m_N^2}{\sqrt{3}\lambda_\Delta} e^{\frac{m_\Delta^2}{M_B^2}} \Bigg\{ \int_{t_0}^{1} dx_2 \int_0^{1-x_2} dx_1 \int_{t_0}^{x_2} dt_1 e^{-\frac{s(t_1,Q^2)}{M_B^2}} \\
&\Bigg[\frac{-2m_N(-1+t_1)}{M_B^2 t_1}(-2\mathcal{A}_{123} + \mathcal{T}_{123})(x_i) + \frac{-2m_N(-1+t_1)(-1+2t_1)}{M_B^2 t_1^2}\mathcal{T}_{127}(x_i) \\
+ &\frac{2m_N^3(2(-1+t_1)^2 t_1 - (1+2(-2+t_1)t_1)x_2)}{M_B^4 t_1^2}(\mathcal{A}_{123456} + \mathcal{T}_{125678})(x_i)\Bigg] \\
+ &\int_{t_0}^{1} dx_2 \int_0^{1-x_2} dx_1 e^{-\frac{s_0}{M_B^2}} \Bigg[\frac{4m_N(-1+t_0)t_0}{Q^2 + m_N^2 t_0^2}\mathcal{A}_{123}(x_i) \\
- &2\frac{m_N(-1+t_0)}{Q^2 + m_N^2 t_0^2}\mathcal{T}_{123}(x_i) - \frac{2m_N(-1+t_0)(-1+2t_0)}{Q^2 + m_N^2 t_0^2}\mathcal{T}_{127}(x_i) \\
+ &\Bigg(\frac{8m_N^5(-1+t_0)^2 t_0^4(-x_2+t_0)}{(Q^2 + m_N^2 t_0^2)^3} - \frac{4m_N^3(-1+t_0)t_0^2(3x_2 + t_0(-4-5x_2+6t_0))}{(Q^2 + m_N^2 t_0^2)^2} \\
+ &\frac{4m_N^3(-1+t_0)^2(-x_2+t_0)}{M_B^2(Q^2 + m_N^2 t_0^2)}\Bigg)(\mathcal{A}_{123456} + \mathcal{T}_{125678})(x_i)\Bigg] \\
+ &\int_{t_0}^{1} dx_3 \int_0^{1-x_3} dx_1 \int_{t_0}^{x_3} dt_1 e^{-\frac{s(t_1,Q^2)}{M_B^2}} \frac{m_N(1-t_1)}{M_B^2 t_1} \\
&\Bigg[\mathcal{A}_{123}(x_i') + \frac{1}{t_1}\mathcal{T}_{123}(x_i') + \frac{(-1+2t_1)}{t_1}\mathcal{T}_{127}(x_i') \\
+ &\frac{2m_N^2(1-t_1)(t_1 - x_3)}{M_B^2 t_1}(\mathcal{V}_{123456} - \frac{1}{2}\mathcal{A}_{123456} + \mathcal{T}_{125678})(x_i')\Bigg] \\
+ &\int_{t_0}^{1} dx_3 \int_0^{1-x_3} dx_1 e^{-\frac{s_0}{M_B^2}} \frac{m_N(-1+t_0)}{Q^2 + m_N^2 t_0^2} \\
\times &\Bigg[t_0\mathcal{A}_{123}(x_i') + \mathcal{T}_{123}(x_i') - (-1+2t_0)\mathcal{T}_{127}(x_i') \\
+ &2m_N^2\Bigg(\frac{2m_N^2(-1+t_0)t_0^4(-x_3+t_0)}{(Q^2 + m_N^2 t_0^2)^2} - \frac{t_0^2(3x_3 + t_0(-4-5x_3+6t_0))}{(Q^2 + m_N^2 t_0^2)} \\
+ &\frac{(-1+t_0)(-x_3+t_0)}{M_B^2}\Bigg)(\mathcal{V}_{123456} - \frac{1}{2}\mathcal{A}_{123456} + \mathcal{T}_{125678})(x_i')\Bigg]\Bigg\},
\end{aligned} \tag{4.24}
$$

where following [26], the following shorthand notations for various combinations of

the DA's are employed:

$$\begin{aligned}
\mathcal{T}_{234578} &= T_2 - T_3 - T_4 + T_5 + T_7 + T_8, \\
\mathcal{T}_{123} &= T_1 + T_2 - 2T_3, \\
\mathcal{T}_{127} &= T_1 - T_2 - 2T_7, \\
\mathcal{T}_{125678} &= -T_1 + T_2 + T_5 - T_6 + 2T_7 + 2T_8, \\
\mathcal{V}_{123} &= V_1 - V_2 - V_3, \\
\mathcal{V}_{123456} &= -V_1 + V_2 + V_3 + V_4 + V_5 - V_6, \\
\mathcal{A}_{123} &= A_1 - A_2 + A_3, \\
\mathcal{A}_{123456} &= A_1 - A_2 + A_3 + A_4 - A_5 + A_6,
\end{aligned} \tag{4.25}$$

and

$$\begin{aligned}
\mathcal{F}(x_i) &= \mathcal{F}(x_1, x_2, 1 - x_1 - x_2), \\
\mathcal{F}(x'_i) &= \mathcal{F}(x_1, 1 - x_1 - x_3, x_3).
\end{aligned} \tag{4.26}$$

The Borel transformation and the continuum subtraction are performed using the following substitutions in Minkowski space (see [25, 26]):

$$\begin{aligned}
\int dt \frac{\rho(t)}{(q - tp)^2} &= -\int_0^1 \frac{dt}{t} \frac{\rho(t)}{s - p'^2} \Rightarrow -\int_{t_0}^1 \frac{dt}{t} \rho(t) e^{-\frac{s}{M_B^2}}, \\
\int dt \frac{\rho(t)}{(q - tp)^4} &= \int_0^1 \frac{dt}{t^2} \frac{\rho(t)}{(s - p'^2)^2} \Rightarrow \frac{1}{M_B^2} \int_{t_0}^1 \frac{dt}{t^2} \rho(t) e^{-\frac{s}{M_B^2}} + \frac{\rho(t_0) e^{-\frac{s_0}{M_B^2}}}{Q^2 + t_0^2 m_N^2}, \\
\int dt \frac{\rho(t)}{(q - tp)^6} &= -\int_0^1 \frac{dt}{t^3} \frac{\rho(t)}{(s - p'^2)^3} \Rightarrow -\frac{1}{2M_B^4} \int_{t_0}^1 \frac{dt}{t^3} \rho(t) e^{-\frac{s}{M_B^2}} \\
&\quad - \frac{\rho(t_0) e^{-\frac{s_0}{M_B^2}}}{2t_0 (Q^2 + t_0^2 m_N^2) M_B^2} \\
&\quad + \frac{t_0^2}{2(Q^2 + t_0^2 m_N^2)} \left[\frac{d}{dt_0} \frac{\rho(t_0)}{t_0 (Q^2 + t_0^2 m_N^2)} \right] e^{-\frac{s_0}{M_B^2}}, \\
s(t, Q^2) &= (1 - t) M^2 + \frac{(1 - t)}{t} Q^2, \\
t_0(s_0, Q^2) &= \frac{\sqrt{(Q^2 + s_0 - m_N^2)^2 + 4 m_N^2 Q^2} - (Q^2 + s_0 - m_N^2)}{2 m_N^2},
\end{aligned} \tag{4.27}$$

where $Q^2 = -q^2$ and t_0 is the solution of the $s(t_0, Q^2) = s_0$. The terms $\sim e^{-\frac{s_0}{M_B^2}}$ are the

so-called surface terms which appear in successive partial integrations to reduce the power of denominators.

4.1.2 Numerical Analysis

From explicit expressions of the sum rules for the axial $N-\Delta$ transition form factors, it follows that the main input parameters are the nucleon distribution amplitudes (DA's). In general, these distribution amplitudes contain hadronic parameters which should be determined by some means. Various methods to determine these parameters give different results. In this work, we considered all three different determinations of these parameters: a) QCD sum rules based DA's, where corrections to the DA's are taken into account and the parameters in DA's are determined from QCD sum rules, b) A model for nucleon DA's where parameters are chosen in a such way that the nucleon electromagnetic and axial form factors are described well within LCQSR and c) Asymptotic forms of DA's of all twists (see for example [25]). The explicit expressions of corresponding DA's can be found in [25] and for completeness we present their expressions in Appendix–A. In this Appendix, the values of the hadronic parameters obtained from three different methods (three sets) are also presented.

For the numerical evaluation of the sum rules for the $N-\Delta$ transition form factors, we need also specify the values of the residue of Δ baryon λ_Δ, the continuum threshold s_0 and Borel parameter M_B^2. The residue λ_Δ and s_0 are determined from analysis of the mass sum rules: $\lambda_\Delta = 0.038\ GeV^3$ and $s_0 = 2.6 - 3\ GeV^2$ [40, 41, 42, 43, 44] which we have used in numerical calculations. The Borel mass parameter M_B^2 is the auxiliary parameter of sum rules. Therefore, we need to find a suitable region of M_B^2, where physical results are independent of this parameter. A suitable region of M_B^2 is determined in the following way. From one side, M_B^2 has to be small enough in order to guarantee suppression of higher resonances and the continuum contributions to the correlation function and from other side, it should be large enough in order to guarantee convergence of the light cone expansion with increasing twist in QCD calculation.

In Figs. 4.1, 4.2, 4.3, and 4.4, we present the dependence of the form factors $C_3(Q^2)$, $C_4(Q^2)$, $C_5(Q^2)$ and $C_6(Q^2)$ on M_B^2 for first set of DA's with two fixed values of s_0 and three fixed values of Q^2 respectively. From these figures it follows that all considered form factors exhibit good stability with respect to variation of M_B^2 in the region $1.2\ GeV^2 \leq M_B^2 \leq 2\ GeV^2$, so this region of M_B^2 can be considered as a working region where form factors are practically independent of M_B^2. We performed similar analysis for the two other sets of DA's and obtained that within the above mentioned region of M_B^2, the form factors are rather stable to variation of M_B^2.

In Figs. 4.5, 4.6, 4.7 and 4.8, we present the dependence of the form factors $C_i(Q^2)$, $i = 3, 4, 5, 6$ on Q^2 at fixed values of M_B^2 and s_0 for all three sets of DA's. From these figures, we see that form factors are very sensitive to the choice of DA's. For form factor $C_3(Q^2)$, the sets 2 and 3 lead to the same result, for $C_4(Q^2)$ and $C_5(Q^2)$ form factors, the sets 1 and 2 give results which are very close to each other and for $C_6(Q^2)$ up to $Q^2 = 4\ GeV^2$ all sets of DA's lead to the different results and when $Q^2 \geq 4\ GeV^2$ all three sets of DA's lead to indistinguishable predictions. Our results on form factors $C_4(Q^2)$ and $C_5(Q^2)$ for three sets of DA's satisfy the relation $C_4(Q^2) = C_5(Q^2)/4$ assumed in the experimental analysis.

Figs. 4.7 and 4.8 contain also the predictions of lattice calculations from [36]. The points correspond to the values obtained using a hybrid action and assuming $Z_A = 1.1$ (see [36] for details of the notation). Note that, due to different conventions used, the lattice results has been multiplied with $\sqrt{2/3}$. From the figures, it is seen that there is a good agreement between the lattice results and our predictions within error bars. Note also that, the biggest difference between sum rules predictions and lattice calculations is seen in $C_5(Q^2)$ when the asymptotic distributions are used, i.e. when the hadronic parameters from Set 3 are used.

And finally, in Fig. 4.9, $R(Q^2)$ is plotted as a function of Q^2. The function $R(Q^2)$ is defined as:

$$R(Q^2) = \frac{C_6^A(Q^2)}{C_5^A(Q^2)} \frac{Q^2 + m_\pi^2}{m_N^2} \tag{4.28}$$

From Eq. (4.3), it is seen that, assuming PCAC and pion dominance, $R(Q^2) = 1$. From

Fig. 4.9, it is seen that at $Q^2 \simeq 1.5\ GeV$, PCAC and pion dominance approximations are valid. But for larger values of Q^2, $R(Q^2)$ deviates considerable from unity, and hence we may conclude that PCAC and pion dominance assumptions break down.

As we have already noted, the axial form factors for the $\Delta \rightarrow N$ transition have also been calculated in the framework of the constituent quark model in [37]. Our predictions on these form factors differ from the results of [37].

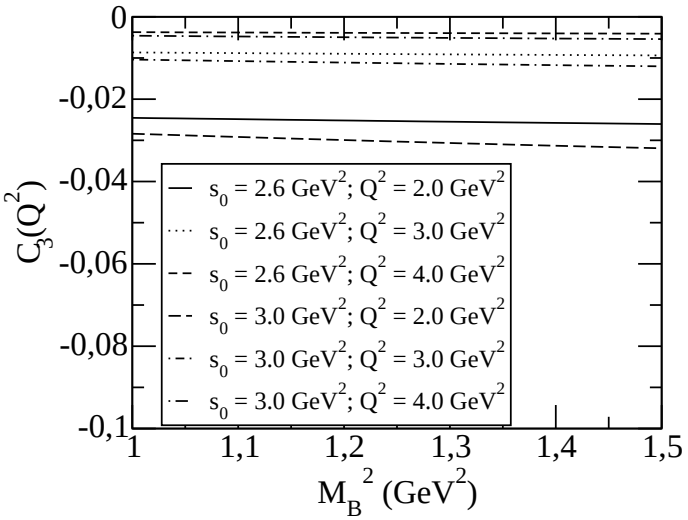

Figure 4.1: The dependence of the form factor $C_3(Q^2)$ on the Borel parameter squared M_B^2 for the values of the continuum threshold $s_0 = 2.6\ GeV^2$ and $s_0 = 3.0\ GeV^2$ and at the values of $Q^2 = 3 \pm 1\ GeV^2$.

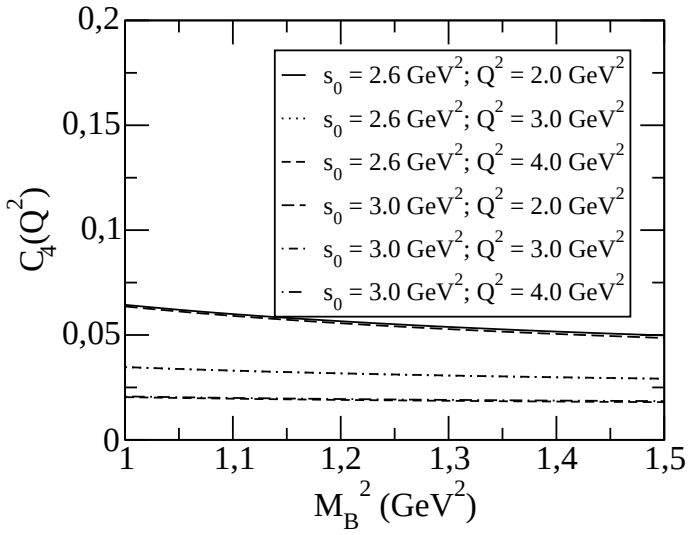

Figure 4.2: The same as Fig. 4.1 but for the form factor $C_4(Q^2)$.

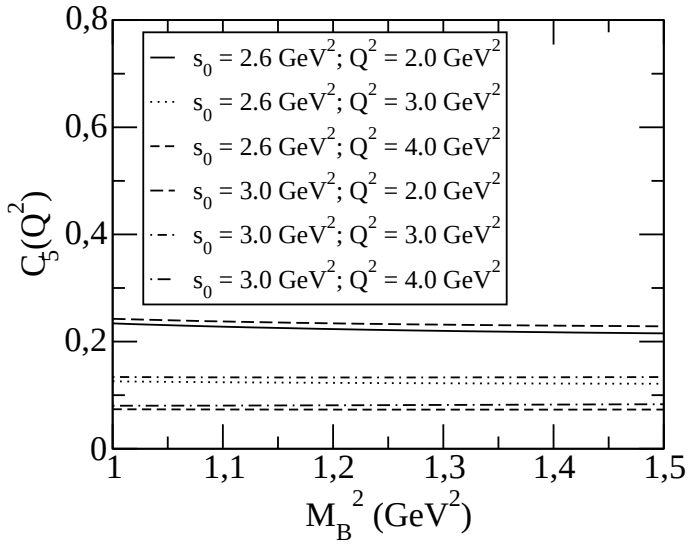

Figure 4.3: The same as Fig. 4.1 but for the form factor $C_5(Q^2)$.

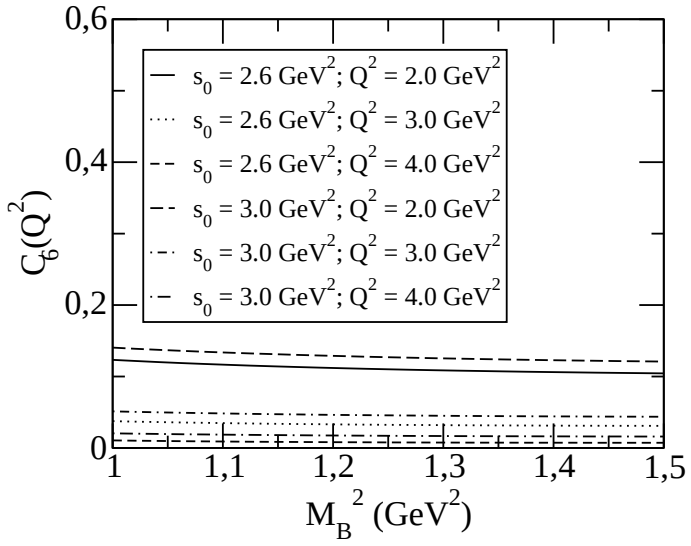

Figure 4.4: The same as Fig. 4.1 but for the form factor $C_6(Q^2)$.

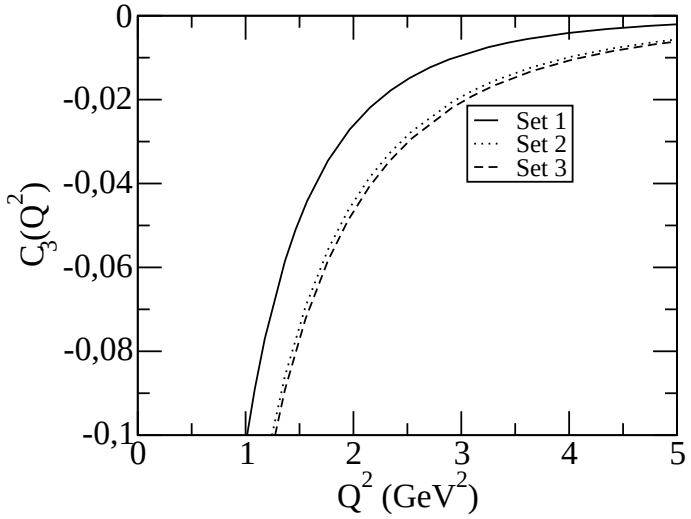

Figure 4.5: The dependence of the form factor $C_3(Q^2)$ on Q^2 for three different sets of distribution amplitudes at the continuum threshold $s_0 = 2.6\ GeV^2$ and the Borel parameter $M_B^2 = 1.5\ GeV^2$.

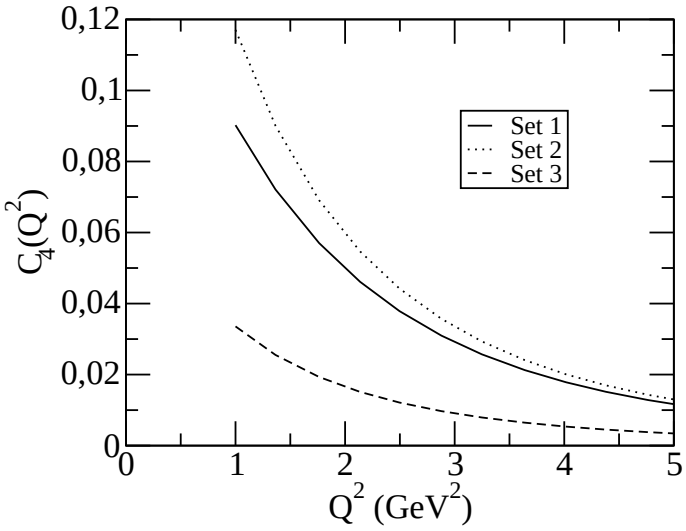

Figure 4.6: The same as Fig. 4.5 but for the form factor $C_4(Q^2)$.

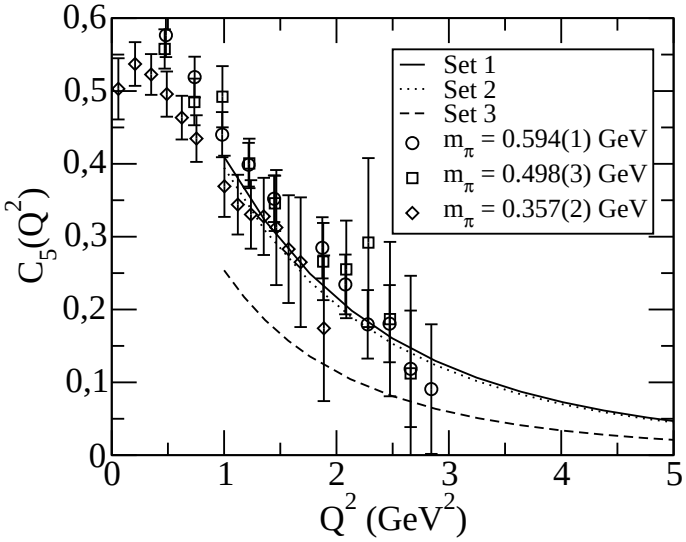

Figure 4.7: The same as Fig. 4.5 but for the form factor $C_5(Q^2)$. Results from the lattice are also shown.

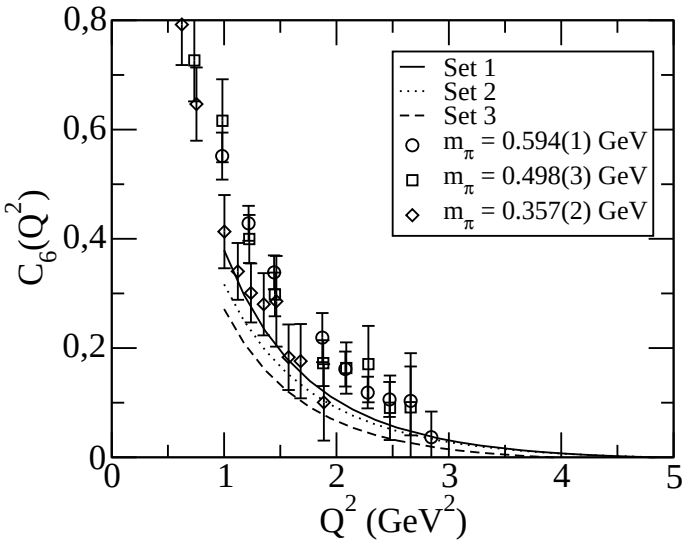

Figure 4.8: The same as Fig. 4.7 but for the form factor $C_6(Q^2)$.

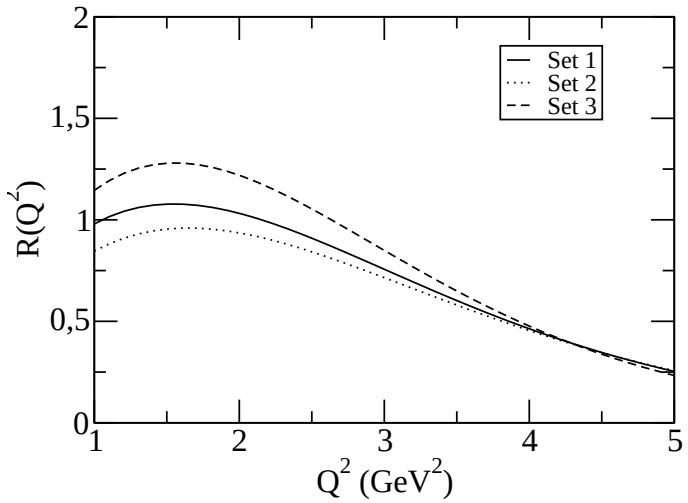

Figure 4.9: The dependence of $R(Q^2)$ as a function of Q^2 for the three sets of DA's.

4.2 Nucleon Electromagnetic Form Factors

The internal structure of the nucleons are usually described in terms of the electromagnetic Dirac and Pauli form factors $F_1(q^2)$ and $F_2(q^2)$ or equivalently the electric and magnetic dipole Sachs form factors $G_E(q^2)$ and $G_M(q^2)$, respectively (for a recent status of experiments and phenomenology of the form factors see [46]).

Until a few years ago, the nucleon electromagnetic form factors are studied in unpolarized elastic electron-nucleon scattering through a virtual photon exchange. It is shown in the pioneering work [47] that the polarization effects, i.e., scattering of polarized electrons from polarized targets, can play essential role for a more accurate determination of the nucleon electromagnetic form factors. The main result of [47] is that, unlike the unpolarized elastic cross section, which is proportional to the sum of the squares of the form factors, the polarized cross section contains also interference terms of the form factors $G_E(q^2)$ and $G_M(q^2)$. Studying various polarization observables allows more accurate determination of these form factors.

Recent developments in experimental instruments allow to produce polarized electron beams and polarized protons, which gives the opportunity for a more precise separation of the $G_E(q^2)$ and $G_M(q^2)$ form factors. The electron-proton scattering experiments, which are performed at Jefferson Laboratory using the polarized electrons and polarized proton, show strong deviation from the theoretical predictions [48, 49, 50, 51], i.e., the ratio $F_2(q^2)/F_1(q^2)$ does not behave as is expected from previous experiments and as is predicted by the perturbative QCD (for a review see [52] and references therein). For understanding this unexpected result, the model-independent, non-perturbative, more attractive and powerful QCD sum rules method can be used. In the next subsection, we calculate the electromagnetic form factors of nucleon using the LCQSR and most general form of the interpolating current for nucleon. In this approach, the form factors of the nucleons are expressed in terms of distribution amplitude of the nucleon. Note that, this problem is investigated for the Ioffe current in the framework of the LCQSR in [26] and the traditional sum rules in [53]. In [25], an improved version of the Chernyak-Zhitnitsky current is used.

4.2.1 Electromagnetic Form Factors of Nucleon in LCQSR

The electromagnetic form factors of nucleon are defined by the matrix element of the electromagnetic current J_λ^{el} between the initial and final nucleon states $\langle N(p') \mid J_\lambda^{el} \mid N(p)\rangle$. The most general form of this matrix element satisfying the Lorentz invariance and electromagnetic current conservation is

$$\langle N(p') \mid J_\lambda^{el}(0) \mid N(p)\rangle = \bar{N}(p')\left[\gamma_\lambda F_1(Q^2) - \frac{i}{2m_N}\sigma_{\lambda\nu}q^\nu F_2(Q^2)\right]N(p), \tag{4.29}$$

where $Q^2 = -q^2$, is the negative of the square of the virtual photon momentum, $q = p - p'$ and F_1 and F_2 are the Dirac and Pauli form factors, respectively.

Another set of nucleon form factors is the so called Sachs form factors, which are defined in terms of the $F_1(Q^2)$ and $F_2(Q^2)$ as follows:

$$\begin{aligned} G_M(Q^2) &= F_1(Q^2) + F_2(Q^2), \\ G_E(Q^2) &= F_1(Q^2) - \frac{Q^2}{4m_N^2}F_2(Q^2), \end{aligned} \tag{4.30}$$

At the static limit, $Q^2 = 0$, $G_E^P(0) = 1$, $G_E^n(0) = 0$, $G_M^P(0) = \mu_P = 2.792847337(29)$ and $G_M^n(0) = \mu_n = -1.91304272(45)$, where μ_P and μ_n are the anomalous magnetic moments of the proton and neutron in units of the Bohr magneton.

Analysis of the experimental results (for review see [52] and references therein) lead that the magnetic form factors of the nucleon are very well described by the dipole formula

$$G_M^{n,p}(Q^2) = \frac{\mu_{n,p}}{\left(1 + \frac{Q^2}{(0.71\ GeV)^2}\right)^2} = \mu_{n,p}G_D. \tag{4.31}$$

The measured values of the electric form factors of the neutron are given in [54, 55].

After these preliminary remarks, we proceed to calculate the electromagnetic form factors of nucleon in LCQSR. The basic object of the LCQSR is a suitably chosen correlation function. In this study, it is chosen as:

$$\Pi_\lambda(p,q) = i\int d^4x e^{iqx}\langle 0 \mid T\{J^N(0)J_\lambda^{el}(x)\} \mid N(p)\rangle, \tag{4.32}$$

which describes the transition of the nucleon $N(p)$ to the nucleon $N(p-q)$ via the EM current. The interpolating current for the nucleon is chosen as

$$J^N(x) = 2\varepsilon^{abc}\sum_{\ell=1}^{2}(u^{Ta}(x)CA_1^\ell d^b(x))A_2^\ell u^c(x), \tag{4.33}$$

where $A_1^1 = I$, $A_1^2 = A_2^1 = \gamma_5$, $A_2^2 = \beta$, and C is the charge conjugation operator, and a, b, c are the color indices. The electromagnetic current is:

$$J_\lambda^{el}(x) = e_u\bar{u}\gamma_\lambda u + e_d\bar{d}\gamma_\lambda d, \tag{4.34}$$

and the choice $\beta = -1$ corresponds to the Ioffe current.

Let us first calculate the physical part of the correlator (4.32). The contribution of the nucleon to the correlation function (4.32) is given by

$$\Pi_\lambda(p,q) = \sum_s \frac{\langle 0 \mid J^N(0) \mid N(p',s)\rangle\langle N(p',s) \mid J_\lambda^{el}(0) \mid N(p)\rangle}{m_N^2 - p'^2}. \tag{4.35}$$

The matrix element $\langle 0 \mid J^N(0) \mid N(p',s)\rangle$ in (4.35) is determined as:

$$\langle 0 \mid J^N(0) \mid N(p',s)\rangle = \lambda_N N(p',s), \tag{4.36}$$

where λ_N is the coupling constant of the nucleon to the current $J^N(0)$. The matrix element $\langle N(p',s) \mid J_\lambda^{el}(0) \mid N(p)\rangle$ is parameterized in terms of the form factors F_1 and F_2 via Eq. (4.29). Summing over spins of the nucleons

$$\sum_s N(p',s)\overline{N}(p',s) = \not{p}' + m_N, \tag{4.37}$$

and using Eqs. (4.29), (4.35) and (4.36), we obtain the following expression for the contribution of nucleon to the correlation function

$$\Pi_\lambda(p,q) = \frac{\lambda_N}{m_N^2 - p'^2}(\not{p}' + m_N)\left[\gamma_\lambda F_1(Q^2) - \frac{i}{2m_N}\sigma_{\lambda\nu}q^\nu F_2(Q^2)\right]N(p) + \cdots \tag{4.38}$$

where $\cdots$ stand for the contributions to the correlation functions from the higher states and continuum. It follows from expression (4.38) that, the correlation function contains numerous structures and in principle all of them can be used in determination of the electromagnetic form factors of nucleons. In further analysis, we choose the independent structures containing p_λ, and $p_\lambda \not{q}$ for obtaining F_1 and F_2, respectively.

The theoretical part of this correlator can also be calculated in LCQSR in deep Euclidean region $p'^2 = (p-q)^2 << 0$ in terms of the nucleon DA's. Using the explicit expression for the currents and carrying out all contractions, the correlation function takes the form

$$\begin{aligned}(\Pi_\lambda)_\rho &= \frac{i}{2}\int d^4x e^{iqx}\sum_{\ell=1}^{2}\Big\{ \\ &\quad e_u(CA_1^\ell)_{\alpha\gamma}\Big[A_2^\ell S_u(-x)\gamma_\lambda\Big]_{\rho\phi}4\epsilon^{abc}\langle 0|u_\alpha^a(0)u_\phi^b(x)d_\gamma^c(0)|N(p)\rangle \\ &+ e_u(A_2^\ell)_{\rho\alpha}\Big[(CA_1^\ell)^T S_u(-x)\gamma_\lambda\Big]_{\gamma\phi}4\epsilon^{abc}\langle 0|u_\alpha^a(0)u_\phi^b(x)d_\gamma^c(0)|N(p)\rangle \\ &+ e_d(A_2^\ell)_{\rho\phi}\Big[CA_1^\ell S_d(-x)\gamma_\lambda\Big]_{\alpha\gamma}4\epsilon^{abc}\langle 0|u_\alpha^a(0)u_\phi^b(0)d_\gamma^c(x)|N(p)\rangle\Big\}, \quad (4.39)\end{aligned}$$

in x representation, where λ is a Lorentz index, and α, γ, ρ and ϕ are spinor indices. Using the expressions for the light quark propagators in Eqs. (4.13)-(4.14) and nucleon DA's in Eq. (4.15) as presented in the previous section, the QCD side of the correlation function is obtained. Omitting the details of calculations of the theoretical part, choosing the coefficients of the structures p_λ, and $p_\lambda \not{q}$, equating both representation of the correlation function and applying the Borel transformation with respect to the variable $p'^2 = (p-q)^2$, which suppress the contributions of the higher states and continuum, we obtain following sum rules for the form factors F_1 and F_2:

$$\begin{aligned}&F_1(Q^2) = \frac{-1}{2\lambda_N}e^{m_N^2/M_B^2} \\ &\Big\{e_u m_N\int_{t_0}^{1}dx_2\int_0^{1-x_2}dx_1 e^{-s(x_2,Q^2)/M_B^2}\Big[2\mathcal{H}_{5,-7}(x_i)(1-\beta) \\ &+4(\mathcal{H}_{17}(x_i)-2\mathcal{H}_{19}(x_i))(1+\beta)\,] \\ &+ e_u m_N\int_{t_0}^{1}dx_2\int_0^{1-x_2}dx_1\int_{t_0}^{x_2}\frac{dt_1}{t_1}e^{-s(t_1,Q^2)/M_B^2}\Big(\\ &-2\Big[\mathcal{H}_{20,-18}(x_i)(1+\beta)-\mathcal{H}_6(x_i)(-1+\beta)\Big] \\ &-\frac{1}{M_B^2}\Big[\Big\{2\mathcal{H}_{20,18}(x_i)(1+\beta)(Q^2+s(t_1,Q^2)+m_N^2(-1+t_1))\Big\}\end{aligned}$$

$$
\begin{aligned}
&+m_N^2\{\mathcal{H}_{15,-14}(x_i)t_1(1-\beta)-4\mathcal{H}_{21,24}(x_i)t_1(1+\beta)\\
&+2\mathcal{H}_{10}(x_i)(-1+\beta)(t_1-x_2)+2(\mathcal{H}_{16}(x_i)(-1+\beta)+2\mathcal{H}_{24}(x_i)(1+\beta))x_2\}\ \Big]\Big)\\
-\ & e_u m_N\int_{t_0}^1 dx_2\int_0^{1-x_2} dx_1 e^{-s_0/M_B^2}\\
&\frac{t_0}{Q^2+m_N^2t_0^2}\Big(2\mathcal{H}_{20,18}(x_i)(1+\beta)(Q^2+s_0+m_N^2(-1+t_0))\\
&+m_N^2\Big[\{\mathcal{H}_{-8,9}(x_i)(1-\beta)-(3\mathcal{H}_{21,24}(x_i)+8\mathcal{H}_{23}(x_i))(1+\beta)\}t_0\\
&+2\mathcal{H}_{10}(x_i)(-1+\beta)(t_0-x_2)+2(\mathcal{H}_{16}(x_i)(-1+\beta)+\mathcal{H}_{24}(x_i)(1+\beta))x_2\Big]\Big)\\
&+e_d\eta_1'(Q^2,\beta)+e_u\eta_1(Q^2,\beta)\Big\},
\end{aligned}
\tag{4.40}
$$

$$
\begin{aligned}
&F_2(Q^2)=\frac{-m_N}{\lambda_N}e^{m_N^2/M_B^2}\\
&\Big\{e_u\int_{t_0}^1 dx_2\int_0^{1-x_2} dx_1 e^{-s(x_2,Q^2)/M_B^2}\left[\frac{2\mathcal{H}_5(x_i)(-1+\beta)}{x_2}\right](x_i)\\
&-e_u m_N^2\int_{t_0}^1 dx_2\int_0^{1-x_2} dx_1\int_{t_0}^{x_2}\frac{dt_1}{t_1}e^{-s(t_1,Q^2)/M_B^2}\Big(\\
&\frac{1}{M_B^2}\Big[\mathcal{H}_{8,-9}(x_i)(1-\beta)+2(\mathcal{H}_{18,20}(x_i)+2\mathcal{H}_{21,22}(x_i)+4\mathcal{H}_{23}(x_i))(1+\beta)\Big]\\
&-\frac{4}{M_B^2t_1}\Big[\mathcal{H}_{22}(x_i)(1+\beta)x_2\Big]\Big)\\
+\ & e_u m_N^2\int_{t_0}^1 dx_2\int_0^{1-x_2} dx_1 e^{-s_0/M_B^2}\Big(\frac{1}{Q^2+m_N^2t_0^2}\Big[\mathcal{H}_{8,-9}(x_i)(-1+\beta)t_0\\
&-2(\mathcal{H}_{18,20}(x_i)+2\mathcal{H}_{21,22}(x_i)+4\mathcal{H}_{23}(x_i))(1+\beta)t_0+4\mathcal{H}_{22}(x_i)(1+\beta)x_2\Big]\Big)\\
&+e_d\eta_2'(Q^2,\beta)+e_u\eta_2(Q^2,\beta)\Big\},
\end{aligned}
\tag{4.41}
$$

where

$$
\begin{aligned}
\mathcal{F}(x_i) &= \mathcal{F}(x_1,x_2,1-x_1-x_2),\\
\mathcal{F}(x_i') &= \mathcal{F}(x_1,1-x_1-x_3,x_3),\\
s(y,Q^2) &= (1-y)m_N^2+\frac{(1-y)}{y}Q^2,
\end{aligned}
\tag{4.42}
$$

with $t_0(s_0, Q^2)$ being solution of the equation $s(t_0, Q^2) = s_0$, and

$$
\begin{aligned}
&\eta_1(Q^2,\beta) = m_N \left\{ \int_{t_0}^{1} dx_3 \int_{0}^{1-x_3} dx_1 e^{-s(x_3,Q^2)/M_B^2} \right. \\
&\left[(\mathcal{H}_{1,17,3}(x_i) - 2\mathcal{H}_{19}(x_i))(1+\beta) + \mathcal{H}_{13,7}(x_i)(-1+\beta) \right] \\
&+ \int_{t_0}^{1} dx_3 \int_{0}^{1-x_3} dx_1 \int_{t_0}^{x_3} dt_1 e^{-s(t_1,Q^2)/M_B^2} \Bigg(\\
&\frac{1}{M_B^4 t_1} \left[-\mathcal{H}_{22}(x_i) m_N^2 (-m_N^2 + Q^2 + s(t_1,Q^2))(1+\beta) x_3 \right] \\
&+ \frac{1}{M_B^4} \left[\mathcal{H}_{22}(x_i) m_N^2 (m_N^2(-1+2t_1-2x_3) + Q^2 + s(t_1,Q^2))(1+\beta) \right] \\
&+ \frac{1}{2M_B^2 t_1} \Big[-(m_N^2 - Q^2 - s(t_1,Q^2)) \{ (\mathcal{H}_{18}(x_i) - 3\mathcal{H}_{20}(x_i))(1+\beta) \\
&2\mathcal{H}_{6,12}(x_i)(-1+\beta) \} + 2(2\mathcal{H}_{22}(x_i) - \mathcal{H}_{24}(x_i)) m_N^2 (1+\beta) x_3 \Big] \\
&+ \frac{1}{M_B^2} \Big[m_N^2 \{ \mathcal{H}_{-12,15,-6,9}(x_i)(1-\beta) + (\mathcal{H}_{18,-2,24,4,21}(x_i) \\
&+ 2\mathcal{H}_{-20,-22,23}(x_i))(1+\beta) \} \Big] \\
&+ \frac{1}{t_1} \left[\mathcal{H}_{12,6}(x_i)(1-\beta) + \mathcal{H}_{-18,20}(x_i)(1+\beta) \right] \Bigg) \\
&+ \int_{t_0}^{1} dx_3 \int_{0}^{1-x_3} dx_1 e^{-s_0/M_B^2} \Bigg(\\
&\frac{1}{M_B^2 t_0 (Q^2 + m_N^2 t_0^2)} \left[\mathcal{H}_{22}(x_i) m_N^2 (1+\beta) t_0^2 (Q^2 + s_0 + m_N^2(-1+2t_0))(t_0 - x_3) \right] \\
&+ \frac{1}{(Q^2 + m_N^2 t_0^2)^3} \left[2\mathcal{H}_{22}(x_i) m_N^4 (1+\beta) t_0^4 (Q^2 + s_0 + m_N^2(-1+2t_0))(t_0 - x_3) \right] \\
&- \frac{1}{(Q^2 + m_N^2 t_0^2)^2} \Big[\mathcal{H}_{22}(x_i) m_N^2 (1+\beta) t_0^2 ((Q^2 + s_0)(2t_0 - x_3) \\
&+ m_N^2 (2t_0(-1+3t_0-2x_3) + x_3)) \Big] \\
&+ \frac{1}{t_0 (Q^2 + m_N^2 t_0^2)} \left[2\mathcal{H}_{22}(x_i) m_N^2 (1+\beta) t_0^2 x_3 \right] + \frac{1}{2(Q^2 + m_N^2 t_0^2)} \Big[\\
&-\mathcal{H}_{20}(x_i)(1+\beta) t_0 \{ 3(Q^2 + s_0) + m_N^2(-3+4t_0) \} \\
&+ 2\mathcal{H}_{6,12}(x_i)(-1+\beta)(Q^2 + s_0 + m_N^2(-1+t_0)) t_0
\end{aligned}
$$

$$
\begin{aligned}
&+2\mathcal{H}_{24}(x_i)m_N^2(1+\beta)t_0(t_0-x_3)\\
&+2\mathcal{H}_{18}(x_i)(1+\beta)t_0(Q^2+s_0+m_N^2(-1+2t_0))\\
&+2m_N^2\mathcal{H}_{9,-15}(x_i)(-1+\beta)t_0^2+2m_N^2(\mathcal{H}_{4,-2,21}(x_i)\\
&+2\mathcal{H}_{23,-22}(x_i))(1+\beta)t_0^2\Big]\Big)\Big\},
\end{aligned}
\tag{4.43}
$$

$$
\begin{aligned}
&\eta_2(Q^2,\beta)=\int_{t_0}^{1}dx_3\int_0^{1-x_3}dx_1e^{-s(x_3,Q^2)/M_B^2}\left[\frac{\mathcal{H}_{11,-5}(x_i)(-1+\beta)}{x_3}\right]\\
&+m_N\int_{t_0}^{1}dx_3\int_0^{1-x_3}dx_1\int_{t_0}^{x_3}dt_1e^{-s(t_1,Q^2)/M_B^2}\Bigg(\frac{-2}{M_B^4}\left[\mathcal{H}_{22}(x_i)m_N^3(1+\beta)\right]\\
&+\frac{1}{M_B^4t_1}\left[\mathcal{H}_{22}(x_i)m_N(1+\beta)(-Q^2-s(t_1,Q^2)+m_N^2(1+2x_3))\right]\\
&+\frac{1}{M_B^4t_1^2}\left[\mathcal{H}_{22}(x_i)m_N(1+\beta)(Q^2+s(t_1,Q^2)-m_N^2)x_3\right]\\
&-\frac{3}{M_B^2t_1^2}\left[\mathcal{H}_{22}(x_i)m_N(1+\beta)x_3\right]+\frac{m_N}{M_B^2t_1}\Big[\mathcal{H}_{12,15,6,-9}(x_i)(-1+\beta)\\
&+(\mathcal{H}_{2,-20,-21,-4}(x_i)+3\mathcal{H}_{22}(x_i)-2\mathcal{H}_{23}(x_i))(1+\beta)\Big]\Bigg)\\
&+m_N\int_{t_0}^{1}dx_3\int_0^{1-x_3}dx_1e^{-s_0/M_B^2}\Bigg(\\
&-\frac{m_N}{M_B^2(Q^2+m_N^2t_0^2)}\left[\mathcal{H}_{22}(x_i)(1+\beta)(Q^2+s_0+m_N^2(-1+2t_0))(t_0-x_3)\right]\\
&+\frac{1}{(Q^2+m_N^2t_0^2)^3}\left[-2\mathcal{H}_{22}(x_i)m_N^3(1+\beta)t_0^3(Q^2+s_0+m_N^2(-1+2t_0))(t_0-x_3)\right]\\
&+\frac{1}{(Q^2+m_N^2t_0^2)^2}\left[\mathcal{H}_{22}(x_i)m_N(1+\beta)t_0^2(Q^2+s_0+m_N^2(-1+4t_0-2x_3))\right]\\
&+\frac{m_N}{(Q^2+m_N^2t_0^2)}\Big[\mathcal{H}_{-12,-15,-6,9}(x_i)(1-\beta)+(\mathcal{H}_{2,-20,-21,22,-4}(x_i)\\
&-2\mathcal{H}_{23}(x_i))(1+\beta)t_0-\mathcal{H}_{22}(x_i)(1+\beta)(3x_3-2t_0)\Big]\Bigg).
\end{aligned}
\tag{4.44}
$$

and $\eta_i'(Q^2,\beta)$, $(i=1,\ 2)$ are obtained from $\eta_i(Q^2,\beta)$ by replacing x_3 with x_2 and replacing $\mathcal{F}(x_i)$ with $\mathcal{F}(x_i')$ in the integrals. In the above equations, we have used the short hand notations for the functions $\mathcal{H}_{\pm i,\pm j,...}=\pm\mathcal{H}_i\pm\mathcal{H}_j...$, and $\mathcal{H}_i$ are defined in

terms of the distribution amplitudes as follows:

$$\begin{aligned}
&\mathcal{H}_1 = S_1 && \mathcal{H}_2 = S_{1,-2} \\
&\mathcal{H}_3 = P_1 && \mathcal{H}_4 = P_{1,-2} \\
&\mathcal{H}_5 = V_1 && \mathcal{H}_6 = V_{1,-2,-3} \\
&\mathcal{H}_7 = V_3 && \mathcal{H}_8 = -2V_{1,-5} + V_{3,4} \\
&\mathcal{H}_9 = V_{4,-3} && \mathcal{H}_{10} = -V_{1,-2,-3,-4,-5,6} \\
&\mathcal{H}_{11} = A_1 && \mathcal{H}_{12} = -A_{1,-2,3} \\
&\mathcal{H}_{13} = A_3 && \mathcal{H}_{14} = -2A_{1,-5} - A_{3,4} \\
&\mathcal{H}_{15} = A_{3,-4} && \mathcal{H}_{16} = A_{1,-2,3,4,-5,6} \\
&\mathcal{H}_{17} = T_1 && \mathcal{H}_{18} = T_{1,2} - 2T_3 \\
&\mathcal{H}_{19} = T_7 && \mathcal{H}_{20} = T_{1,-2} - 2T_7 \\
&\mathcal{H}_{21} = -T_{1,-5} + 2T_8 && \mathcal{H}_{22} = T_{2,-3,-4,5,7,8} \\
&\mathcal{H}_{23} = T_{7,-8} && \mathcal{H}_{24} = -T_{1,-2,-5,6} + 2T_{7,8},
\end{aligned} \tag{4.45}$$

where for any distribution amplitudes, $X_{\pm i,\pm j,\ldots} = \pm X_i \pm X_j \ldots$ are also used. The overlap amplitude of the nucleon interpolating current with nucleon is determined from sum rule and its expression is [56]

$$\begin{aligned}
\lambda_N^2 = e^{m_N^2/M_B^2} \Bigg\{ &\frac{M_B^6}{256\pi^4} E_2(x)(5 + 2\beta + \beta^2) + \frac{< \bar{u}u >}{6} \Bigg[- 6(1 - \beta^2) < \bar{d}d > \\
&+(-1 + \beta)^2 < \bar{u}u > \Bigg] - \frac{m_0^2}{24M_B^2} < \bar{u}u > \Bigg[- 12(1 - \beta^2) < \bar{d}d > \\
&+(-1 + \beta)^2 < \bar{u}u > \Bigg] \Bigg\},
\end{aligned} \tag{4.46}$$

where, $x = s_0/M_B^2$ and the functions

$$E_n(x) = 1 - e^{-x} \sum_{k=1}^{n} \frac{x^k}{k!}, \tag{4.47}$$

are used to subtract the contribution of higher states and continuum.

4.2.2 Numerical Results

It follows from the explicit expressions of the sum rules for the nucleon electromagnetic form factors that the nucleon DA's are the principal input parameters, whose explicit expressions and the values of parameters inside them is presented in the Appendix–A.

The continuum threshold that appears in the continuum subtraction is determined from the mass sum rules as $s_0 = 2.25\ GeV^2$. There are two auxiliary parameters of the sum rules: the Borel parameter M_B^2 and the parameter β. The Borel mass square M_B^2 is the artificial parameter of the sum rules and therefore we need to find a region of M_B^2, where physically measurable quantities, in our case electromagnetic form factors, are independent of M_B^2. Lower bound of M_B^2 is determined from condition that contribution from higher states and continuum in the correlator should be enough small, upper bound of M_B^2 is determined from condition that series of the light cone expansion with increasing twist should be convergent. Our numerical analysis shows that both conditions are satisfied in the region $1GeV^2 \leq M_B^2 \leq 2GeV^2$, which we will use in numerical analysis.

The other auxiliary parameter β is chosen in a region such that, the predictions are independent of the precise value of β in that region. In our analysis, it is found that in the region $-0.5 \leq cos\theta \leq 0.5$ the form factors are practically insensitive to the variation of β, where θ is defined as $tan\theta = \beta$. Note that the analysis of mass sum rules and magnetic moments of octet baryons [56] leads to the very close region for $cos\theta$, i.e. $-0.6 \leq cos\theta \leq 0.3$. Also, it is observed in [57] that the optimal value of β is $\beta = -1.2(\cos\theta = -0.64)$, which follows from a Monte Carlo analysis.

In Fig. 4.10, we present the dependence of the proton magnetic form factor $G_M^p/\mu_p G_D$ on Q^2 at $s_0 = 2.25\ GeV^2$, $M_B^2 = 1.2\ GeV^2$ for two sets (set1 and set3 or asymptotic) of DA's, at fixed values of parameter β. In this figure, we also present the experimental results [58, 59, 60]. From this figure, we see that the Q^2 dependencies, as well as the magnitude of proton magnetic form factor are in rather good agreement with the experimental data, especially for the set 1 of DA's and Ioffe current ($\beta = -1$).

The dependence of the ratio of the proton electric form factor to the magnetic form factor $\mu_p G_E^p/G_M^p$ on Q^2 at $s_0 = 2.25\ GeV^2$, $M_B^2 = 1.2\ GeV^2$ for two sets of DA's, at fixed values of parameter β is depicted in Fig. 4.11. From this figure it follows that, practically, both sets of DA's well describe the existing experimental results, except for $\beta = 5$ and $\beta = -1$ of set 1. For large values of Q^2, $Q^2 > 4\ GeV^2$, the experimental results obtained in [49] and in [59, 60] are not in agreement. Whereas $\beta = -1$ describes better the data in [49], larger values of $|\beta|$ (smaller value of $|cos\theta|$) describe better the data in [60].

The LCQSR results for the neutron magnetic (normalized to the dipole form factor) and electric form factors are given in Fig. 4.12 and Fig. 4.13, respectively. From Fig. 4.12, we see that the magnetic form factor of neutron reproduce experimental data [61] very well at $\beta = -1$ for both sets of DA's. Neutron electric form factor is in a good agreement with the experimental result for all cases.

In [62, 63], the following large Q^2 behavior of the electromagnetic form factors is obtained

$$\frac{F_2(Q^2)}{F_1(Q^2)} \sim \frac{ln^2(Q^2/\Lambda^2)}{Q^2} \tag{4.48}$$

where $\Lambda = 300\ MeV$. In Figs. 4.14 and 4.15 , we present the logarithmic scale prediction, i.e. $(1/15)ln^{-2}(Q^2/\Lambda^2)Q^2F_2(Q^2)/F_1(Q^2)$ for the proton (neutron), with available experimental data [64] at fixed values of β for two sets of DA's. From these figures, we see that our prediction for the proton for $ln^{-2}(Q^2/\Lambda^2)Q^2F_2(Q^2)/F_1(Q^2)$ is in good agreement with experimental data except for $\beta = -1$ case for both DA's, and $\beta = -5$ case for set1. For the neutron case only set1 for $\beta = -1$ describes quite successfully the existing experimental data.

Finally, in Fig. 4.16, as an example on the dependence of the predictions on β, we present the dependence of proton magnetic form factor normalized to the dipole form factor $G_M^p/\mu_p G_D$ on $cos\theta$, for both sets of DA's at two fixed values of Q^2. It follows from this graph that, in the chosen region of β, i.e. in the region $-0.5 \leq cos\theta \leq 0.5$, the form factor G_M^p is practically insensitive to the variation of β.

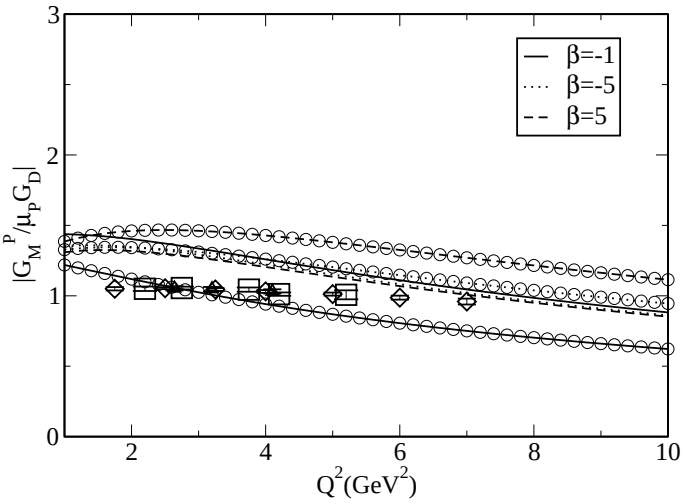

Figure 4.10: The dependence of $G_M^P/\mu_P G_D$ on Q^2 at $s_0 = 2.25\ GeV^2, M_B^2 = 1.2\ GeV^2$ for $\beta = -1,\ -5$ and 5. The boxes correspond to experimental data in [58], the diamonds to [59] and the up-triangles to [60] . The lines with circles correspond to set1 and the lines without any circles correspond to the asymptotic DA's.

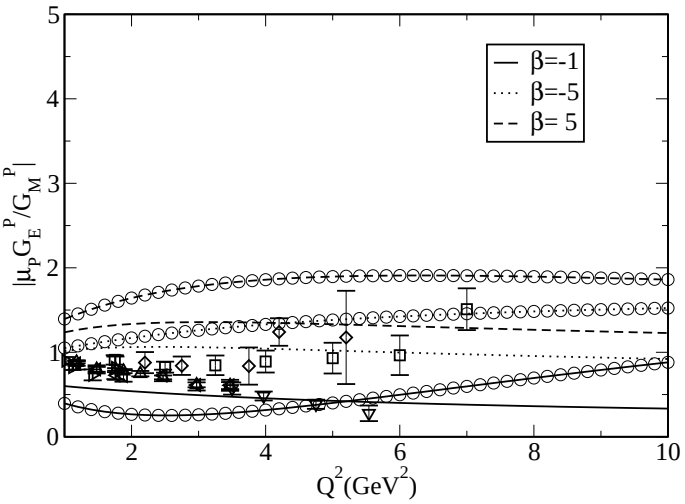

Figure 4.11: The same as Fig. 4.10, but for $\mu_P G_E^P/G_M^P$. The boxes/diamonds/up-triangles/down-triangles/right-triangles/left-triangles correspond to experimental data given in [58, 59, 51, 49, 50, 48], respectively.

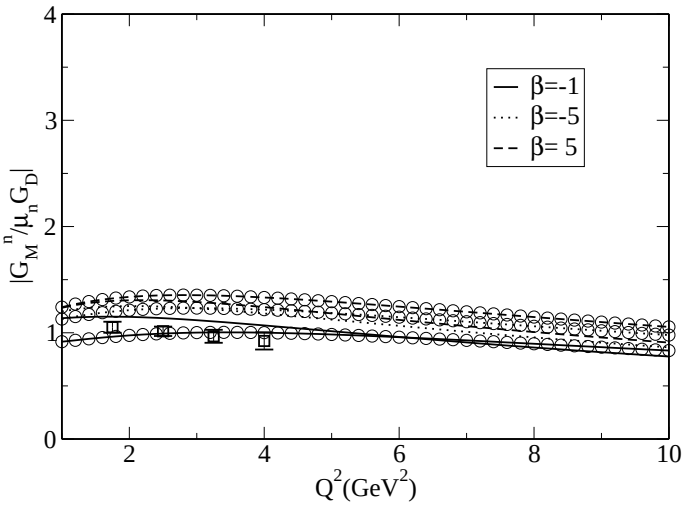

Figure 4.12: The same as Fig. 4.10 but for $G_M^n/\mu_n G_D$. The boxes correspond to experimental data ([61]).

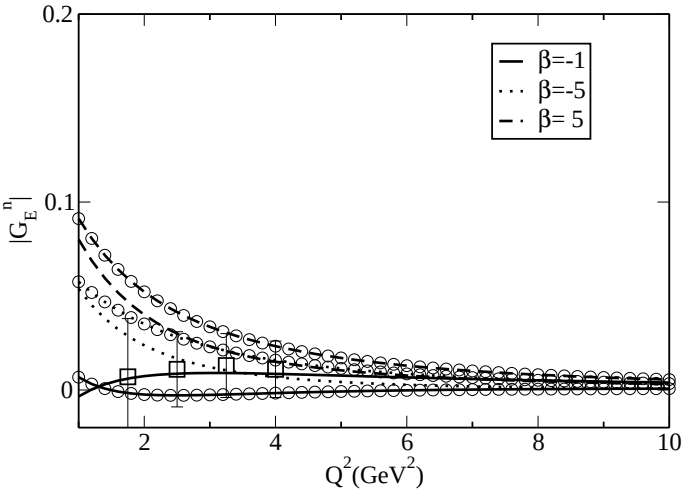

Figure 4.13: The same as Fig. 4.10 but for G_E^n. The boxes are correspond to experimental data ([61]).

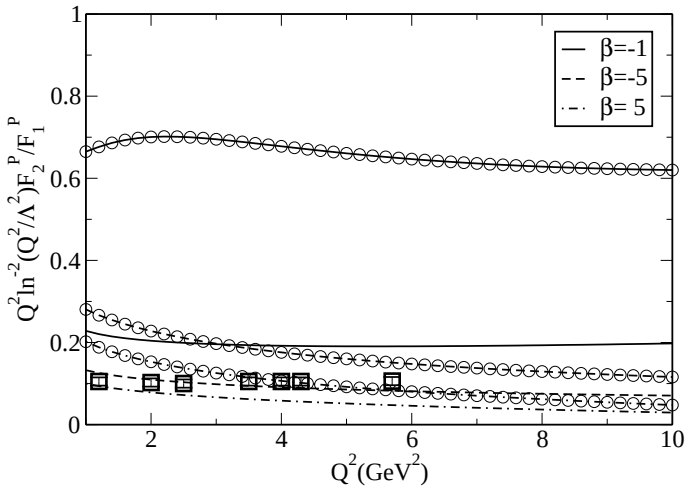

Figure 4.14: The same as Fig. 4.10 but for $Q^2 ln^{-2}(\frac{Q^2}{\Lambda^2})F_2^p/F_1^p$ where $\Lambda = 300MeV$. The boxes correspond to experimental data ([64])

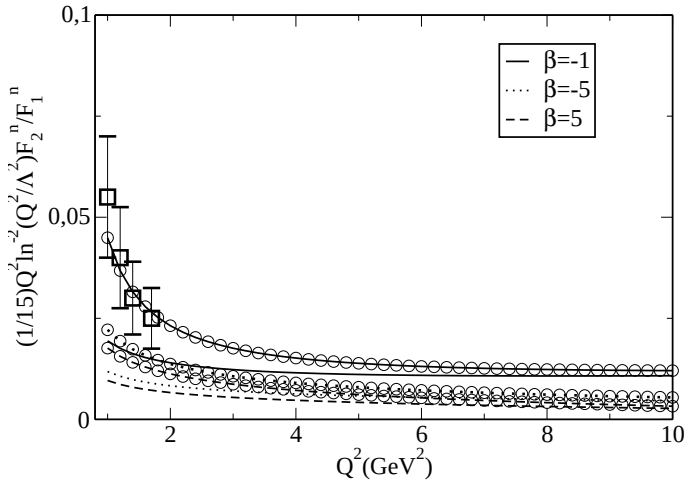

Figure 4.15: The dependence of $\frac{1}{15}Q^2 ln^{-2}(\frac{Q^2}{\Lambda^2})F_2^n/F_1^n$ on Q^2 at $s_0 = 2.25\ GeV^2, M_B^2 = 1.2\ GeV^2, \Lambda = 300MeV$. The boxes correspond to experimental data ([64]).

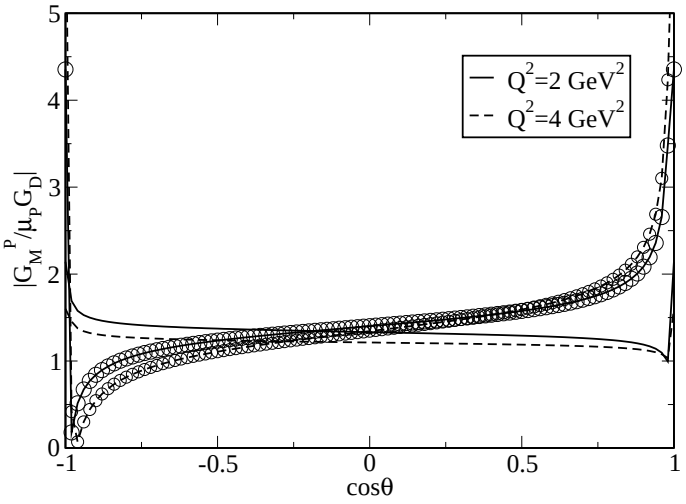

Figure 4.16: The dependence of $G_M^P/\mu_P G_D$ on $cos\theta$ at $s_0 = 2.25\ GeV^2, M_B^2 = 1.2\ GeV^2$ for two different values of Q^2, i.e. $Q^2 = 2\ GeV^2$ and $Q^2 = 4\ GeV^2$. The lines with circles correspond to set1 and the lines without any circles correspond to the asymptotic wave functions.

CHAPTER 5

PHENOMENOLOGY OF THE HEAVY BARYONS

During the last few years, exciting experimental results are obtained in the baryon sector containing a single b-quark. The CDF Collaboration observed the states $\Sigma_b^{\pm}$ and $\Sigma_b^{*\pm}$ [8], while both DO [10] and CDF [9] Collaborations have seen Ξ_b. Recently, BaBar Collaboration reported the discovery of Ω_c^* with mass splitting $m_{\Omega_c^*} - m_{\Omega_c} = (70.8 \pm 1.0 \pm 1.1)MeV$ [11]. The CDF sensitivity appears adequate to observe new heavy baryons.

The masses of the heavy baryons have been studied in the framework of various phenomenological models [65]- [73] and also in the framework of QCD sum rules method [74]- [86]. Along with their masses, another static parameter of the heavy baryons is their magnetic moment. Study of the magnetic moments can give valuable information about the internal structures of hadrons.

The magnetic moments of heavy baryons have been studied in the framework of different methods. In [87, 88] the magnetic moments of charmed baryons are calculated within naive quark model. In [89, 90], magnetic moments of charmed and bottom baryons are analyzed in quark model and in [91] heavy baryon magnetic moments are studied in bound state approach. Magnetic moments of heavy baryons are calculated in the relativistic three-quark model [92], hyper central model [93], Chiral perturbation model [94], soliton model [95], skyrmion model [96] and nonrelativistic constituent quark model with light and strange $\bar{q}q$ pairs [97]. In [98] the magnetic moments of Σ_c and Λ_c baryons are calculated in QCD sum rules in external electromagnetic field. In [99, 100], the light cone QCD sum rules method is applied to study

the magnetic moments of the Λ_Q, ($Q = c, b$) and $\Sigma_Q\Lambda_Q$ transitions. For more about the calculation of the mass and magnetic moments of the heavy flavored baryons in different approaches see also [101, 102, 103, 104]. In this chapter, first we calculate the magnetic moments of the heavy spin 1/2, Ξ_Q baryons. Then, we calculate the mass and magnetic moments of the heavy flavored spin 3/2 bayons (Σ_Q^*, Ξ_Q^* and Ω_Q^*) in the framework of the LCQSR.

5.1 Magnetic Moments of Heavy Ξ_Q Baryons

The aim of the present section is the calculation of the magnetic moments of the Ξ_b baryons recently observed by DO and CDF Collaborations within the light cone QCD sum rules framework. The plan of the section is as follows. In the next subsection, using the general form of the the baryon current, the light cone QCD sum rules for magnetic moment of the Ξ_b and Ξ_c baryons are calculated. Then, we present our numerical calculations on the magnetic moment of the Ξ_b and Ξ_c baryons and also present a comparison of our results with the predictions of other approaches.

5.1.1 Light Cone QCD Sum Rules for the Ξ_Q Magnetic Moments

In order to calculate the magnetic moments of Ξ_Q ($Q = b, c$) in the framework of the light cone QCD sum rules, we need the expression for the interpolating current of Ξ_Q. To construct it, we follow [71], i.e., we assume that the strange and light quarks (sq) in Ξ_Q are in a relative spin zero state (scalar or pseudo scalar diquarks). Therefore, the most general current without derivatives and with the quantum numbers of Ξ_Q can be constructed from the combination of aforementioned scalar or pseudoscalar diquarks in the following way

$$\eta_Q = \varepsilon_{abc}[(q^{aT}Cs^b)\gamma_5 + \beta(q^{aT}C\gamma_5 s^b)]Q^c, \tag{5.1}$$

here a, b and c are color indices, C is the charge conjugation operator, $Q = b$, or c, $q = u$, or d and β is an arbitrary parameter. Having the explicit expression for the interpolating current, our next task is to construct light cone QCD sum rules for the

magnetic moments of Ξ_Q baryons. It is constructed from the following correlation function:

$$\Pi(p,q) = i \int d^4x e^{ipx} < \gamma \mid T\{\eta_Q(x)\bar{\eta}_Q(0) \mid\}0 > . \tag{5.2}$$

The calculation of the phenomenological side at the hadronic level proceeds by inserting into the correlation function a complete set of hadronic states with the quantum numbers of Ξ_Q. We get

$$\Pi = \sum_i \frac{< 0 \mid \eta_Q \mid \Xi_{Q_i}(p_2) >}{p_2^2 - m_{\Xi_Q}^2} < \Xi_{Q_i}(p_2) \mid \Xi_{Q_i}(p_1) >_\gamma \frac{< \Xi_{Q_i}(p_1) \mid \bar{\eta}_Q \mid 0 >}{p_1^2 - m_{\Xi_Q}^2}. \tag{5.3}$$

Isolating the ground state's contributions, Eq. (5.3) can be written as

$$\begin{aligned} \Pi &= \frac{< 0 \mid \eta_Q \mid \Xi_Q(p_2) >}{p_2^2 - m_{\Xi_Q}^2} < \Xi_Q(p_2) \mid \Xi_Q(p_1) >_\gamma \frac{< \Xi_Q(p_1) \mid \bar{\eta}_Q \mid 0 >}{p_1^2 - m_{\Xi_Q}^2} \\ &+ \sum_{h_i} \frac{< 0 \mid \eta_{Qi} \mid h_i(p_2) >}{p_2^2 - m_{h_i}^2} < h_i(p_2) \mid h_i(p_1) >_\gamma \frac{< h_i(p_1) \mid \bar{\eta}_Q \mid 0 >}{p_1^2 - m_{h_i}^2}, \end{aligned} \tag{5.4}$$

where $p_1 = p + q$, $p_2 = p$ and q is the photon momentum. The second term in Eq. (5.4) describes the higher resonances and continuum contributions. The coupling of the interpolating current with the baryons Ξ_Q is determined as

$$< 0 \mid \eta_Q \mid \Xi_Q(p) >= \lambda_Q u_{\Xi_Q}(p), \tag{5.5}$$

where $u_{\Xi_Q}(p)$ is a spinor describing the baryon Ξ_Q with four momentum p and λ_Q is the corresponding residue.

The last step for obtaining the expression for the physical part of the correlator function is to write down the matrix element $< \Xi_Q(p_2) \mid \Xi_Q(p_1) >_\gamma$ in terms of the form factors. Using Lorentz covariance, this matrix element can be written as

$$\begin{aligned} < \Xi_Q(p_1) \mid \Xi_Q(p_2) >_\gamma &= \varepsilon^\mu \overline{u}_{\Xi_Q}(p_1) \left[f_1 \gamma_\mu - i \frac{\sigma_{\mu\alpha} q_\alpha}{2m_{\Xi_Q}} f_2 \right] u_{\Xi_Q}(p_2) \\ &= \overline{u}_{\Xi_Q}(p_1) \left[(f_1 + f_2)\gamma_\mu + \frac{(p_1 + p_2)_\mu}{2m_{\Xi_Q}} f_2 \right] u_{\Xi_Q}(p_2) \varepsilon^\mu, \end{aligned} \tag{5.6}$$

where $f_1(q^2)$ and $f_2(q^2)$ are the form factors and ε^μ is the photon polarization vector.

For calculation of the Ξ_Q magnetic moments, the values of the form factors only at $q^2 = 0$ are needed because the photon is real in our problem. Using Eqs. (5.4-5.6) for physical part of the correlator and summing over the spins of initial and final Ξ_Q baryons, the correlation function becomes

$$\Pi = -\lambda_Q^2 \varepsilon^\mu \frac{\not{p}_2 + m_{\Xi_Q}}{p_2^2 - m_{\Xi_Q}^2} \left[(f_1 + f_2)\gamma_\mu + \frac{(p_1 + p_2)_\mu}{2m_{\Xi_Q}} f_2 \right] \frac{\not{p}_1 + m_{\Xi_Q}}{p_1^2 - m_{\Xi_Q}^2}. \tag{5.7}$$

From this expression, we see that there are various structures which can be chosen for studying the magnetic moments of Ξ_Q. In the present work, following [105], we choose the structure $\not{p}_2 \not{\varepsilon} \not{q}$ that contains magnetic form factor $f_1 + f_2$ and at $q^2 = 0$ it gives the magnetic moment of Ξ_Q in units of $e\hbar/2m_{\Xi_Q}$. Choosing this structure in the physical part of the correlator, for the magnetic moments of Ξ_Q we obtain

$$\Pi = -\lambda_Q^2 \frac{1}{p_1^2 - m_{\Xi_Q}^2} \mu_{\Xi_Q} \frac{1}{p_2^2 - m_{\Xi_Q}^2}, \tag{5.8}$$

where $\mu_{\Xi_Q} = (f_1 + f_2)\,|_{q^2=0}$ are the magnetic moments of Ξ_Q in units of $e\hbar/2m_{\Xi_Q}$.

In order to calculate the magnetic moments of Ξ_Q baryons, the expression of the theoretical part of the correlation function is needed. After simple calculations for the theoretical part of the correlation function in QCD we obtain

$$\begin{aligned} \Pi &= -i\epsilon_{abc}\epsilon_{a'b'c'} \int d^4x e^{ipx} \langle \gamma(q) \mid \{\gamma_5 S_Q^{cc'} \gamma_5 Tr(S_q^{ba'} S_s'^{ab'}) \\ &+ \beta\gamma_5 S_Q^{cc'} Tr(S_q^{ba'} \gamma_5 S_s'^{ab'}) + \beta S_Q^{cc'} \gamma_5 Tr(\gamma_5 S_q^{ba'} S_s'^{ab'}) \\ &+ \beta^2 S_Q^{cc'} Tr(\gamma_5 S_s^{ab'} \gamma_5 S_q'^{ba'})\} \mid 0\rangle, \end{aligned} \tag{5.9}$$

where $S_i' = CS_i^T C$ and C and T are the charge conjugation and transposition operators, respectively and S_Q and $S_{q(s)}$ are the heavy and light(strange) quark propagators.

The correlation function from QCD part receives three different contributions: a) perturbative contributions, b) nonperturbative contributions, where photon is emitted from the freely propagating quark (in other words at short distance) c) nonperturbative contributions, when photon is radiated at long distances. To obtain the expression for the contribution from the emission of photon at short distances, the following

procedure can be used: Each one of the quarks can emit the photon, and hence each term in Eq. (5.9) corresponds to three terms in which the propagator of the photon emitting quark is replaced by:

$$S^{ab}_{\alpha\beta} \Rightarrow \left\{ \int d^4y S^{free}(x-y) \not{A} S^{free}(y) \right\}^{ab}_{\alpha\beta}. \tag{5.10}$$

Note that, the explicit expressions of free and full light quark propagator had been given in chapter 3. The free part of the heavy quark propagator in x representation is:

$$S^{free}_{Q} = \frac{m_Q^2}{4\pi^2} \frac{K_1(m_Q\sqrt{-x^2})}{\sqrt{-x^2}} - i\frac{m_Q^2 \not{x}}{4\pi^2 x^2} K_2(m_Q\sqrt{-x^2}), \tag{5.11}$$

where K_i are Bessel functions, $m_{u,d} = 0$ and $m_s \neq 0$. The expression for the nonperturbative contributions to the correlation function can be obtained from Eq. (5.9) by replacing one of the light quark propagator by

$$S^{ab}_{\alpha\beta} \to -\frac{1}{4}\bar{q}^a \Gamma_j q^b (\Gamma_j)_{\alpha\beta}\,, \tag{5.12}$$

where $\Gamma_j = \left\{1,\ \gamma_5,\ \gamma_\alpha,\ i\gamma_5\gamma_\alpha,\ \sigma_{\alpha\beta}/\sqrt{2}\right\}$ and sum over Γ_j is implied, and the other two propagators are the full propagators involving both perturbative and nonperturbative contributions. In order to calculate the correlation function from QCD side, we need the explicit expressions of the heavy and light quark propagators in the presence of external field.

The light cone expansion of the heavy propagator in external field is also obtained in [43]. It receives contributions from various $\bar{q}Gq$, $\bar{q}GGq$, $\bar{q}q\bar{q}q$ nonlocal operators , where G is the gluon field strength tensor. In this work, we consider operators with only one gluon field and contributions coming from three particle nonlocal operators and neglect terms with two gluons $\bar{q}GGq$, and four quarks $\bar{q}q\bar{q}q$ [106]. In this approximation the expressions for the heavy quark propagator is:

$$\begin{aligned} iS_Q(x) &= iS^{free}_Q(x) - ig_s \int \frac{d^4k}{(2\pi)^4} e^{-ikx} \int_0^1 dv \Bigg[\frac{\not{k} + m_Q}{(m_Q^2 - k^2)^2} G^{\mu\nu}(vx)\sigma_{\mu\nu} \\ &+ \frac{1}{m_Q^2 - k^2} v x_\mu G^{\mu\nu}\gamma_\nu \Bigg], \end{aligned} \tag{5.13}$$

In order to calculate the theoretical part, from Eqs. (5.9)-(5.13) it follows that the matrix elements of nonlocal operators $\bar{q}\Gamma_i q$ between the photon and vacuum states are needed, i.e.$\langle\gamma(q)\mid\bar{q}(x_1)\Gamma_i q(x_2)\mid 0\rangle$. These matrix elements can be expanded near the light cone $x^2=0$ in terms of the photon distribution amplitudes [16].

$$\langle\gamma(q)|\bar{q}(x)\sigma_{\mu\nu}q(0)|0\rangle = -ie_q\bar{q}q(\varepsilon_\mu q_\nu-\varepsilon_\nu q_\mu)\int_0^1 due^{i\bar{u}qx}\left(\chi\varphi_\gamma(u)+\frac{x^2}{16}\mathbb{A}(u)\right)$$
$$-\frac{i}{2(qx)}e_q\langle\bar{q}q\rangle\left[x_\nu\left(\varepsilon_\mu-q_\mu\frac{\varepsilon x}{qx}\right)-x_\mu\left(\varepsilon_\nu-q_\nu\frac{\varepsilon x}{qx}\right)\right]\int_0^1 due^{i\bar{u}qx}h_\gamma(u)$$
$$\langle\gamma(q)|\bar{q}(x)\gamma_\mu q(0)|0\rangle = e_q f_{3\gamma}\left(\varepsilon_\mu-q_\mu\frac{\varepsilon x}{qx}\right)\int_0^1 due^{i\bar{u}qx}\psi^v(u)$$
$$\langle\gamma(q)|\bar{q}(x)\gamma_\mu\gamma_5 q(0)|0\rangle = -\frac{1}{4}e_q f_{3\gamma}\epsilon_{\mu\nu\alpha\beta}\varepsilon^\nu q^\alpha x^\beta\int_0^1 due^{i\bar{u}qx}\psi^a(u)$$
$$\langle\gamma(q)|\bar{q}(x)g_s G_{\mu\nu}(vx)q(0)|0\rangle = -ie_q\langle\bar{q}q\rangle\left(\varepsilon_\mu q_\nu-\varepsilon_\nu q_\mu\right)\int\mathcal{D}\alpha_i e^{i(\alpha_{\bar{q}}+v\alpha_g)qx}\mathcal{S}(\alpha_i)$$
$$\langle\gamma(q)|\bar{q}(x)g_s\tilde{G}_{\mu\nu}i\gamma_5(vx)q(0)|0\rangle = -ie_q\langle\bar{q}q\rangle\left(\varepsilon_\mu q_\nu-\varepsilon_\nu q_\mu\right)\int\mathcal{D}\alpha_i e^{i(\alpha_{\bar{q}}+v\alpha_g)qx}\tilde{\mathcal{S}}(\alpha_i)$$
$$\langle\gamma(q)|\bar{q}(x)g_s\tilde{G}_{\mu\nu}(vx)\gamma_\alpha\gamma_5 q(0)|0\rangle = e_q f_{3\gamma}q_\alpha(\varepsilon_\mu q_\nu-\varepsilon_\nu q_\mu)\int\mathcal{D}\alpha_i e^{i(\alpha_{\bar{q}}+v\alpha_g)qx}\mathcal{A}(\alpha_i)$$
$$\langle\gamma(q)|\bar{q}(x)g_s G_{\mu\nu}(vx)i\gamma_\alpha q(0)|0\rangle = e_q f_{3\gamma}q_\alpha(\varepsilon_\mu q_\nu-\varepsilon_\nu q_\mu)\int\mathcal{D}\alpha_i e^{i(\alpha_{\bar{q}}+v\alpha_g)qx}\mathcal{V}(\alpha_i)$$
$$\langle\gamma(q)|\bar{q}(x)\sigma_{\alpha\beta}g_s G_{\mu\nu}(vx)q(0)|0\rangle =$$
$$e_q\langle\bar{q}q\rangle\left\{\left[\left(\varepsilon_\mu-q_\mu\frac{\varepsilon x}{qx}\right)\left(g_{\alpha\nu}-\frac{1}{qx}(q_\alpha x_\nu+q_\nu x_\alpha)\right)q_\beta\right.\right.$$
$$-\left(\varepsilon_\mu-q_\mu\frac{\varepsilon x}{qx}\right)\left(g_{\beta\nu}-\frac{1}{qx}(q_\beta x_\nu+q_\nu x_\beta)\right)q_\alpha$$
$$-\left(\varepsilon_\nu-q_\nu\frac{\varepsilon x}{qx}\right)\left(g_{\alpha\mu}-\frac{1}{qx}(q_\alpha x_\mu+q_\mu x_\alpha)\right)q_\beta$$
$$\left.+\left(\varepsilon_\nu-q_\nu\frac{\varepsilon x}{q.x}\right)\left(g_{\beta\mu}-\frac{1}{qx}(q_\beta x_\mu+q_\mu x_\beta)\right)q_\alpha\right]\int\mathcal{D}\alpha_i e^{i(\alpha_{\bar{q}}+v\alpha_g)qx}\mathcal{T}_1(\alpha_i)$$
$$+\left[\left(\varepsilon_\alpha-q_\alpha\frac{\varepsilon x}{qx}\right)\left(g_{\mu\beta}-\frac{1}{qx}(q_\mu x_\beta+q_\beta x_\mu)\right)q_\nu\right.$$
$$-\left(\varepsilon_\alpha-q_\alpha\frac{\varepsilon x}{qx}\right)\left(g_{\nu\beta}-\frac{1}{qx}(q_\nu x_\beta+q_\beta x_\nu)\right)q_\mu$$
$$-\left(\varepsilon_\beta-q_\beta\frac{\varepsilon x}{qx}\right)\left(g_{\mu\alpha}-\frac{1}{qx}(q_\mu x_\alpha+q_\alpha x_\mu)\right)q_\nu$$
$$\left.+\left(\varepsilon_\beta-q_\beta\frac{\varepsilon x}{qx}\right)\left(g_{\nu\alpha}-\frac{1}{qx}(q_\nu x_\alpha+q_\alpha x_\nu)\right)q_\mu\right]\int\mathcal{D}\alpha_i e^{i(\alpha_{\bar{q}}+v\alpha_g)qx}\mathcal{T}_2(\alpha_i)$$
$$+\frac{1}{qx}(q_\mu x_\nu-q_\nu x_\mu)(\varepsilon_\alpha q_\beta-\varepsilon_\beta q_\alpha)\int\mathcal{D}\alpha_i e^{i(\alpha_{\bar{q}}+v\alpha_g)qx}\mathcal{T}_3(\alpha_i)$$

$$+\frac{1}{qx}(q_\alpha x_\beta - q_\beta x_\alpha)(\varepsilon_\mu q_\nu - \varepsilon_\nu q_\mu)\int \mathcal{D}\alpha_i e^{i(\alpha_{\bar{q}}+v\alpha_g)qx}\mathcal{T}_4(\alpha_i)\Bigg\}, \tag{5.14}$$

where χ is the magnetic susceptibility of the quarks, $\varphi_\gamma(u)$ is the leading twist 2, $\psi^v(u)$, $\psi^a(u)$, $\mathcal{A}$ and $\mathcal{V}$ are the twist 3 and $h_\gamma(u)$, $\mathbb{A}$, $\mathcal{T}_i$ ($i = 1,\ 2,\ 3,\ 4$) are the twist 4 photon distribution amplitudes (DA's), respectively. The explicit expressions of DA's are presented in numerical analysis section. The mesure $\mathcal{D}\alpha_i$ is defined as

$$\int \mathcal{D}\alpha_i \ = \ \int_0^1 d\alpha_{\bar{q}} \int_0^1 d\alpha_q \int_0^1 d\alpha_g \delta(1-\alpha_{\bar{q}}-\alpha_q-\alpha_g). \tag{5.15}$$

The theoretical part of the correlation function can be obtained in terms of QCD parameters by substituting photon DA's and expressions for heavy and light quarks propagators. Sum rules for the Ξ_Q magnetic moments are obtained by equating two representations of the correlation function. The higher states and continuum contributions are modeled using the hadron-quark duality. Applying double Borel transformations on the variables $p_1^2 = (p+q)^2$ and $p_2^2 = p^2$ on both sides of the correlator, for the Ξ_Q baryon magnetic moments we get:

$$\begin{aligned}
-\ & \lambda_Q^2(\beta)\mu_{\Xi_Q} e^{-m_{\Xi_Q}^2/M_B^2} = \int_{m_Q^2}^{s_0} e^{\frac{-s}{M_B^2}}\rho(s)ds \\
+\ & \frac{(\beta^2-1)e^{\frac{-m_Q^2}{M_B^2}}}{288\pi^2}\Bigg\{\gamma_E(6e_Q+e_s)m_s m_0^2 < \bar{q}q > \Bigg\} \\
-\ & \frac{(\beta^2-1)e^{\frac{-m_Q^2}{M_B^2}} m_Q^2}{72M_B^4}\Bigg\{(e_s+e_q)m_0^2 < \bar{s}s >< \bar{q}q > \eta_1\Bigg\} \\
+\ & \frac{e^{\frac{-m_Q^2}{M_B^2}} m_Q^2}{432M_B^4}\Bigg\{(\beta^2-1)m_0^2 < \bar{s}s >< \bar{q}q > \Bigg[36e_Q + (e_s+e_q)\mathbb{A}(u_0)\Bigg] \\
+\ & (\beta^2+1)f_{3\gamma}e_q m_s m_0^2 < \bar{s}s > (\eta_2 + \psi^a(u_0))\Bigg\} \\
+\ & \frac{e^{\frac{-m_Q^2}{M_B^2}}}{72}\Bigg\{(1-\beta^2) < \bar{s}s >< \bar{q}q > \Bigg[12e_Q - (e_s+e_q)[\eta_1 - m_0^2\chi_i\varphi_\gamma(u_0)]\Bigg] \\
-\ & 3e_q(\beta^2+1)f_{3\gamma}m_s < \bar{s}s > \eta_2\Bigg\}
\end{aligned}$$

$$
\begin{aligned}
&- \frac{(\beta^2-1)e^{\frac{-m_Q^2}{M_B^2}} M_B^2 m_s}{96\pi^2 m_Q^2}\left[(6e_Q+e_s)\gamma_E m_0^2 < \bar{q}q > \right] \\
&- \frac{e^{\frac{-m_Q^2}{M_B^2}} m_s}{288\pi^2}\left(3(\beta^2-1)e_Q m_0^2 < \bar{q}q > \left\{ -3+2\gamma_E+2ln[\frac{\Lambda^2}{m_Q^2}]\right\}\right. \\
&+ \left. e_q m_0^2 < \bar{s}s > (1+\beta^2) + e_s m_0^2 < \bar{q}q > \left[(1-\beta^2)(\gamma_E + ln[\frac{\Lambda^2}{m_Q^2}])\right]\right) \\
&+ \frac{9e_Q m_Q^2 m_s}{144\pi^2}\left\{ < \bar{s}s > (1+\beta^2) + 2 < \bar{q}q > (1-\beta^2)\right\},
\end{aligned}
\tag{5.16}
$$

where $M_B^2 = \frac{M_1^2 M_2^2}{M_1^2+M_2^2}$ and $u_0 = \frac{M_1^2}{M_1^2+M_2^2}$. Since the masses of the initial and final baryons are the same, we will set $M_1^2 = M_2^2$ and $u_0 = 1/2$. The functions appearing in Eq. (5.16) are defined as:

$$
\begin{aligned}
\eta_1 &= \int \mathcal{D}\alpha_i \int_0^1 dv \mathcal{S}(\alpha_i)\delta(\alpha_q + v\alpha_g - u_0), \\
\eta_2 &= \int \mathcal{D}\alpha_i \int_0^1 dv \mathcal{V}(\alpha_i)\delta'(\alpha_q + v\alpha_g - u_0), \\
\rho(s) &= \frac{(\beta^2-1)}{144\pi^2 M_B^2}\left\{ m_0^2(6e_Q+e_s)m_s < \bar{q}q > \ln(\frac{-{m_Q}^2+s}{\Lambda^2})\right\} \\
&+ \frac{3(1+\beta^2)e_Q m_Q^4}{64\pi^4}\left\{\frac{13}{2} + \psi_{10} - \frac{1}{6}\psi_{20} - \frac{1}{6}\psi_{30} + [\psi_{10}+\frac{3}{2}]ln(\frac{s}{m_Q^2}) + \frac{1}{6}\psi_{41}\right\} \\
&+ \frac{(1-\beta^2)m_s < \bar{q}q > \psi_{10}}{48\pi^2 m_Q^2}\left\{2e_q m_Q^2\eta_1 - (e_s+e_q)m_0^2\left[8 + ln(\frac{s-m_Q^2}{\Lambda^2})\right]\right\} \\
&- \frac{m_s}{288\pi^2 m_Q^2}\left\{(\beta^2-1)m_0^2(e_s+6e_Q) < \bar{q}q > \right. \\
&\quad \left.\left[3ln(\frac{s-m_Q^2}{\Lambda^2}) - (4\gamma_E + ln[\frac{\Lambda^2}{m_Q^2}])\right]\right. \\
&+ \left. 6e_Q\left[3m_Q^2\{(1+\beta^2) < \bar{s}s > +2(1-\beta^2) < \bar{q}q > \}\psi_{10}\right]\right\} \\
&+ \frac{m_Q^2}{576\pi^2}\left((e_s+12e_Q)\left\{\frac{(\beta^2-1)}{m_Q^4}m_0^2 m_s < \bar{q}q > \left[-(1+\gamma_E)(\psi_{22}+2\psi_{12})\right.\right.\right. \\
&- \left.\left.\left.\psi_{02} - \psi_{32} - \psi_{22} - \frac{\gamma_E}{2}\psi_{20}\right.\right.\right.
\end{aligned}
$$

$$
\begin{aligned}
&+ \quad 3(2\psi_{32}+3\psi_{22}+\psi_{02})ln(\frac{s-m_Q^2}{\Lambda^2})-ln(\frac{\Lambda^2}{m_Q^2})\Big]\Big\} \\
&+ \quad 12e_q\Big\{\frac{2}{m_Q^2}(\beta^2-1)m_s<\bar{q}q>\eta_1\psi_{21} \\
&+ \quad (1+\beta^2)f_{3\gamma}\eta_2\left[\psi_{21}-\psi_{10}+\frac{1}{2}\psi_{20}+\frac{1}{2}\psi_{00}+ln(\frac{m_Q^2}{s})\right]\Big\}\Big),
\end{aligned}
\tag{5.17}
$$

and functions ψ_{nm} are defined as

$$
\psi_{nm} \quad = \quad \frac{(s-{m_Q}^2)^n}{s^m(m_Q^2)^{n-m}}. \tag{5.18}
$$

Note that the contributions of the terms $\sim< G^2 >$ are also calculated, but their numerical values are very small and therefore for customary in Eq. (5.16) these terms are omitted. From Eq. (5.16) it follows that for the determination of the Ξ_Q baryon magnetic moments, we need to know the residue λ_Q. The residue can be obtained from the two-point sum rules and is calculated in [85]. For the current given in eq. (5.1) it takes the following form:

$$
\begin{aligned}
\lambda_Q^2(\beta) \quad &= \quad e^{{m_{\Xi_Q}}^2/M_B^2}\Bigg(\int_{m_Q^2}^{s_0} ds\, e^{-s/M_B^2}\Bigg\{\frac{(1+\beta^2)m_Q^4}{2^9\pi^4} \\
&\times \quad \left[(1-x^2)\left(\frac{1}{x^2}-\frac{8}{x}+1\right)-12\ln x\right] \\
&+ \quad \frac{m_s}{2^4\pi^2}(1-x^2)\left[(1-\beta^2)\langle\bar{q}q\rangle+\frac{(1+b^2)\langle\bar{s}s\rangle}{2}\right] \\
&+ \quad \frac{(1+\beta^2)<g^2G^2>}{2^{10}3\pi^4}(1-x)(1+5x)\Bigg\} \\
&+ \quad \frac{m_s}{2^5\pi^2}\Bigg\{\frac{(1+\beta^2)m_0^2<\bar{s}s>}{6}e^{-m_Q^2/M_B^2}-(1-\beta^2)m_0^2<\bar{q}q>\Big[e^{-m_Q^2/M_B^2} \\
&+ \quad \int_0^1 d\alpha(1-\alpha)e^{\frac{-m_Q^2}{(1-\alpha)M_B^2}}\Big]\Bigg\}-\frac{\langle\bar{q}q\rangle\langle\bar{s}s\rangle}{6}(1-\beta^2)e^{-m_Q^2/M_B^2}\Bigg),
\end{aligned}
\tag{5.19}
$$

where, $x = m_Q^2/s$.

5.1.2 Numerical Analysis

The present section is devoted to the numerical analysis of the magnetic moments of Ξ_Q baryons. The values of the input parameters, appearing in the sum rules expression for magnetic moments are: $\langle\bar{u}u\rangle(1\ GeV) = \langle\bar{d}d\rangle(1\ GeV) = -(0.243)^3\ GeV^3$, $\langle\bar{s}s\rangle(1\ GeV) = 0.8\langle\bar{u}u\rangle(1\ GeV)$, $m_0^2(1\ GeV) = 0.8\ GeV^2$ [107], , $\Lambda = 300\ MeV$ and $f_{3\gamma} = -0.0039\ GeV^2$ [16]. The value of the magnetic susceptibility $\chi(1\ GeV) = -3.15 \pm 0.3\ GeV^{-2}$ was obtained by a combination of the local duality approach and QCD sum rules [16]. Recently, from the analysis of radiative heavy meson decay, $\chi(1\ GeV) = -(2.85 \pm 0.5)\ GeV^{-2}$ was obtained [108], which is in good agreement with the instanton liquid model prediction [109], but slightly below the QCD sum rules prediction [16]. Note that firstly the magnetic susceptibility in the framework of QCD sum rules is calculated in [110] and it is obtained that $\chi(1\ GeV) = -4.4\ GeV^{-2}$. In the numerical analysis, we have used all three value of χ existing in the litrature and obtained that the values of the magnetic moments of Ξ_Q baryons are practically insensitive to the value of χ. The photon DA's entering the sum rules for the magnetic moments of Ξ_Q are calculated in [16] and their expressions are:

$$
\begin{aligned}
\varphi_\gamma(u) &= 6u\bar{u}\Big(1+\varphi_2(\mu)C_2^{\frac{3}{2}}(u-\bar{u})\Big),\\
\psi^v(u) &= 3\Big(3(2u-1)^2-1\Big)+\frac{3}{64}\Big(15w_\gamma^V-5w_\gamma^A\Big)\Big(3-30(2u-1)^2+35(2u-1)^4\Big),\\
\psi^a(u) &= \Big(1-(2u-1)^2\Big)\Big(5(2u-1)^2-1\Big)\frac{5}{2}\Big(1+\frac{9}{16}w_\gamma^V-\frac{3}{16}w_\gamma^A\Big),\\
\mathcal{A}(\alpha_i) &= 360\alpha_q\alpha_{\bar{q}}\alpha_g^2\Big(1+w_\gamma^A\frac{1}{2}(7\alpha_g-3)\Big),\\
\mathcal{V}(\alpha_i) &= 540w_\gamma^V(\alpha_q-\alpha_{\bar{q}})\alpha_q\alpha_{\bar{q}}\alpha_g^2,\\
h_\gamma(u) &= -10\,(1+2\kappa^+)\,C_2^{\frac{1}{2}}(u-\bar{u}),\\
\mathbb{A}(u) &= 40u^2\bar{u}^2\,(3\kappa-\kappa^++1)\\
&\quad +8(\zeta_2^+-3\zeta_2)\,[u\bar{u}(2+13u\bar{u})\\
&\quad +2u^3(10-15u+6u^2)\ln(u)+2\bar{u}^3(10-15\bar{u}+6\bar{u}^2)\ln(\bar{u})\Big],\\
\mathcal{T}_1(\alpha_i) &= -120(3\zeta_2+\zeta_2^+)(\alpha_{\bar{q}}-\alpha_q)\alpha_{\bar{q}}\alpha_q\alpha_g,\\
\mathcal{T}_2(\alpha_i) &= 30\alpha_g^2(\alpha_{\bar{q}}-\alpha_q)\Big((\kappa-\kappa^+)+(\zeta_1-\zeta_1^+)(1-2\alpha_g)+\zeta_2(3-4\alpha_g)\Big),
\end{aligned}
$$

$$
\begin{aligned}
\mathcal{T}_3(\alpha_i) &= -120(3\zeta_2 - \zeta_2^+)(\alpha_{\bar{q}} - \alpha_q)\alpha_{\bar{q}}\alpha_q\alpha_g, \\
\mathcal{T}_4(\alpha_i) &= 30\alpha_g^2(\alpha_{\bar{q}} - \alpha_q)\Big((\kappa + \kappa^+) + (\zeta_1 + \zeta_1^+)(1 - 2\alpha_g) + \zeta_2(3 - 4\alpha_g)\Big), \\
\mathcal{S}(\alpha_i) &= 30\alpha_g^2\{(\kappa + \kappa^+)(1 - \alpha_g) + (\zeta_1 + \zeta_1^+)(1 - \alpha_g)(1 - 2\alpha_g) \\
&+ \zeta_2[3(\alpha_{\bar{q}} - \alpha_q)^2 - \alpha_g(1 - \alpha_g)]\}, \\
\tilde{\mathcal{S}}(\alpha_i) &= -30\alpha_g^2\{(\kappa - \kappa^+)(1 - \alpha_g) + (\zeta_1 - \zeta_1^+)(1 - \alpha_g)(1 - 2\alpha_g) \\
&+ \zeta_2[3(\alpha_{\bar{q}} - \alpha_q)^2 - \alpha_g(1 - \alpha_g)]\}. \qquad (5.20)
\end{aligned}
$$

The constants appearing in the wave functions are given as [16] $\varphi_2(1\ GeV) = 0$, $w_\gamma^V = 3.8 \pm 1.8$, $w_\gamma^A = -2.1 \pm 1.0$, $\kappa = 0.2$, $\kappa^+ = 0$, $\zeta_1 = 0.4$, $\zeta_2 = 0.3$, $\zeta_1^+ = 0$ and $\zeta_2^+ = 0$.

From the explicit expressions of the magnetic moments of Ξ_Q baryons, it follows that it contains three auxiliary parameters: Borel mass squared M_B^2, continuum threshold s_0 and β which enters the expression of the interpolating current for Ξ_Q. The physical quantity, magnetic moment μ_{Ξ_Q}, should be independent of these auxiliary parameters. In other words we should find the "working regions" of these auxiliary parameters, where the magnetic moments are independent of them.

The value of the continuum threshold is fixed from the analysis of the two- point sum rules, where the mass and residue λ_{Ξ_Q} of the Ξ_Q baryons are determined [85], which leads to the value $s_0 = 6.5^2\ GeV^2$ for Ξ_b and $s_0 = 3.0^2\ GeV^2$ for Ξ_c. If we choose the value $s_0 = 6.4^2\ GeV^2$ for Ξ_b and $s_0 = 8\ GeV^2$ for Ξ_c. the results remain practically unchanged. Next, we try to find the working region of M_B^2 where μ_{Ξ_Q} are independent of it at fixed value of β and the above mentioned values of s_0. The upper bound of M_B^2 is obtained requiring that the continuum contribution should be less than the contribution of the first resonance. The lower bound of M_B^2 is determined by requiring that the highest power of $1/M_B^2$ be less than $30^0/_0$ of the highest power of M_B^2. These two conditions are both satisfied in the region $15\ GeV^2 \leq M_B^2 \leq 20\ GeV^2$ and $5\ GeV^2 \leq M_B^2 \leq 8\ GeV^2$ for Ξ_b and Ξ_c, respectively.

In Figs. 5.1 and 5.2, we depict the dependence of $\mu_{\Xi_b^0}$ and $\mu_{\Xi_b^-}$ on M_B^2 at fixed value of β and $s_0 = 6.5^2\ GeV^2$. In Figs. 5.3 and 5.4, we present the dependence of $\mu_{\Xi_c^0}$ and $\mu_{\Xi_c^+}$ on M_B^2 at fixed value of β and $s_0 = 3.0^2\ GeV^2$. From these figures, we see

that the values of the magnetic moments of Ξ_b and Ξ_c exhibit good stability when M_B^2 varies in the region 15 $GeV^2 \leq M_B^2 \leq 20\ GeV^2$ and 5 $GeV^2 \leq M_B^2 \leq 8\ GeV^2$, respectively. The last step of our analysis is the determination of the working region for the auxiliary parameter β. For this aim, in Figs. 5.5, 5.6, 5.7, and 5.8 we present the dependence of the magnetic moments of Ξ_Q baryons on $\cos\theta$ where $\tan\theta = \beta$, using the values of M_B^2 from the "working region" which we already determined and at fixed values of s_0.

From these figures we obtained that the prediction of the magnetic moment μ_{Ξ_b} (μ_{Ξ_c}) is practically independent of the value of the auxiliary parameter β. From all these analysis we deduce the final results for the magnetic moments in Table 5.1 for $\chi = -3.15\ GeV^2$. Comparison of our results on the magnetic moments of Ξ_Q baryons with predictions of other approaches, as we already noted, is also presented in Table 5.1.

Table 5.1: Results for the magnetic moments of Ξ_Q baryons in different approaches.

	$\mu_{\Xi_b^0}$	$\mu_{\Xi_b^-}$	$\mu_{\Xi_c^0}$	$\mu_{\Xi_c^+}$
Our results	-0.045 ± 0.005	-0.08 ± 0.02	0.35 ± 0.05	0.50 ± 0.05
RQM [92]	-0.06	-0.06	0.39	0.41
NQM [92]	-0.06	-0.06	0.37	0.37
[93]	-	-	$-1.02 \div -1.06$	$0.45 \div 0.48$
[94]	-	-	0.32	0.42
[95]	-	-	0.38	0.38
[96]	-	-	0.28	0.28
[97]	-	-	$0.28 \div 0.34$	$0.39 \div 0.46$

We see that within errors our predictions on the magnetic moments are in good agreement with the quark model predictions. Our results on the magnetic moments of Ξ_c are also close to the predictions of the other approaches except the prediction of [93] on $\mu_{\Xi_c^0}$.

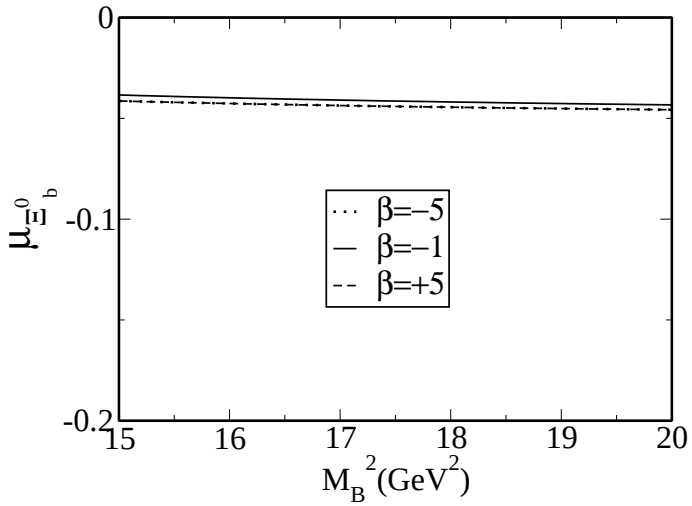

Figure 5.1: The dependence of magnetic moment $\mu_{\Xi_b^0}$ on M_B^2 at $s_0 = 6.5^2\ GeV^2$ and $\beta = \pm 5,\ -1$.

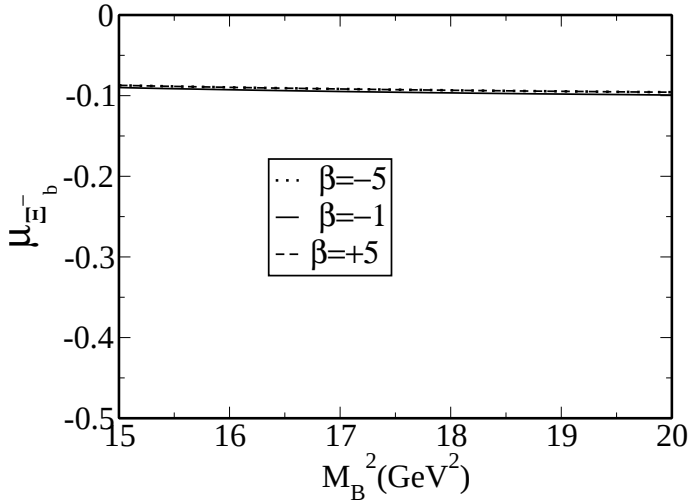

Figure 5.2: The same as Fig. 5.1 but for $\mu_{\Xi_b^-}$.

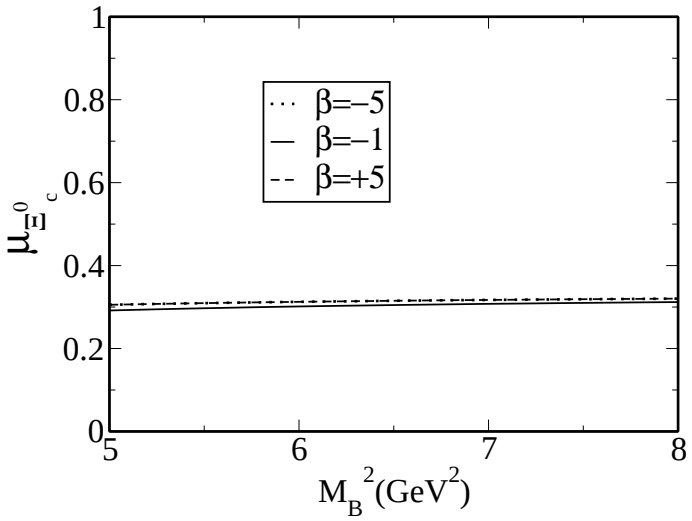

Figure 5.3: The same as Fig. 5.1 but for $\mu_{\Xi_c^0}$ and at $s_0 = 3.0^2\ GeV^2$.

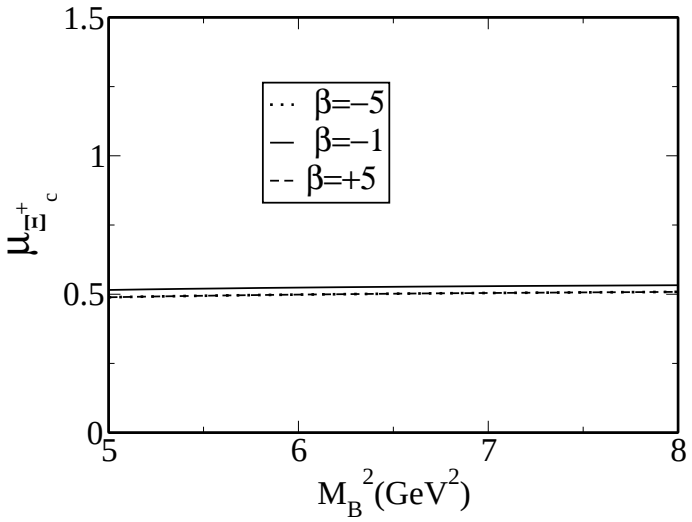

Figure 5.4: The same as Fig. 5.3 but for $\mu_{\Xi_c^+}$.

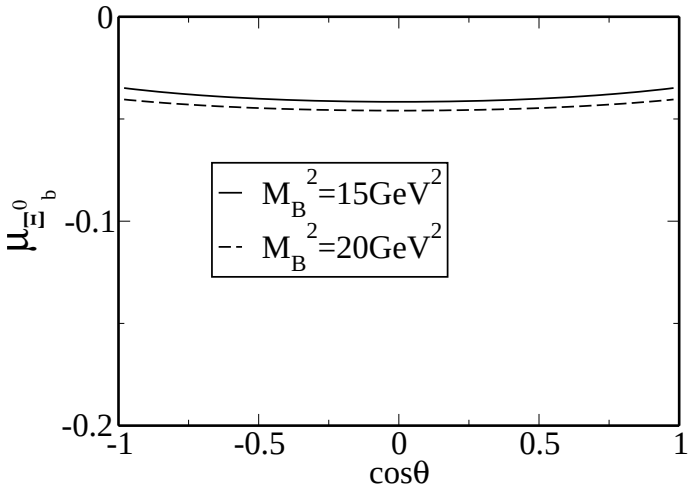

Figure 5.5: The dependence of the magnetic moment $\mu_{\Xi_b^0}$ on $cos\theta$ at $s_0 = 6.5^2\ GeV^2$ and for $M_B^2 = 15\ GeV^2$ and $M_B^2 = 20\ GeV^2$.

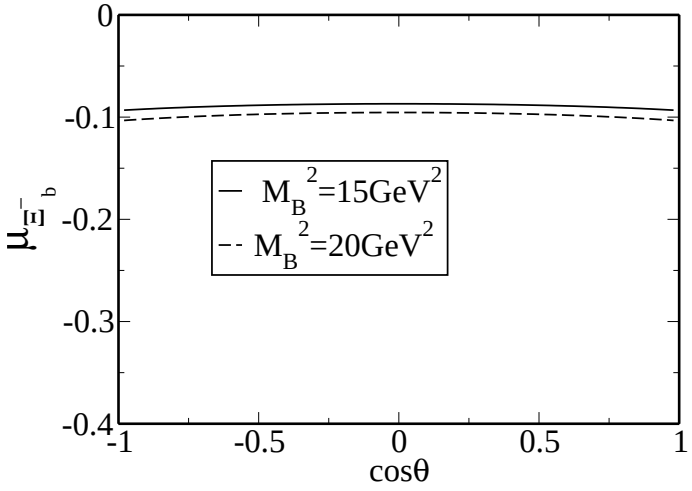

Figure 5.6: The same as Fig. 5.5 but for $\mu_{\Xi_b^-}$.

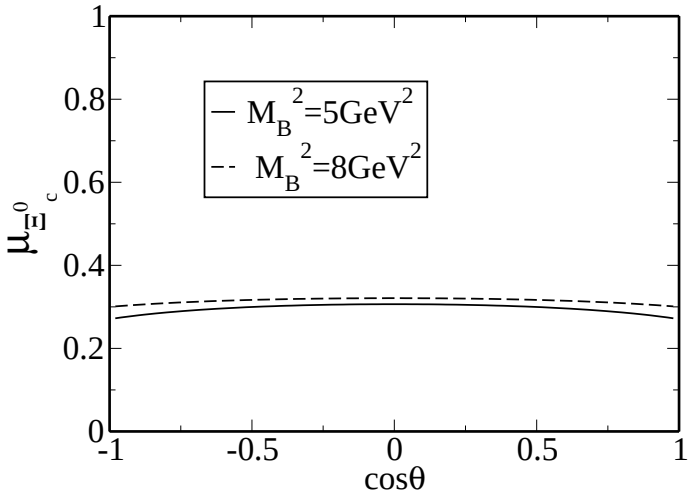

Figure 5.7: The same as Fig. 5.5 but for $\mu_{\Xi_c^0}$ and $s_0 = 3.0^2\ GeV^2$ and for $M_B^2 = 5\ GeV^2$ and $M_B^2 = 8\ GeV^2$.

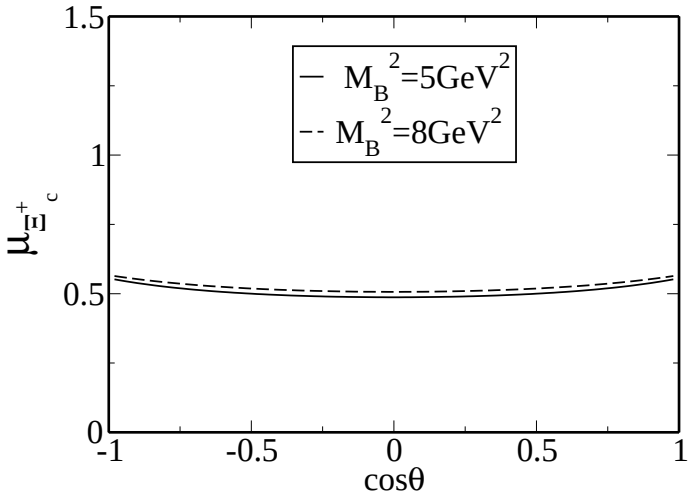

Figure 5.8: The same as Fig. 5.7 but for $\mu_{\Xi_c^+}$.

5.2 Mass and Magnetic Moments of the Heavy Flavored Baryons with $J = \frac{3}{2}$

In this section, we study the masses and magnetic moments of the ground state baryons with total angular momentum 3/2 and containing one heavy quark. First, the light cone QCD sum rules for mass and magnetic moments of heavy baryons are calculated. Then, the numerical analysis of the sum rules for mass and magnetic moments as well as our discussion are presented.

5.2.1 Light Cone QCD Sum Rules for the Mass and Magnetic Moments of the Heavy Flavored Baryons

To calculate the magnetic moments and masses of the heavy flavored hadrons, we start again with the basic object in LCSR method which is the correlation function where hadrons are represented by the interpolating quark currents. For this aim, we consider the correlator

$$T_{\mu\nu} = i \int d^4x e^{ipx} \langle 0 \mid T\{\eta_\mu(x)\bar{\eta}_\nu(0)\} \mid 0\rangle_\gamma, \tag{5.21}$$

where η_μ is the interpolating current of the heavy baryon and γ means the electromagnetic field. In QCD sum rules method, this correlation function is calculated in two different approaches: On the quark level, it describes a hadron as quarks and gluons interacting in QCD vacuum. In the phenomenological side, it is saturated by a tower of hadrons with the same flavor quantum numbers.The magnetic moments are determined by matching two different representations of the correlator function, i.e., theoretical and phenomenological forms, using the dispersion relations.

The phenomenological part of the correlation function can be obtained by inserting the complete set of states between the interpolating currents in (5.21) with quantum numbers of heavy baryons.

$$T_{\mu\nu} = \frac{\langle 0 \mid \eta_\mu \mid B(p_2)\rangle}{p_2^2 - m_B^2} \langle B(p_2) \mid B(p_1)\rangle_\gamma \frac{\langle B(p_1) \mid \bar{\eta}_\nu \mid 0\rangle}{p_1^2 - m_B^2}, \tag{5.22}$$

where $p_1 = p + q$, $p_2 = p$ and q is the photon momentum. The vacuum to baryon

matrix element of the interpolating current is defined as

$$\langle 0 \mid \eta_\mu(0) \mid B(p,s)\rangle = \lambda_B u_\mu(p,s), \tag{5.23}$$

where λ_B is the residue and $u_\mu(p,s)$ is the Rarita-Schwinger spinor. The matrix element $\langle B(p_2) \mid B(p_1)\rangle_\gamma$ entering Eq. (5.22) can be parameterized in the following way

$$\begin{aligned}\langle B(p_2) \mid B(p_1)\rangle_\gamma &= \varepsilon_\rho \bar{u}_\mu(p_2)\Bigg\{-g_{\mu\nu}\left[\gamma_\rho(f_1+f_2) + \frac{(p_1+p_2)_\rho}{2m_B}f_2 + q_\rho f_3\right] \\ &- \frac{q_\mu q_\nu}{(2m_B)^2}\left[\gamma_\rho(G_1+G_2) + \frac{(p_1+p_2)_\rho}{2m_B}G_2 + q_\rho G_3\right]\Bigg\}\bar{u}_\nu(p_1),\end{aligned} \tag{5.24}$$

where ε_ρ is the photon polarization vector, f_i and G_i are the form factors and they are functions of $q^2 = (p_1 - p_2)^2$. In order to obtain the explicit expressions of the correlation function, we perform summation over spins of the spin 3/2 particles using

$$\sum_s u_\mu(p,s)\bar{u}_\nu(p,s) = \frac{(\not{p} + m)}{2m}\{-g_{\mu\nu} + \frac{1}{3}\gamma_\mu\gamma_\nu - \frac{2p_\mu p_\nu}{3m^2} - \frac{p_\mu\gamma_\nu - p_\nu\gamma_\mu}{3m}\}. \tag{5.25}$$

Using Eqs. (5.22-5.25) in principle one can write down the phenomenological part of the correlator. But, the following two drawbacks appear: a) all Lorentz structures are not independent, b) not only spin 3/2, but spin 1/2 states also contribute to the correlation function. Indeed the matrix element of the current η_μ between vacuum and spin 1/2 states is nonzero and is determined as

$$\langle 0 \mid \eta_\mu(0) \mid B(p, s = 1/2)\rangle = \alpha(4p_\mu - m\gamma_\mu)u(p, s = 1/2), \tag{5.26}$$

where the condition $\gamma_\mu \eta^\mu = 0$ is imposed.

There are two different ways to remove the unwanted spin 1/2 contribution and retain only independent structures in the correlation function: 1) Introduce projection operators for the spin 3/2 states, which kill the spin 1/2 contribution, 2) Order Dirac matrices in a specific form and eliminate the structures that receive contributions from spin 1/2 states. In this work, we will follow the second method and choose the ordering for Dirac matrices as $\gamma_\mu \not{p} \not{\varepsilon} \not{q}\gamma_\nu$. With this ordering for the correlator, we

get

$$T_{\mu\nu} = \lambda_B^2 \frac{1}{(p_1^2 - m_B^2)(p_2^2 - m_B^2)} \Big[g_{\mu\nu} \not{p} \not{\epsilon} \not{q} \frac{g_M}{3} + \text{other structures with } \gamma_\mu \text{ at the beginning or } \gamma_\nu \text{ at the end or which are proportional to } p_{2\mu} \text{or } p_{1\nu} \Big], \quad (5.27)$$

where $g_M/3 = f_1 + f_2$ and at $q^2 = 0$, g_M is the magnetic moment of the baryon in units of its natural magneton, $e\hbar/2m_Bc$. The factor 3 is due the fact that in the nonrelativistic limit the interaction Hamiltonian with magnetic field is equal to $g_M B = 3(f_1 + f_2)B$.

From Eq. (5.21), it follows that to calculate the correlation function from QCD side, we need the explicit expressions of the interpolating currents of heavy baryons with the angular momentum $J^P = 3/2^+$. The main condition for constructing the interpolating currents from quark field is that they should have the same quantum numbers as the baryons under consideration. For the heavy baryons with $J^P = 3/2^+$, the interpolating current is chosen in the following general form

$$\eta_\mu = A\epsilon_{abc} \Big\{ (q_1^{aT} C\gamma_\mu q_2^b) Q^c + (q_2^{aT} C\gamma_\mu Q^b) q_1^c + (Q^{aT} C\gamma_\mu q_1^b) q_2^c \Big\}, \quad (5.28)$$

where C is the charge conjugation operator and a, b and c are color indices. The value of A and quark fields q_1 and q_2 for each heavy baryons is given in Table 5.2. After

Table 5.2: The value of A and quark fields q_1 and q_2 for the corresponding baryons.

	A	q_1	q_2
$\Sigma_{b(c)}^{*+(++)}$	$1/\sqrt{3}$	u	u
$\Sigma_{b(c)}^{*0(+)}$	$\sqrt{2/3}$	u	d
$\Sigma_{b(c)}^{*-(0)}$	$1/\sqrt{3}$	d	d
$\Xi_{b(c)}^{*0(+)}$	$\sqrt{2/3}$	s	u
$\Xi_{b(c)}^{*-(0)}$	$\sqrt{2/3}$	s	d
$\Omega_{b(c)}^{*-(0)}$	$1/\sqrt{3}$	s	s

contracting out the quark pairs in Eq. (5.21) using the Wick's theorem, we get the

following expression for the correlation function in terms of quark propagators

$$\begin{aligned}\Pi_{\mu\nu} &= -iA^2\epsilon_{abc}\epsilon_{a'b'c'}\int d^4x e^{ipx}\langle 0[\gamma(q)] \mid \{S_Q^{ca'}\gamma_\nu S_{q_2}^{\prime bb'}\gamma_\mu S_{q_1}^{ac'} \\ &+ S_Q^{cb'}\gamma_\nu S_{q_1}^{\prime aa'}\gamma_\mu S_{q_2}^{bc'} + S_{q_2}^{ca'}\gamma_\nu S_{q_1}^{\prime bb'}\gamma_\mu S_Q^{ac'} + S_{q_2}^{cb'}\gamma_\nu S_Q^{\prime aa'}\gamma_\mu S_{q_1}^{bc'} \\ &+ S_{q_1}^{cb'}\gamma_\nu S_{q_2}^{\prime aa'}\gamma_\mu S_Q^{bc'} + S_{q_1}^{ca'}\gamma_\nu S_Q^{\prime bb'}\gamma_\mu S_{q_2}^{ac'} + Tr(\gamma_\mu S_{q_1}^{ab'}\gamma_\nu S_{q_2}^{\prime ba'})S_Q^{cc'} \\ &+ Tr(\gamma_\mu S_Q^{ab'}\gamma_\nu S_{q_1}^{\prime ba'})S_{q_2}^{cc'} + Tr(\gamma_\mu S_{q_2}^{ab'}\gamma_\nu S_Q^{\prime ba'})S_{q_1}^{cc'}\} \mid 0\rangle, \end{aligned} \tag{5.29}$$

where $S' = CS^TC$ and $S_Q(S_q)$ is the full heavy (light) quark propagator. In calculation of the correlation function from QCD side, we take into account terms linear in m_q and neglect quadratic terms.The correlator contains three different contributions (for these three contributions and the methods of their calculations see the previous section).

Using the expressions of the light and heavy full quark propagators and the photon DA's and separating the coefficient of the structure $g_{\mu\nu}\ \not{p}\ \not{\varepsilon}\ \not{q}$, the expression of the correlation function from QCD side is obtained. Separating the coefficient of the same structure from phenomenological part and equating these representations of the correlator, we get sum rules for the magnetic moments of the $J^P = 3/2^+$ heavy baryons. In order to suppress the contribution of higher states and continuum, Borel transformation with respect to the variables $p_2^2 = p^2$ and $p_1^2 = (p+q)^2$ is applied.

Before presenting the sum rules for the magnetic moments, few words about the relations between the correlation functions are in order. Note that the correlation function (more precisely, coefficient of the structure $g_{\mu\nu}\ \not{p}\ \not{\varepsilon}\ \not{q}$) can be written in the form

$$\Pi(q_1,q_2,Q) = e_{q_1}\Pi_1(q_1,q_2,Q) + e_{q_2}\Pi_1'(q_1,q_2,Q) + e_Q\Pi_2(q_1,q_2,Q). \tag{5.30}$$

where Π_1 corresponds to the emission of the photon from the quark q_1, Π_1' to emission from q_2 and Π_2 to emission from the heavy quark Q. Note that the functions $\Pi_i(q_1,q_2,q_3)$ $(i = 1,\ 2)$ do not depend on the quark charges in the limit where we neglect electromagnetic corrections.

From the explicit form of the interpolating current it follows that it is symmetric under the exchange of the light quarks, i.e. $q_1 \longleftrightarrow q_2$, and for this reason $\Pi_1(q_1,q_2,Q) = \Pi_1'(q_2,q_1,Q)$.

Due to the symmetries between the interpolating currents, any interpolating current can be obtained from the interpolating current for $\Sigma_{b(c)}^{*0(+)}$. This also leads to relations between their correlation functions. In terms of the defined $\Pi_1(q_1, q_2, Q)$ and $\Pi_2(q_1, q_2, Q)$, all the correlation functions can be written as:

$$\begin{aligned}
\Pi^{\Sigma_b^{*0}} &= e_u\Pi_1(u,d,b) + e_d\Pi_1(d,u,b) + e_b\Pi_2(u,d,b),\\
\Pi^{\Sigma_b^{*+}} &= \Pi^{\Sigma_b^{*0}}(d\to u) = 2e_u\Pi_1(u,u,b) + e_b\Pi_2(u,u,b),\\
\Pi^{\Sigma_b^{*-}} &= \Pi^{\Sigma_b^{*0}}(u\to d) = 2e_d\Pi_1(d,d,b) + e_b\Pi_2(d,d,b),\\
\Pi^{\Xi_b^{*0}} &= \Pi^{\Sigma_b^{*0}}(d\to s) = e_u\Pi_1(u,s,b) + e_s\Pi_1(s,u,b) + e_b\Pi_2(u,s,b),\\
\Pi^{\Xi_b^{*-}} &= \Pi^{\Sigma_b^{*0}}(u\to s) = e_s\Pi_1(s,d,b) + e_d\Pi_1(d,s,b) + e_b\Pi_2(s,d,b),\\
\Pi^{\Omega_b^{*-}} &= \Pi^{\Sigma_b^{*0}}(u\to s, d\to s) = 2e_s\Pi_1(s,s,b) + e_b\Pi_2(s,s,b),
\end{aligned} \tag{5.31}$$

and the relations for the charmed baryons can simply be obtained from Eq. (5.31), by $b \to c$. Note that in the $SU(3)_f$ limit, the correlation functions can be expressed as:

$$\begin{aligned}
\Pi^{\Sigma_b^{*0}} &= \frac{1}{3}\Pi_1(b) - \frac{1}{3}\Pi_2(b),\\
\Pi^{\Sigma_b^{*+}} &= \frac{4}{3}\Pi_1(b) - \frac{1}{3}\Pi_2(b),\\
\Pi^{\Sigma_b^{*-}} &= -\frac{2}{3}\Pi_1(b) - \frac{1}{3}\Pi_2(b),\\
\Pi^{\Xi_b^{*0}} &= \frac{1}{3}\Pi_1(b) - \frac{1}{3}\Pi_2(b),\\
\Pi^{\Xi_b^{*-}} &= -\frac{2}{3}\Pi_1(b) - \frac{1}{3}\Pi_2(b),\\
\Pi^{\Omega_b^{*-}} &= -\frac{2}{3}\Pi_1(b) - \frac{1}{3}\Pi_2(b),
\end{aligned} \tag{5.32}$$

where, for simplicity, we have used the short hand notation $\Pi_i(q_1, q_2, Q) = \Pi_i(Q)$ ($i = 1,\ 2$) since in the assumed $SU(3)_f$ limit, all the light quarks have the same mass, condensates, etc.

From Eq. (5.32) follows the well known $SU(3)_f$ relations between the correlation functions, and hence the magnetic moments (part of these relations were derived in

[111]):

$$\begin{aligned}
\Pi^{\Sigma_b^{*+}} + \Pi^{\Sigma_b^{*-}} &= 2\Pi^{\Sigma_b^{*0}}, \\
\Pi^{\Sigma_b^{*-}} &= \Pi^{\Xi_b^{*-}} = \Pi^{\Omega_b^{*-}}, \\
\Pi^{\Sigma_b^{*+}} + \Pi^{\Omega_b^{*-}} &= 2\Pi^{\Xi_b^{*0}}, \\
\Pi^{\Sigma_b^{*+}} + 2\Pi^{\Xi_b^{*-}} &= \Pi^{\Sigma_b^{*-}} + 2\Pi^{\Xi_b^{*0}}, \\
\Pi^{\Sigma_b^{*0}} &= \Pi^{\Xi_b^{*0}},
\end{aligned} \tag{5.33}$$

and the corresponding expressions for the charmed baryons. Any deviation from these relations in the magnetic moments is a sign of $SU(3)_f$ violation. Note that the first relation in Eq. (5.33) is a direct consequence of the isospin subgroup of $SU(3)_f$. Since in this work, set $m_u = m_d$ and $\langle \bar{u}u \rangle = \langle \bar{d}d \rangle$, i.e. we assume isospin symmetry, our results satisfy this relation exactly. And hence, in the following, we will not show numerical results form the magnetic moment of $\Sigma_{b(c)}^{*0(+)}$.

Once the explicit forms of the functions $\Pi_i(q_1, q_2, Q)(i = 1, 2)$ are known, the sum rules for the magnetic moments can be obtained using Eq. 5.31 and

$$-\lambda_B^2 \frac{\mu_{B_Q}}{3} e^{\frac{-m_{B_Q}^2}{M^2}} = A^2 \Pi^{B_Q}. \tag{5.34}$$

The functions $\Pi_i(q_1, q_2, Q)$ can be written as:

$$\Pi_i = \int_{m_Q^2}^{s_0} e^{\frac{-s}{M^2}} \rho_i(s) ds + e^{\frac{-m_Q^2}{M^2}} \Gamma_i. \tag{5.35}$$

where

$$
\begin{aligned}
\rho_1(s) &= < q_1q_1 >< q_2q_2 > \left[-\frac{1}{6}\chi_i\varphi_\gamma(u_0)\right] \\
&+ m_0^2 < q_2q_2 > \left[\{-\frac{m_Q^2}{16\pi^2M^4} - \frac{19}{288\pi^2M^2}\}m_{q_1}ln(\frac{s-m_Q^2}{\Lambda^2})\right. \\
&+ \frac{1}{288\pi^2m_Q^2}\{8(1+\psi_{11})m_Q - [-9+4\psi_{02}+5\psi_{10}+8\psi_{12}-9\psi_{21}+8\psi_{22} \\
&+ 4\gamma_E(23+\psi_{02}+2\psi_{12}+\psi_{22})+4\psi_{32}]m_{q_1} - 6(-1+2\psi_{12}+\psi_{22})m_{q_2} \\
&+ 6(16+2\psi_{02}-18\psi_{03}-50\psi_{10}+9\psi_{21}+93\psi_{23}-4\psi_{32}+120\psi_{33}+45\psi_{43}) \\
&\times \left. m_{q_1}ln(\frac{s-m_Q^2}{\Lambda^2})\}\right] \\
&+ < q_2q_2 > \frac{1}{16\pi^2}\left[4(\psi_{10}-\psi_{21})m_Q - \{-1+4\psi_{01}-\psi_{02}+2\psi_{11}+\psi_{22}\right. \\
&+ 2\gamma_E(1+\psi_{02}+2\psi_{12}+\psi_{22})\}m_{q_1} - (1+\psi_{02})m_{q_2} + 2m_{q_1}\{ln(\frac{\Lambda^2}{m_Q^2}) \\
&+ \left.(2-\psi_{02}-2\psi_{10}+3\psi_{22}+2\psi_{32})ln(\frac{s-m_Q^2}{\Lambda^2}) + ln(\frac{m_Q^2(s-m_Q^2)}{\Lambda^2 s})\}\right] \\
&+ < q_1q_1 > \frac{1}{96\pi^2}\left[-3\{(\psi_{10}-\psi_{21})m_Q + m_{q_2}\}\mathbb{A}(u_0)\right. \\
&+ 2\left(\{-1+4\psi_{01}-\psi_{02}+2\psi_{11}+\psi_{22}+2\gamma_E(1+\psi_{02}+2\psi_{12}+\psi_{22})\}\right. \\
&\times m_{q_2}(\eta_1-3\eta_2) + 2(\psi_{21}-\psi_{10})\{m_Q(\eta_1+3\eta_2) \\
&+ 2m_{q_2}\eta_1 - (m_Q+m_{q_2})(\eta_4-\eta_3)\} \\
&- 2(\eta_1-3\eta_2)\left\{ m_Q ln(\frac{s}{m_Q^2}) + m_{q_2}\{ln(\frac{\Lambda^2}{m_Q^2})\right. \\
&+ \left.\left.(2-\psi_{02}-2\psi_{10}+3\psi_{22}+2\psi_{32})ln(\frac{s-m_Q^2}{\Lambda^2}) + ln(\frac{m_Q^2(s-m_Q^2)}{\Lambda^2 s})\}\right\}\right. \\
&+ \left. 3m_Q^2\chi_i\{2m_Q\psi_{10} - (m_Q-m_{q_2})(\psi_{20}-\psi_{31}) + 2m_Q ln(\frac{m_Q^2}{s})\}\,\varphi_\gamma(u_0)\right)\Bigg] \\
&+ \frac{m_Q^3}{256\pi^4}\left[m_Q(12\psi_{10}-6\psi_{20}+4\psi_{30}-5\psi_{42}\right. \\
&- 4\psi_{52} + m_{q_1}(18-18\psi_{01}+114\psi_{10} \\
&- \left. 66\psi_{20}+12\psi_{31}) - 24m_{q_2}(2\psi_{10}-\psi_{20}+\psi_{31}) - 12\{6+\psi_{10}+12ln(\frac{\Lambda^2}{m_Q^2})\}\right. \\
&\times m_{q_1}ln(\frac{\Lambda^2}{m_Q^2}) - 12m_Q ln(\frac{s}{m_Q^2}) + 12\left(\{2+\psi_{01}-ln(\frac{\Lambda^2}{s})\}m_{q_1}ln(\frac{\Lambda^2}{s})\right. \\
&+ \left. ln(\frac{m_Q^2}{s})\{2(1-4ln(\frac{s-m_Q^2}{\Lambda^2}))m_{q_1} - 4m_{q_2}\} + m_{q_1}\{(1+\psi_{01}-7\psi_{10}+3\psi_{20}\right.
\end{aligned}
$$

$$
\begin{aligned}
&+ \quad 2ln(\frac{s}{m_Q^2}))ln(\frac{s-m_Q^2}{\Lambda^2}) - (3+\psi_{10})ln(\frac{m_Q^2(s-m_Q^2)}{\Lambda^2 s}) \\
&+ \quad \psi_{01}ln(\frac{s(s-m_Q^2)}{\Lambda^2 m_Q^2})\} \Big) - 24\{4Li_2(1-\frac{m_Q^2}{s}) - Li_2(1-\frac{s}{m_Q^2})\}m_{q_1} \Big] \\
&+ \quad \frac{f_{3\gamma}m_Q^2}{48\pi^2}\Big[-2\eta'\{\psi_{10} + ln(\frac{m_Q^2}{s})\} + (3\psi_{31}+4\psi_{32}+3\psi_{42})\psi^a(u_0)\Big],
\end{aligned}
\tag{5.36}
$$

$$
\begin{aligned}
\rho_2(s) &= m_0^2 < q_1 q_1 > \\
&\times \Big[-\frac{5(1+\psi_{11})}{288\pi^2 m_Q} + \frac{m_{q_2}}{18\pi^2 M^2}ln(\frac{s-m_Q^2}{\Lambda^2}) - \frac{m_{q_2}}{36\pi^2 m_Q^2}\{\psi_{02}-\psi_{10} \\
&+ 2(\psi_{12}+\psi_{22}) + \gamma_E(-4+\psi_{02}+2\psi_{12}+\psi_{22}) + \psi_{32} + 3(1-\psi_{02}-2\psi_{10} \\
&+ 3\psi_{22}+2\psi_{32})ln(\frac{s-m_Q^2}{\Lambda^2})\} \Big] \\
&+ m_0^2 < q_2 q_2 > \\
&\times \Big[-\frac{5(1+\psi_{11})}{288\pi^2 m_Q} + \frac{m_{q_1}}{18\pi^2 M^2}ln(\frac{s-m_Q^2}{\Lambda^2}) - \frac{m_{q_1}}{36\pi^2 m_Q^2}\{\psi_{02}-\psi_{10} \\
&+ 2(\psi_{12}+\psi_{22}) + \gamma_E(-4+\psi_{02}+2\psi_{12}+\psi_{22}) + \psi_{32} + 3(1-\psi_{02}-2\psi_{10} \\
&+ 3\psi_{22}+2\psi_{32})ln(\frac{s-m_Q^2}{\Lambda^2})\} \Big] \\
&+ < q_1 q_1 > \frac{1}{16\pi^2} \\
&\times \Big[(\psi_{02}-1)m_{q_1} - 2(\psi_{10}-\psi_{21})(m_Q - 2m_{q_2}) + 2m_Q ln(\frac{s}{m_Q^2}) \Big] \\
&+ < q_2 q_2 > \frac{1}{16\pi^2} \\
&\times \Big[(\psi_{02}-1)m_{q_2} - 2(\psi_{10}-\psi_{21})(m_Q - 2m_{q_1}) + 2m_Q ln(\frac{s}{m_Q^2}) \Big] \\
&+ \frac{m_Q^3}{768\pi^4}\Big[(-4\psi_{30}+5\psi_{42}+4\psi_{52})m_Q + 18\psi_{31}(m_{q_1}+m_{q_2}) \\
&- 12\psi_{10}\{7m_Q - 9(m_{q_1}+m_{q_2})\} - 6\psi_{20}\{m_Q + 3(m_{q_1}+m_{q_2})\} \\
&- 24\{2(1+\psi_{10})m_Q - 3(m_{q_1}+m_{q_2})\}ln(\frac{m_Q^2}{s}) \\
&+ 36\{m_Q - (1+\psi_{10})(m_{q_1}+m_{q_2})\}ln(\frac{s}{m_Q^2}) \Big],
\end{aligned}
\tag{5.37}
$$

$$
\begin{aligned}
\Gamma_1 &= m_0^2 < q_1q_1 >< q_2q_2 > \left[\frac{m_Q^5 m_{q_2} \mathbb{A}(u_0)}{288M^8} - \frac{m_Q^3}{864M^6}\{-4m_{q_2}(\eta_1 - 3\eta_2) \right. \\
&+ (9m_Q + 10m_{q_2})\mathbb{A}(u_0)\} - \frac{m_Q}{2164M^4}\{m_{q_2}(\eta_1 - 3\eta_2) + 3m_Q(2\eta_1 + \eta_3 - 2\eta_4) \\
&- (m_Q + m_{q_2})\mathbb{A}(u_0) + 3m_Q^2 m_{q_2}\chi_i\varphi_\gamma(u_0)\} - \frac{m_Q}{216M^2}(9m_Q + 4m_{q_2})\chi_i\varphi_\gamma(u_0) \\
&+ \left. \frac{5}{216}\chi_i\varphi_\gamma(u_0) \right] \\
&+ < q_1q_1 >< q_2q_2 > \\
&\times \left[-\frac{m_Q^3 m_{q_2}\mathbb{A}(u_0)}{48M^4} + \frac{m_Q}{72M^2}\{2m_{q_2}(-\eta_1 + 3\eta_2) + 3m_Q\mathbb{A}(u_0)\} \right. \\
&+ \left. \frac{1}{72}\{2(4\eta_1 + 2\eta_3 - 4\eta_4) + 3\mathbb{A}(u_0) + 6m_Q m_{q_2}\chi_i\varphi_\gamma(u_0)\} \right] \\
&+ m_0^2 < q_2q_2 > \left[\frac{\gamma_E m_{q_1} M^2}{3\pi^2 m_Q^2} + \frac{m_Q^2}{96\pi^2 M^2}\{2m_{q_2} - 3m_{q_1} ln(\frac{\Lambda^2}{m_Q^2})\} \right. \\
&- \frac{1}{288\pi^2}\{18m_Q + 9m_{q_1} + 14m_{q_1}(2\gamma_E + ln(\frac{\Lambda^2}{m_Q^2})) + 4m_{q_2}\} \\
&+ \left. \frac{f_{3\gamma} m_Q^2 m_{q_2}(\eta' + 4\psi^a(u_0))}{216M^4} \right] \\
&+ < q_2q_2 > \left[\frac{\gamma_E M^2 m_{q_1}}{4\pi^2} - \frac{1}{36} f_{3\gamma} m_{q_2}(\eta' + 3\psi^a(u_0)) \right] \\
&- < q_1q_1 > \left[\frac{\gamma_E M^2 m_{q_2}}{12\pi^2}(\eta_1 - 3\eta_2) \right], \qquad (5.38)
\end{aligned}
$$

$$
\begin{aligned}
\Gamma_2 &= m_0^2 < q_1q_1 >< q_2q_2 > \left[-\frac{5m_Q^3(m_{q_1} + m_{q_2})}{144M^6} + \frac{m_Q(24m_Q + 5(m_{q_1} + m_{q_2})}{144M^4} \right] \\
&+ < q_1q_1 >< q_2q_2 > \left[-\frac{1}{3} + \frac{m_Q(m_{q_1} + m_{q_2})}{12M^2} \right] \\
&+ m_0^2 < q_1q_1 > \left[-\frac{\gamma_E m_{q_2} M^2}{12\pi^2 m_Q^2} + \frac{1}{144\pi^2}\{(-9 + 8\gamma_E + 4ln(\frac{\Lambda^2}{m_Q^2}))m_{q_2} + m_{q_1}\} \right] \\
&+ m_0^2 < q_2q_2 > \left[-\frac{\gamma_E m_{q_1} M^2}{12\pi^2 m_Q^2} + \frac{1}{144\pi^2}\{(-9 + 8\gamma_E + 4ln(\frac{\Lambda^2}{m_Q^2}))m_{q_1} + m_{q_2}\} \right], \\
&\qquad (5.39)
\end{aligned}
$$

Where $Li_2(x)$ is the dilogarithm function. The functions entering Eqs. (5.36-5.39) are

given as

$$\begin{aligned}\eta_i &= \int \mathcal{D}\alpha_i \int_0^1 dv f_i(\alpha_i)\delta(\alpha_q + v\alpha_g - u_0),\\ \eta' &= \int \mathcal{D}\alpha_i \int_0^1 dv \mathcal{V}(\alpha_i)\delta'(\alpha_q + v\alpha_g - u_0),\end{aligned} \tag{5.40}$$

and $f_1(\alpha_i) = \mathcal{S}(\alpha_i)$, $f_2(\alpha_i) = \tilde{\mathcal{S}}(\alpha_i)$, $f_3(\alpha_i) = \mathcal{T}_4(\alpha_i)$ and $f_4(\alpha_i) = v\mathcal{T}_4(\alpha_i)$ are the photon distribution amplitudes. Note that in the above equations, the Borel parameter M^2 is defined as $M^2 = \frac{M_1^2 M_2^2}{M_1^2+M_2^2}$ and $u_0 = \frac{M_1^2}{M_1^2+M_2^2}$. Since the masses of the initial and final baryons are the same, we will set $M_1^2 = M_2^2 = 2M^2$ and hence $u_0 = 1/2$. The contributions of the terms $\sim< G^2 >$ are also calculated , but their numerical values are very small and therefore for customary in the expressions these terms are omitted.

For calculation of the magnetic moments of the considered baryons, their residues λ_B as well as their masses are needed (see Eq. (5.34)). Note that many of the considered baryons are not discovered yet in the experiments. The residue is determined from two point sum rules. For the interpolating current given in Eq. (5.28), we obtain the following result for λ_B^2:

$$\lambda_B^2 e^{\frac{-m_{B_Q}^2}{M^2}} = A^2\Big[\Pi' + \Pi'(q_1 \longleftrightarrow q_2)\Big], \tag{5.41}$$

where

$$\begin{aligned}\Pi' &= \int_{m_Q^2}^{s_0} ds\, e^{-s/M^2}\left\{m_0^2 < q_1q_1 > \left[\frac{(m_{q_1} - 6m_Q)(\psi_{22} + 2\psi_{12} - 1)}{192m_Q^2\pi^2}\right]\right.\\
&- < q_1q_1 > \left[\frac{2(\psi_{02} + 2\psi_{10} - 2\psi_{21} - 1)m_Q + (\psi_{02} - 1)(3m_{q_1} - 2m_{q_2})}{32\pi^2}\right]\\
&- \frac{m_Q^3}{512\pi^4}\Big[- 8(3\psi_{31} + 2\psi_{32})m_{q_1}\\
&+ 3\{(2\psi_{30} - 4\psi_{41} + \frac{5}{2}\psi_{42} + 2\psi_{52})m_Q - 4\psi_{42}m_{q_1}\}\\
&+ \left.6(2\psi_{10} - \psi_{20})(\frac{3}{2}m_Q - 2m_{q_1}) - 6(4m_{q_1} - 3m_Q)ln(\frac{m_Q^2}{s})\Big]\right\}\end{aligned}$$

$$
\begin{aligned}
&+ \quad e^{-m_Q^2/M^2}\left\{m_0^2 < q_1q_1 >< q_2q_2 > \right.\\
&\times \quad \left[\frac{-5m_Q^3 m_{q_1}}{144M^6} + \frac{m_Q(m_Q+5m_{q_1})}{24M^4} - \frac{5}{24M^2}\right]\\
&+ \quad < q_1q_1 >< q_2q_2 > \left[\frac{1}{12} - \frac{m_Q m_{q_1}}{12M^2}\right] + m_0^2 < q_1q_1 > \left.\left[\frac{6m_{q_2}-7m_{q_1}}{192\pi^2}\right]\right\}
\end{aligned}
\tag{5.42}
$$

The masses of the considered baryons can also be determined from sum rules. For this aim, one can get the derivative from both side of Eq. (5.41) with respect to $-1/M^2$ and divide the obtained result to the Eq. (5.41), i.e.,

$$
m_{B_Q}^2 = \frac{-\frac{d}{d(1/M^2)}\left[\Pi' + \Pi'(q_1 \longleftrightarrow q_2)\right]}{\left[\Pi' + \Pi'(q_1 \longleftrightarrow q_2)\right]}. \tag{5.43}
$$

5.2.2 Numerical Analysis

In this section, we perform numerical analysis for the mass and magnetic moments of the heavy flavored baryons. Firstly, we present the input parameters used in the analysis of the sum rules: $\langle\bar{u}u\rangle(1\ GeV) = \langle\bar{d}d\rangle(1\ GeV) = -(0.243)^3\ GeV^3$, $\langle\bar{s}s\rangle(1\ GeV) = 0.8\langle\bar{u}u\rangle(1\ GeV)$, $m_0^2(1\ GeV) = (0.8 \pm 0.2)\ GeV^2$ [107], factorization parameter in light quark propagator, $\Lambda = 1\ GeV$ and $f_{3\gamma} = -0.0039\ GeV^2$ [16]. The value of the magnetic susceptibility was obtained in various papers as $\chi(1\ GeV) = -3.15 \pm 0.3\ GeV^{-2}$ [16], $\chi(1\ GeV) = -(2.85 \pm 0.5)\ GeV^{-2}$ [108] and $\chi(1\ GeV) = -4.4\ GeV^{-2}$[110].

Before proceeding to the results for the magnetic moments, we calculate the masses of heavy flavored baryons predicted from mass sum rules. Obviously, the masses should not depend on the Borel mass parameter M^2 in a complete theory. This condition for bottom (charmed) baryons are satisfied when M^2 varies in the interval $15\ GeV^2 < M^2 < 30\ GeV^2$ ($4\ GeV^2 < M^2 < 12\ GeV^2$). In Figs. 5.9-5.14, we presented the dependence of the mass of the heavy flavored baryons on M^2. From these figures, we see very good stability with respect to M^2. The sum rule predictions of the mass of the heavy flavored baryons are presented in Table 5.3 in comparison

with some theoretical predictions and experimental results. Note that the masses of the heavy flavored baryons are calculated in the framework of heavy quark effective theory (HQET) using the QCD sum rules method in [112].

Table 5.3: Comparison of mass of the heavy flavored baryons in GeV from present work and other approaches and with experiment.

	$m_{\Omega_b^*}$	$m_{\Omega_c^*}$	$m_{\Sigma_b^*}$	$m_{\Sigma_c^*}$	$m_{\Xi_b^*}$	$m_{\Xi_c^*}$
this work	6.08 ± 0.40	2.72 ± 0.20	5.85 ± 0.35	2.51 ± 0.15	5.97 ± 0.40	2.66 ± 0.18
[112]	$6.063^{+0.083}_{-0.082}$	$2.790^{+0.109}_{-0.105}$	$5.835^{+0.082}_{-0.077}$	$2.534^{+0.096}_{-0.081}$	$5.929^{+0.088}_{-0.079}$	$2.634^{+0.102}_{-0.094}$
[69]	6.088	2.768	5.834	2.518	5.963	2.654
[65]	-	-	5.805	2.495	-	-
[66]	6.090	2.770	5.850	2.520	5.980	2.650
[113]	-	2.768	-	2.518	-	-
[67]	6.083	2.760	5.840	-	5.966	-
[68]	6.060	2.752	5.871	2.5388	5.959	2.680
Exp[114]	-	2.770	5.836	2.520	-	2.645

After determination of the masses as well as residues of the heavy flavored baryons our next task is the calculation of the numerical values of their magnetic moments. For this aim, from sum rules for the magnetic moments it follows that the photon DA's are needed (see Eq. (5.20)).

The sum rules for magnetic moments also contain the auxiliary parameters: Borel parameter M^2 and continuum threshold s_0. Similar to mass sum rules, the magnetic moments should also be independent of these parameters. In the general case, the working region of M^2 and s_0 for the mass and magnetic moments should be different. To find the working region for M^2, we proceed as follows. The upper bound is obtained requiring that the contribution of higher states and continuum should be less than the ground state contribution. The lower bound of M^2 is determined from condition that the highest power of $1/M^2$ be less than say $30^0/_0$ of the highest power of M^2. These two conditions are both satisfied in the region $15\ GeV^2 \leq M^2 \leq 30\ GeV^2$ and $4\ GeV^2 \leq M^2 \leq 12\ GeV^2$ for baryons containing b and c-quark, respectively. The working region for the Borel parameter for mass and magnetic moments practically coincide, but again we should stress that, this circumstance is accidental.

In Figs. 5.15-5.24, we present the dependence of the magnetic moment of heavy flavored baryons on M^2 at two fixed values of continuum threshold s_0. From these figures, we see that the magnetic moments weakly depend on s_0. The maximal change of results is about $10\,{}^0/_0$ with variation of s_0. The magnetic moments also are practically insensitive to the variation of Borel mass parameter when it varies in the working region. We should also stress that our results practically don't change considering three values of χ which we presented at the beginning of this section. Our final results on the magnetic moments of heavy flavored baryons are presented in Table 5.4. For comparison, the predictions of hyper central model [93] are also presented. The quoted errors in Table 5.4 are due to the uncertainties in m_0^2, variation of s_0 and M^2 as well as errors in the determination of the input parameters.

Table 5.4: The magnetic moments of the heavy flavored baryons in units of nucleon magneton.

	Our results	hyper central model[93]
$\mu_{\Omega_b^{*-}}$	-1.40 ± 0.35	$-1.178 \div -1.201$
$\mu_{\Omega_c^{*0}}$	-0.62 ± 0.18	$-0.827 \div -0.867$
$\mu_{\Sigma_b^{*-}}$	-1.50 ± 0.36	$-1.628 \div -1.657$
$\mu_{\Sigma_b^{*0}}$	0.50 ± 0.15	$0.778 \div 0.792$
$\mu_{\Sigma_b^{*+}}$	2.52 ± 0.50	$3.182 \div 3.239$
$\mu_{\Sigma_c^{*0}}$	-0.81 ± 0.20	$-0.826 \div -0.850$
$\mu_{\Sigma_c^{*+}}$	2.00 ± 0.46	$1.200 \div 1.256$
$\mu_{\Sigma_c^{*++}}$	4.81 ± 1.22	$3.682 \div 3.844$
$\mu_{\Xi_b^{*-}}$	-1.42 ± 0.35	$-1.048 \div -1.098$
$\mu_{\Xi_b^{*0}}$	0.50 ± 0.15	$1.024 \div 1.042$
$\mu_{\Xi_c^{*0}}$	-0.68 ± 0.18	$-0.671 \div -0.690$
$\mu_{\Xi_c^{*+}}$	1.68 ± 0.42	$1.449 \div 1.517$

Although the $SU(3)_f$ breaking effects have been taken into account through a nonzero s-quark mass and different strange quark condensate, we predict that $SU(3)_f$ symmetry violation in the magnetic moments is very small, except the relations $\mu_{\Sigma_c^{*+}} = \mu_{\Xi_c^{*+}}$ and $\Pi^{\Sigma_c^{*++}} + \Pi^{\Omega_c^{*0}} = 2\Pi^{\Xi_c^{*+}}$, where the $SU(3)_f$ symmetry violation is large. For the values of the magnetic moments, our results are consistent with the results of [93] except for the $\mu_{\Omega_b^{*-}}$, $\mu_{\Xi_b^{*-}}$ and especially for the $\mu_{\Sigma_c^{*+}}$, $\mu_{\Xi_b^{*0}}$ which we see a big discrepancy between two predictions.

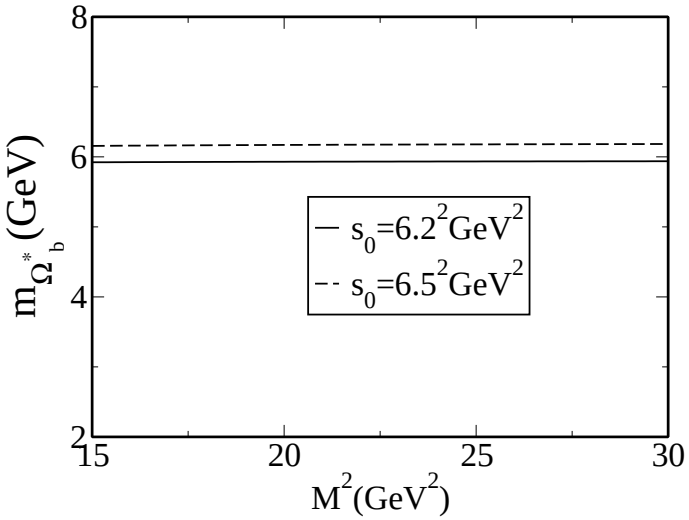

Figure 5.9: The dependence of mass of the Ω_b^* on the Borel parameter M^2 for two fixed values of continuum threshold s_0.

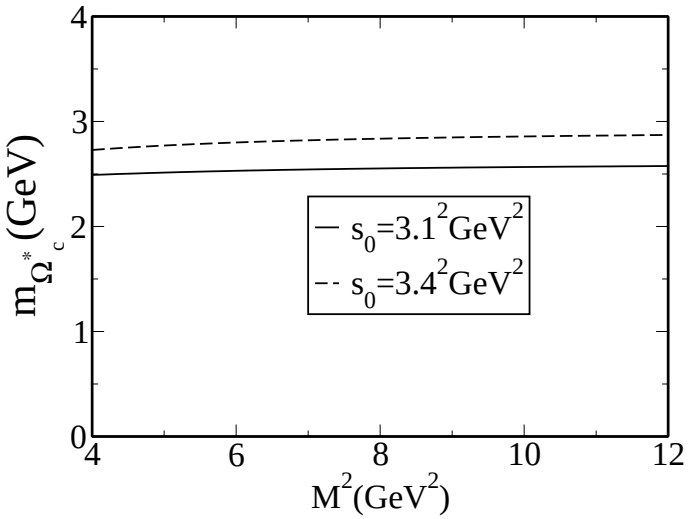

Figure 5.10: The dependence of mass of the Ω_c^* on the Borel parameter M^2 for two fixed values of continuum threshold s_0.

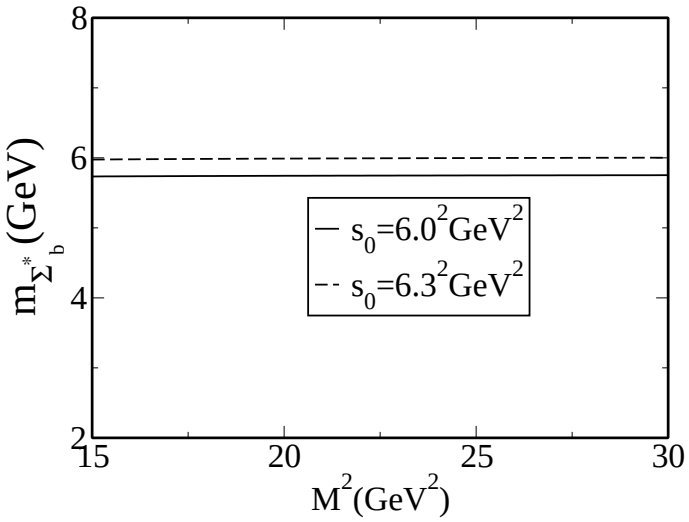

Figure 5.11: The same as Fig. 5.9, but for Σ_b^*.

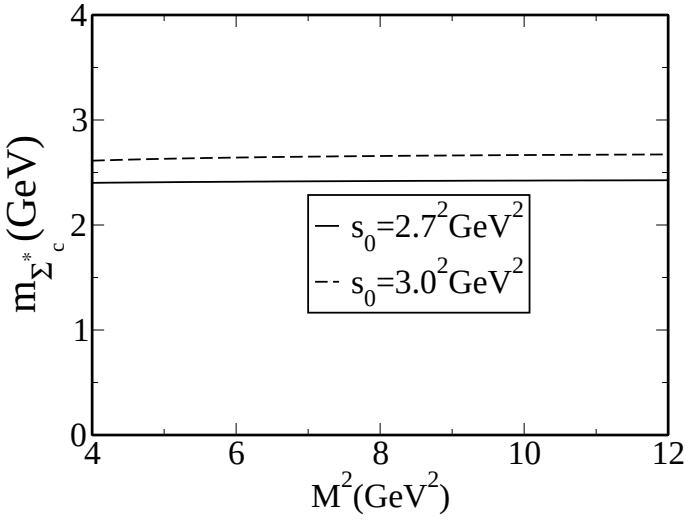

Figure 5.12: The same as Fig. 5.10, but for Σ_c^*.

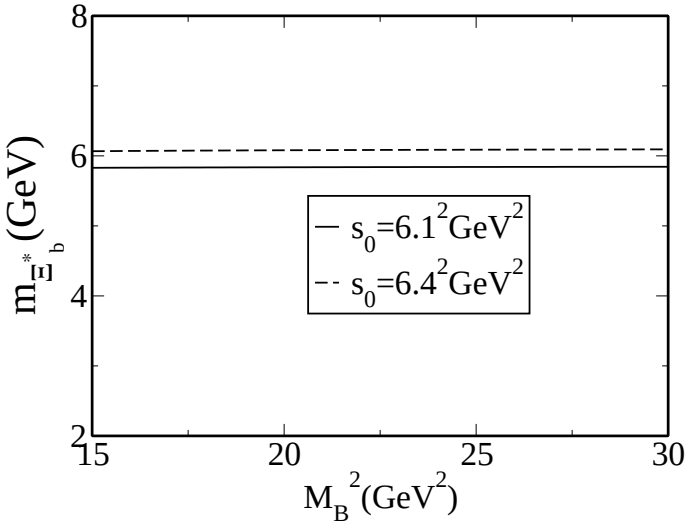

Figure 5.13: The same as Fig. 5.9, but for Ξ_b^*.

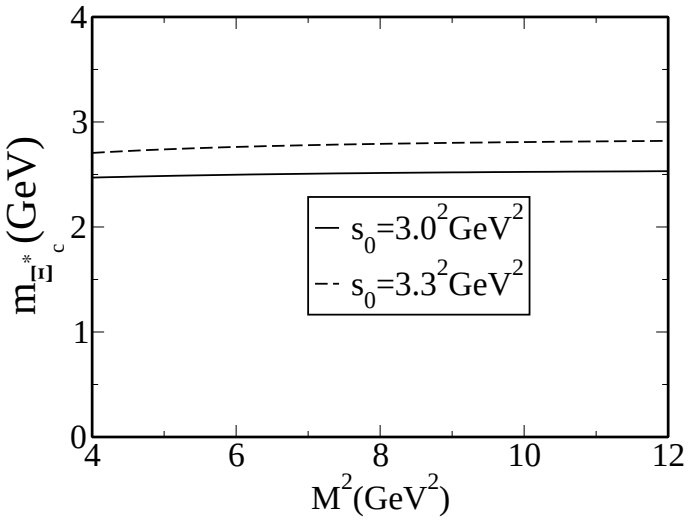

Figure 5.14: The same as Fig. 5.10, but for Ξ_c^*.

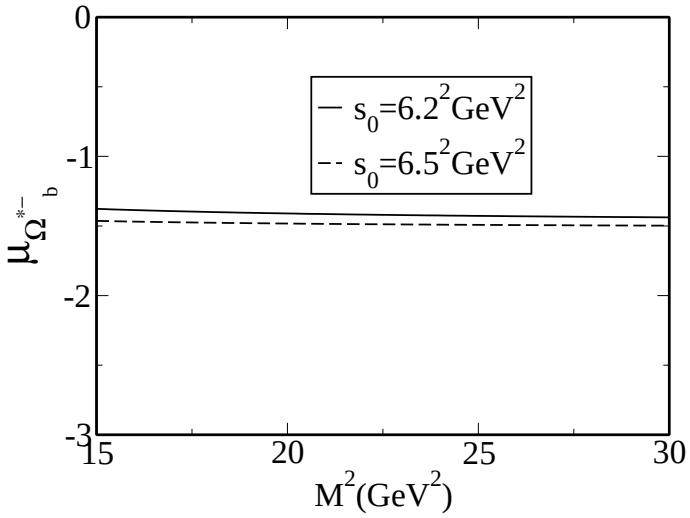

Figure 5.15: The dependence of the magnetic moment of Ω_b^{*-} on Borel parameter M^2 (in units of nucleon magneton) at two fixed values of s_0.

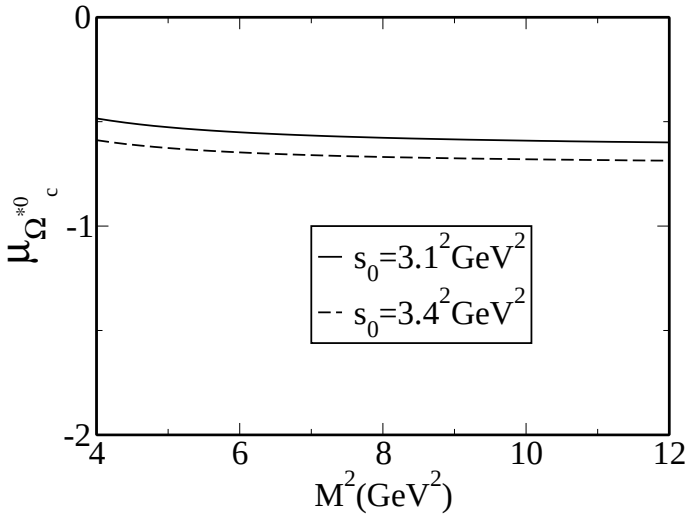

Figure 5.16: The dependence of the magnetic moment of Ω_c^{*0} on Borel parameter M^2 (in units of nucleon magneton) at two fixed values of s_0.

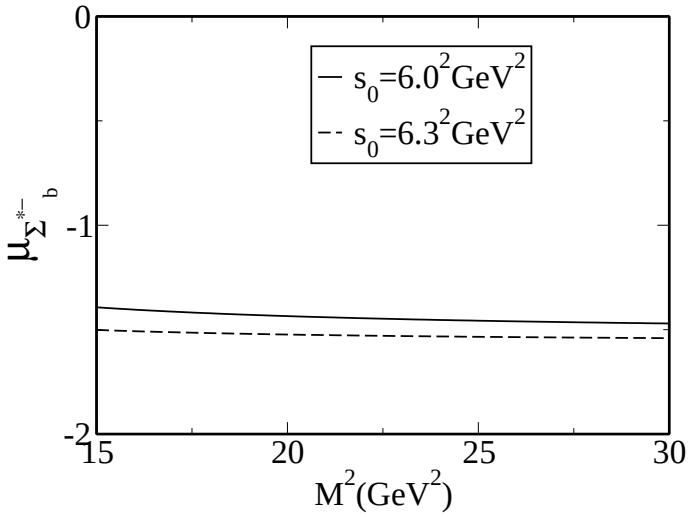

Figure 5.17: The same as Fig. 5.15, but for Σ_b^{*-}.

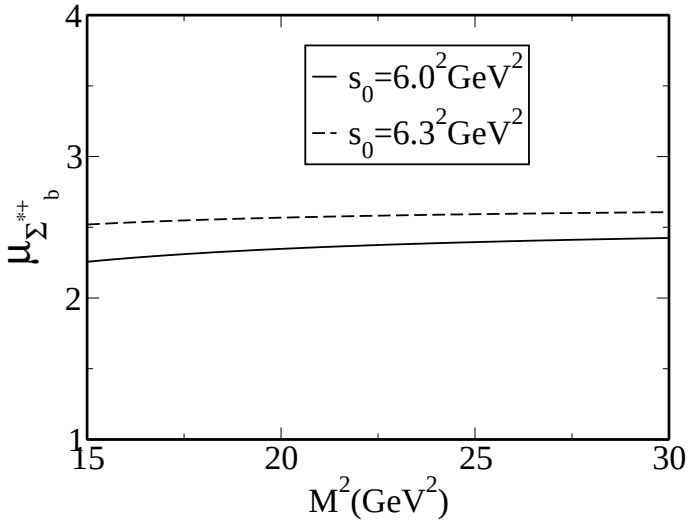

Figure 5.18: The same as Fig. 5.15, but for Σ_b^{*+}.

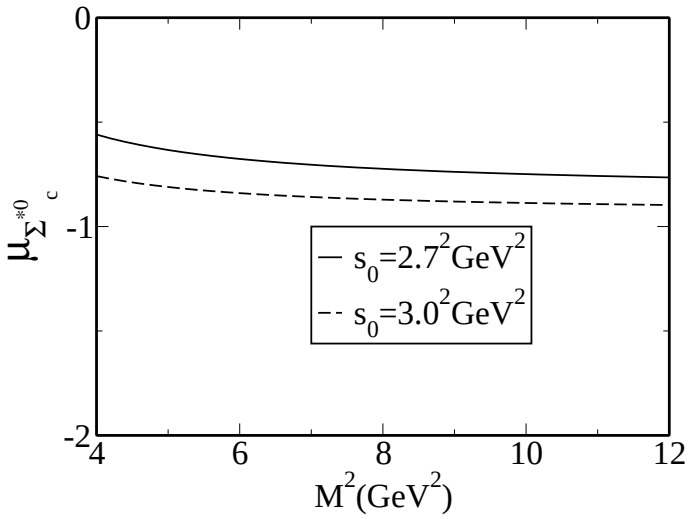

Figure 5.19: The same as Fig. 5.16, but for Σ_c^{*0}.

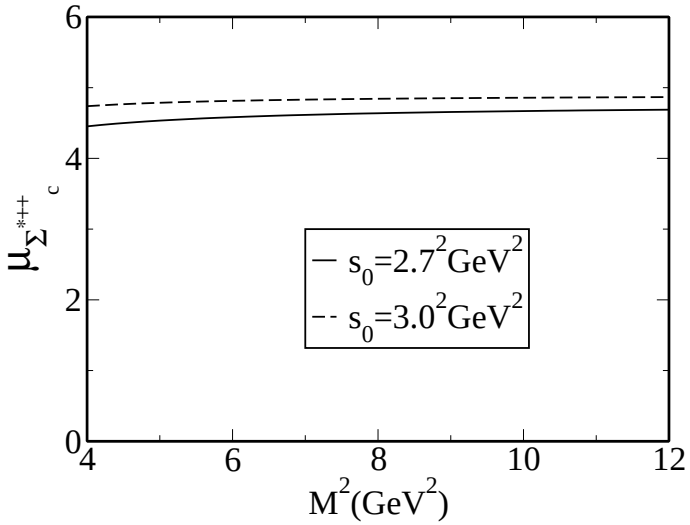

Figure 5.20: The same as Fig. 5.16, but for Σ_c^{*++}.

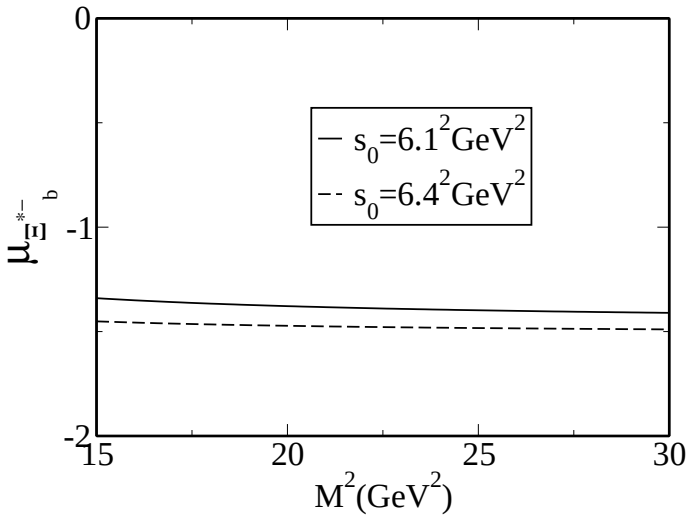

Figure 5.21: The same as Fig. 5.15, but for Ξ_b^{*-}.

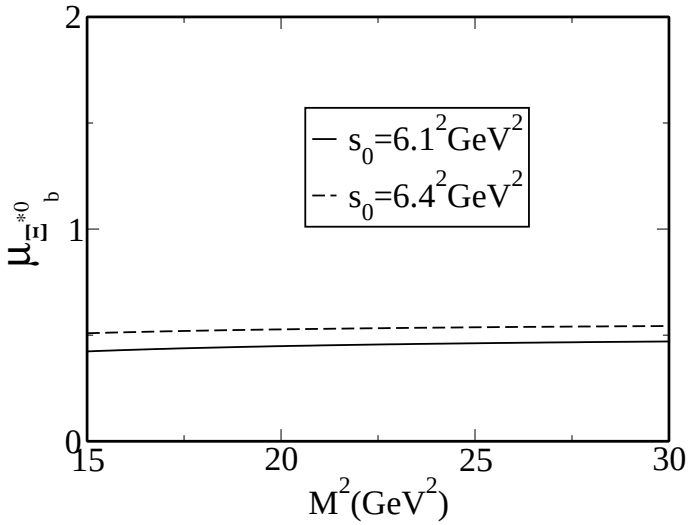

Figure 5.22: The same as Fig. 5.15, but for Ξ_b^{*0}.

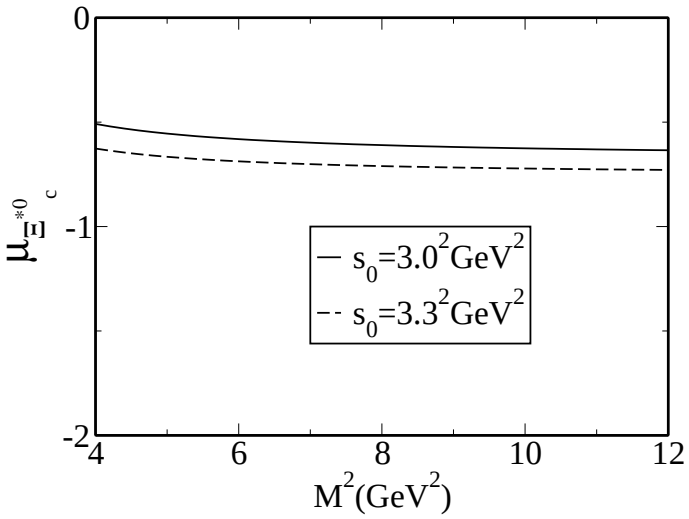

Figure 5.23: The same as Fig. 5.16, but for Ξ_c^{*0}.

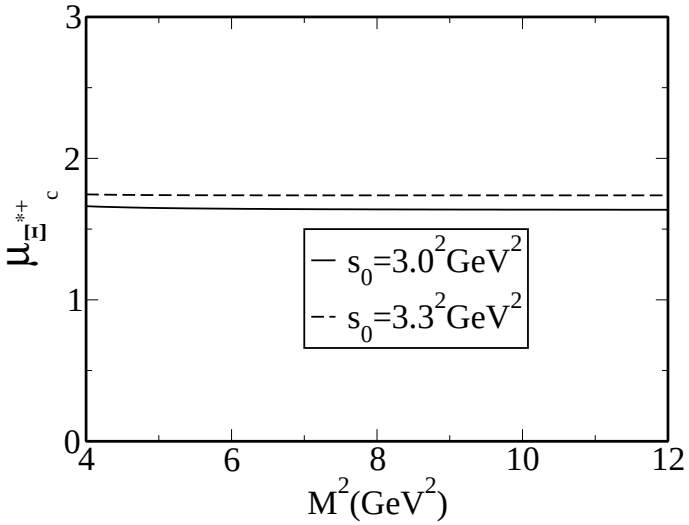

Figure 5.24: The same as Fig. 5.16, but for Ξ_c^{*+}.

CHAPTER 6

CONCLUSION

In this thesis, we investigated some properties, such as transition form factors, mass and magnetic moments, of the light octet, decuplet and heavy baryons containing a single heavy quark within the framework of the light cone QCD sum rules as a more powerful and attractive non-perturbative method. In the recent years, substantial experimental progress has been made in the discovery of those baryons and the experimental studies on the properties of such baryons and their decays have been made. Theoretical and phenomenological calculations of those properties and their comparison with the experimental results can give essential information about the structure of these baryons and strong interactions inside them.

First, we constructed the light and heavy baryons in the content of the representation of the unitary groups. Then, the QCD sum rules and one of its extensions, the light cone QCD sum rules, were discussed. In principle, the QCD Lagrangian is responsible for all properties of the hadrons and hadronic processes, but a direct use of that is possible only within the limited framework of the perturbation theory. In very high energies, the quarks and gluons interact weakly, a property called the asymptotic freedom. Therefore, in very high energies, we can use the perturbation theory. However, in low energy and hadronic size, we need a non-perturbative method to analyze the properties of the baryons and their transitions. Among all non-perturbative approaches, the QCD sum rules has received special attention since it is based on the fundamental QCD Lagrangian.

Understanding the nucleons' properties is one of the major goals of the quantum

chromodynamics. To investigate the properties of the nucleons, we calculated axial $N-\Delta$ transition form factors using the nucleon distribution amplitudes and 3 sets of the independent parameters entered to those DA's. These form factors play important role for understanding the dynamics of weak $N-\Delta$ transition as well as the internal structure of the nucleon and its first resonance Δ, complementary to that obtained from electromagnetic transition. Furthermore, the measurement of axial form factors for $N-\Delta$ transition, allows us to check off diagonal Goldberger-Treiman relation and order of conservation of the axial current. We also compared our results for the related form factors with existing lattice and quark model predictions. Our results reproduce the existing data from the lattice QCD. Our predictions for these axial form factors can be tested in the future experiments.

In order to analyze other properties of the nucleon, the nucleon electromagnetic form factors were calculated using the most general form of the nucleon interpolating current in the light cone QCD sum rules. It is more than forty years that the electromagnetic form factors of the nucleons have been of interest from both experimental and theoretical points of view. Using two forms of the DA's, we obtained the sum rules for these form factors. These form factors were used to calculate the electric and magnetic dipole moments for the proton and neutron. We also compared the obtained results for the form factors and electromagnetic moments with existing experimental data. We obtain that our results are in a good agreement with the existing experimental data. More precisely, at different values of β, which is a general parameter in the interpolating current of the nucleon, our results for the form factors reproduce the experimental data. Finally, we obtained the "working region for β". Our final remark in this regard is that in order to answer the question which β is more preferable, both theoretical and experimental studies have to be refined. From theoretical part $O(\alpha_s)$ corrections to the distributions amplitudes and more accurate determination of the DA's are needed. From experimental side, the discrepancies between various data have to be eliminated.

As to the phenomenology of the heavy baryons, the magnetic moments of the heavy spin 1/2, Ξ_Q baryons, which were discovered recently (more precisely Ξ_b was discov-

ered) were calculated in framework of light cone QCD sum rules. To calculate the magnetic moments of the Ξ_Q, the general form of their interpolating currents have been used. Our results on magnetic moments are close to the predictions of the other non-perturbative approaches existing in the literature. These results can also be tested in the future experiments.

Finally, inspired by recent experimental discovery of the heavy flavored baryons, the mass and magnetic moments of these baryons with $J^P = 3/2^+$ (Σ_Q^*, Ξ_Q^* and Ω_Q^*) were calculated within the light cone QCD sum rules. Our results on the masses are consistent with the experimental data as well as predictions of other approaches. Our results on the masses of the Ω_b^*, and Ξ_b^* can be tested in experiments which will be held in the near future. The predictions on the magnetic moments also can verified in the future experiments.

The results of this thesis have been published in the following papers:

1) T. M. Aliev, K. Azizi, A. Ozpineci, Nucl. Phys. A **799** (2008) 105.

2) T. M. Aliev, K. Azizi, A. Ozpineci, Phys. Rev. D **77** (2008) 114014.

3) T. M. Aliev, K. Azizi, A. Ozpineci, Phys. Rev. D **77** (2008) 114006.

4) T. M. Aliev, K. Azizi, A. Ozpineci, Nucl. Phys. B **808** (2009) 137.

REFERENCES

[1] P. Colangelo, A. Khodjamirian, "At the Frontier of Particle Physics: Handbook of QCD" ed. by M. Shifman (World Scientific, Singapore, 2001), V. 3,1995.

[2] A.V. Radyushkin, Published in " Strong Interactions at Low and Intermediate Energies", Proceedings of the 13th Annual HUGS at CEBAF, 26May-12 June 1998; Edited by J.L. Goity, World Scientific (2000) pp. 91-150, arXiv:hep-ph/0101227.

[3] E. D. Rafael, Published in " Les Houches 1997, Probing the standard model of particle interactions", Pt. 2 1171-1218, arXiv:hep-ph/9802448.

[4] V. M. Braun, Plenary talk given at " 4th International Workshop on Progress in Heavy Quark Physics", Rostock, Germany, 20-22 Sep 1997, arXiv: hep-ph/9801222 (1998).

[5] M. A. Shifman, A. I. Vainshtein, V. I. Zakharov, Nucl. Phys. B **147** (1979) 385.

[6] B. Krusche et al., Phys. Rev. Lett. **74** (1995) 3736.

[7] C. B. Crawford et al., Phys. Rev. Lett. **98** (2007) 052301.

[8] T. Aaltonen et al., CDF Collaboration, Phys. Rev. Lett. **99** (2007) 202001.

[9] T. Aaltonen et al., CDF Collaboration, Phys. Rev. Lett. **99** (2007) 052002.

[10] V. Abazov et al., DO Collaboration, Phys. Rev. Lett. **99** (2007) 052001.

[11] B. Aubert et al., BaBar Collaboration, Phys. Rev. Lett. **97** (2006) 232001.

[12] V. Zamiralov, D. V. Skobeltsyn Institute of Nuclear Physics, Moscow, Russia, Lecture Notes on " Introduction to Group Theory and Its Representaions and Some Applications to Particle Physics" Given at Middle East Technical University on February 2007.

[13] A. Valcarce, H. Garcilazo, J. Vijande, Eur. Phys. J. A **37** (2008) 217.

[14] A. Ozpineci, Ph.D. thesis, Submitted to the Graduate School of Natural and Applied Sciences of the Middle East Technical University, September (2001).

[15] P. Ball, V. M. Braun, H. G. Dosch, Phys. Rev. D **44** (1991) 3567.

[16] P. Ball, V. M. Braun, N. Kivel, Nucl. Phys. B **649** (2003) 263.

[17] H. Y. Gao, Int. J. Mod. Phys. E, **12** (2003) 1 (Erratum-ibid E **12** (2003) 567).

[18] J. Friedrich, T. Walcer, Eur. Phys. J. A, **17** (2003) 607.

[19] C. E. Hyde-Wright, K. de Jager, Ann. Rev. Nucl. Part. Science, **54** (2004) 217.

[20] D. Day, Nucl. Phys. A, **755** (2005) 157.

[21] C. Mertz *et al.*, Phys. Rev. Lett. **86** (2001) 2963.

[22] K. Joe *et al.*, Phys. Rev. Lett. **88** (2002) 122001.

[23] V. M. Braun, A. Lenz, G. Peters, A. V. Radyushkin, Phys. Rev. D **73**(2006) 034020.

[24] L. Elouadrhiri, New body systems suppl. **11** (1999) 130 ; S. P. Wells, N. Simicevic, K. Johnston and T. A. Forest, JLAB E 97-104, PAC(2004).

[25] V. M. Braun, A. Lenz, N. Mahnke, E. Stein, Phys. Rev. D **65** (2002) 074011.

[26] V. M. Braun, A. Lenz, M. Wittmann, Phys. Rev. D **73** (2006) 094019.

[27] V. Braun, R. J. Fries, N. Mahnke, E. Stein, Nucl. Phys. B **589** (2000) 381, Erratum-ibid. B **607** (2001) 433.

[28] M.-Q. Huang, D.-W. Wang, Phys. Rev. D **69** (2004) 094003.

[29] Z.-G. Wang, S.-L. Wang, W.-M. Yang, Phys. Rev. D **73** (2006) 094011.

[30] T. M. Aliev, M. Savci, Phys. Rev. D **75** (2007) 045006.

[31] Z.-G. Wang, S.-L. Wan, W.-M. Yanh, Eur. Phys. J. C **47** (2006) 375.

[32] T. M. Aliev, M. Savci, Phys. Lett. B **656** (2007) 56.

[33] Z.-G. Wang, J. Phys. G **34** (2007) 493.

[34] M.-Q. Huang, D.-W. Wang, hep-ph/0608170 (2006).

[35] C. Alexandrou, T. Leontiou, J. W. Negele, A. Tsapalis, Phys. Rev. Lett. **98** (2007) 052003.

[36] C. Alexandrou, et. al, arXiv:0706.3011 [hep-lat].

[37] D. Barquilla-Cano, A. J. Buchman, E. Hernandez, Phys. Rev, C **75** (2007) 065203.

[38] S.L. Adler, Ann. Phys. (NY) **50** (1968) 189; Phys.Rev. D **12** (1975) 2644 .

[39] C. M. Llewellyn Smith, Phys. Rep. **3 C** (1972) 261.

[40] B. L. Ioffe, Nucl. Phys. B, **188** (1981) 317; Erratum-ibid B **191** (1981) 591.

[41] W. Y. P. Hwang, K. C. Yang, Phys. Rev. D **49** (1994) 460.

[42] F. X. Lee, Phys. Rev. D **57** (1998) 1801.

[43] I. I. Balitsky, V. M. Braun, Nucl. Phys. B **311** (1989) 541; V. M. Belyaev, B. L. Ioffe, Sov. Phys. JETP. **56** (1982) 493.

[44] T. M. Aliev, A. Ozpineci, Nucl. Phys . B **732** (2006) 291.

[45] K. G. Chetyrkin, A. Khodjamirian, A. A. Pivovarov, Phys. Lett. B **661** (2008)250; I. I. Balitsky, V. M. Braun, A. V. Kolesnichenko, Nucl. Phys. B **312** (1989) 509.

[46] J. Arringtin, C. D. Roberts, J. M. Zanotti, J. Phys. G **34** (2007) 523.

[47] A. I. Akhiezer, M. P. Rekalo, Sov. Phys. Dokl **13** (1968) 572.

[48] M. K. Jones *et al.*, Phys. Rev. Lett. **84** (2000) 1398

[49] O. Gayou *et al.*, Phys. Rev. Lett. **88** (2002) 092301.

[50] O. Gayou *et al.*, Phys. Rev. C. **64** (2001) 0382002.

[51] V. Punjabi *et al.*, Phys. Rev. C. **91** (2005) 055202.

[52] C. F. Perdrisat, V. Punjabi, M. Vanderhaegheu, Prog. Part. Nucl. Phys. **59** (2007) 694.

[53] H. Castillo, C. A. Dominguez, M. Loewe, JHEP **0503** (2005) 12.

[54] H. Zhon *et al.*, Phys. Rev. Lett. **87** (2001) 081801.

[55] D. Rohe, Phys. Rev. Lett. **83** (1999) 4257.

[56] T. M. Aliev, A. Ozpineci, M. Savci, Phys. Rev. D. **66** (2002) 016002.

[57] D.B. Leinweber, Ann. Phys. **254** (1997) 328.

[58] Christy ME, et al., Phys. Rev. C **70** (2004) 015206.

[59] Andivahis L, et al., Phys. Rev. D **50** (1994) 5491.

[60] I. A. Qattan *et al.*, Phys. Rev. Lett. **94** (2005) 142301, Phys. Rev. C **71**, 055202 (2005).

[61] A. Lung et al., Phys. Rev. Lett. **70** (1993) 718.

[62] S. J. Brodsky et al., Phys. Rev. D **69** (2004) 076001.

[63] A. V. Belitsky, X. Li, F. Yuan, Phys. Rev. Lett. **91** (2003) 092003.

[64] K. de Jager, AIP Conference Proceeding, **904** (2007) 95, arXiv:nucl-ex/0612026.

[65] S. Capstick, N. Isgur, Phys. Rev. D **34** (1986) 2809.

[66] R. Roncaglia, D. B. Lichtenberg, E. Predazzi, Phys. Rev. D **52** (1995) 1722.

[67] E. Jenkins, Phys. Rev. D **54** (1996) 4515.

[68] N. Mathur, R. Lewis , R. M. Woloshyn, Phys. Rev. D **66** (2002) 014502.

[69] D. Ebert, R. N. Faustov, V. O. Galkin, Phys. Rev. D **72** (2005) 034026.

[70] M. Karliner, H. J. Lipkin, Phys. Lett. B **660** (2008) 539; arXiv:hep-ph/ 0307343.

[71] M. Karliner, B. Kereu-Zura, H. J. Lipkin, J. L. Rosner, arXiv:hep-ph/ 0706.2163.

[72] J. L. Rosner, Phys. Rev. D **75** (2007) 013009.

[73] M. Karliner, H. J. Lipkin, Phys. Lett. B **575** (2003) 249.

[74] M. A. Shifman, A. I. Vainshtein, V. I. Zakharov, Nucl. Phys. B **147** (1979) 385.

[75] E. Bagan, M. Chabab, H. G. Dosch, S. Narison, Phys. Lett. B **278** (1992) 367; ibid; Phys. Lett. B **287** (1992) 176; ibid; Phys. Lett. B **301** (1993) 243.

[76] C. S. Navarra, M. Nielsen, Phys. Lett. B **443** (1998) 285.

[77] E. V. Shuryak, Nucl. Phys. B **198** (1982) 83.

[78] A. G. Grozin, O. I. Yakovlev, Phys. Lett. B **285** (1992) 254.

[79] Y. B. Dai, C. S. Huang, C. Liu, C. D. Lu, Phys. Lett. B **371** (1996) 99.

[80] D. W. Wang, M. Q. Huang, C. Z. Li, Phys. Rev. D **65** (2002) 094036.

[81] S. L. Zhu, Phys. Rev. D **61** (2000) 114019.

[82] C. S. Huang, A. L. Zhang, S. L. Zhu, Phys. Lett. B **492** (2000) 288.

[83] D. W. Wang, M. Q. Huang, Phys. Rev. D **68** (2003) 034019.

[84] Z. G. Wang, Eur. Phys. J. C **54** (2008) 231.

[85] F. O. Duraes, M. Nielsen, Phys. Lett. B **658** (2007) 40.

[86] X. Liu, H. X. Chen, Y. R. Liu, A. Hosaka, S. L. Zhu, Phys. Rev. D **77** (2008) 014031.

[87] A. L. Choudhury, V. Joshi, Phys. Rev. D **13** (1976) 3115.

[88] D. B. Lichtenberg, Phys. Rev. D **15** (1977) 345.

[89] L. Y. Glozman, D. O. Riska, Nucl. Phys. A **603** (1996) 326.

[90] B. Julia-Diaz, D. O. Riska, Nucl. Phys. A **739** (2004) 69.

[91] S. Scholl, H. Weigel, Nucl. Phys. A **735** (2004) 163.

[92] A. Faessler et. al, Phys. Rev. D **73** (2006) 094013.

[93] B. Patel, A. K. Rai, P. C. Vinodkumar, arXiv: 0803.0221 (hep-ph).

[94] M. Savage, Phys. Lett. B **326** (1994) 303.

[95] D. O. Riska, Nucl. Instrum. Meth. B **119** (1996) 259.

[96] Y. Oh, D. P. Min, M. Rho, N. N. Scoccola, Nucl. Phys. A **534** (1991) 493.

[97] C. S. An, Nucl. Phys. A **797** (2007) 131, Erratum-ibid; A **801** (2008) 82.

[98] S. L. Zhu, W. Y. Hwang, Z. S. Yang, Phys. Rev. D **56** (1997) 7273.

[99] T. M. Aliev, A. Ozpineci, M. Savci, Phys. Rev. D **65** (2002) 096004.

[100] T. M. Aliev, A. Ozpineci, M. Savci, Phys. Rev. D **65** (2002) 056008.

[101] R. J. Johnson, M. Shah-Jahan, Phys. Rev. D **15** (1977) 1400.

[102] S. K. Bose, L. P. Singh, Phys. Rev. D **22** (1980) 773.

[103] S. Scholl, H. Weigel, Nucl. Phys. A **735** (2004) 163.

[104] Y. S. Oh, B. Y. Park, Mod. Phys. Lett. A **11** (1996) 653.

[105] T. M. Aliev, A. Ozpineci, M. Savci, Phys. Rev. D **66** (2002) 016002, Erratum-ibid; D **67** (2003) 039901.

[106] V. M. Braun, I. E. Filyanov, Z. Phys. C **48** (1990) 239.

[107] V. M. Belyaev, B. L. Ioffe, JETP **56** (1982) 493.

[108] J. Rohrwild, JHEP **0709** (2007) 073.

[109] A. E. Dorokhov, Eur. J. Phys. C **42** (2005) 309.

[110] V. M. Belyaev, I. I. Kogan, Yad. Fiz. **40** (1984) 1035.

[111] M. C. Banuls, I. Scimemi, J. Bernabeu, V. Gimenez, A. Pich, Phys. Rev. D **61** (2000) 074007.

[112] X. Liu, H. X. Chen, Y. R. Liu, A. Hosaka, S. L. Zhu, Phys. Rev. D **77** (2008) 014031.

[113] M. J. Savage, Phys. Lett. B **359** (1995) 189.

[114] C. Amsler et al., (Particle Data Group), Phys. Lett. B **667** (2008) 1.

APPENDIX A

In Eqs. (4.16), (4.17), (4.18) and (4.19), the distribution amplitudes depend on normalization scale and can be expanded with the conformal operators. To the next-to-leading conformal spin accuracy, they are obtained as [25, 26, 27]:

$$
\begin{aligned}
V_1(x_i,\mu) &= 120x_1x_2x_3[\phi_3^0(\mu)+\phi_3^+(\mu)(1-3x_3)],\\
V_2(x_i,\mu) &= 24x_1x_2[\phi_4^0(\mu)+\phi_3^+(\mu)(1-5x_3)],\\
V_3(x_i,\mu) &= 12x_3\{\psi_4^0(\mu)(1-x_3)+\psi_4^-(\mu)[x_1^2+x_2^2-x_3(1-x_3)]\\
&\quad +\psi_4^+(\mu)(1-x_3-10x_1x_2)\},\\
V_4(x_i,\mu) &= 3\{\psi_5^0(\mu)(1-x_3)+\psi_5^-(\mu)[2x_1x_2-x_3(1-x_3)]\\
&\quad +\psi_5^+(\mu)[1-x_3-2(x_1^2+x_2^2)]\},\\
V_5(x_i,\mu) &= 6x_3[\phi_5^0(\mu)+\phi_5^+(\mu)(1-2x_3)],\\
V_6(x_i,\mu) &= 2[\phi_6^0(\mu)+\phi_6^+(\mu)(1-3x_3)],\\
A_1(x_i,\mu) &= 120x_1x_2x_3\phi_3^-(\mu)(x_2-x_1),\\
A_2(x_i,\mu) &= 24x_1x_2\phi_4^-(\mu)(x_2-x_1),\\
A_3(x_i,\mu) &= 12x_3(x_2-x_1)\{(\psi_4^0(\mu)+\psi_4^+(\mu))+\psi_4^-(\mu)(1-2x_3)\},\\
A_4(x_i,\mu) &= 3(x_2-x_1)\{-\psi_5^0(\mu)+\psi_5^-(\mu)x_3+\psi_5^+(\mu)(1-2x_3)\},\\
A_5(x_i,\mu) &= 6x_3(x_2-x_1)\phi_5^-(\mu)\\
A_6(x_i,\mu) &= 2(x_2-x_1)\phi_6^-(\mu),\\
T_1(x_i,\mu) &= 120x_1x_2x_3[\phi_3^0(\mu)+\frac{1}{2}(\phi_3^- -\phi_3^+)(\mu)(1-3x_3)],\\
T_2(x_i,\mu) &= 24x_1x_2[\xi_4^0(\mu)+\xi_4^+(\mu)(1-5x_3)],
\end{aligned}
$$

$$
\begin{aligned}
T_3(x_i,\mu) &= 6x_3\{(\xi_4^0+\phi_4^0+\psi_4^0)(\mu)(1-x_3)\\
&\quad +(\xi_4^-+\phi_4^--\psi_4^-)(\mu)[x_1^2+x_2^2-x_3(1-x_3)]\\
&\quad +(\xi_4^++\phi_4^++\psi_4^+)(\mu)(1-x_3-10x_1x_2)\},\\
T_4(x_i,\mu) &= \frac{3}{2}\{(\xi_5^0+\phi_5^0+\psi_5^0)(\mu)(1-x_3)+(\xi_5^-+\phi_5^--\psi_5^-)(\mu)\\
&\quad [2x_1x_2-x_3(1-x_3)]+(\xi_5^++\phi_5^++\psi_5^+)(\mu)(1-x_3-2(x_1^2+x_2^2))\},\\
T_5(x_i,\mu) &= 6x_3[\xi_5^0(\mu)+\xi_5^+(\mu)(1-2x_3)],\\
T_6(x_i,\mu) &= 2[\phi_6^0(\mu)+\frac{1}{2}(\phi_6^--\phi_6^+)(\mu)(1-3x_3)],\\
T_7(x_i,\mu) &= 6x_3\{(-\xi_4^0+\phi_4^0+\psi_4^0)(\mu)(1-x_3)+(-\xi_4^-+\phi_4^--\psi_4^-)(\mu)\\
&\quad [x_1^2+x_2^2-x_3(1-x_3)]+(-\xi_4^++\phi_4^++\psi_4^+)(\mu)(1-x_3-10x_1x_2)\},\\
T_8(x_i,\mu) &= \frac{3}{2}\{(-\xi_5^0+\phi_5^0+\psi_5^0)(\mu)(1-x_3)+(-\xi_5^-+\phi_5^--\psi_5^-)(\mu)\\
&\quad [2x_1x_2-x_3(1-x_3)]+(-\xi_5^++\phi_5^++\psi_5^+)(\mu)(1-x_3-2(x_1^2+x_2^2))\},\\
S_1(x_i,\mu) &= 6x_3(x_2-x_1)\Big[(\xi_4^0+\phi_4^0+\psi_4^0+\xi_4^++\phi_4^++\psi_4^+)(\mu)\\
&\quad +(\xi_4^-+\phi_4^--\psi_4^-)(\mu)(1-2x_3)]\\
S_2(x_i,\mu) &= \frac{3}{2}(x_2-x_1)\Big[-\left(\psi_5^0+\phi_5^0+\xi_5^0\right)(\mu)+\left(\xi_5^-+\phi_5^--\psi_5^0\right)(\mu)x_3\\
&\quad +\left(\xi_5^++\phi_5^++\psi_5^0\right)(\mu)(1-2x_3)\Big]\\
P_1(x_i,\mu) &= 6x_3(x_2-x_1)\Big[(\xi_4^0-\phi_4^0-\psi_4^0+\xi_4^+-\phi_4^+-\psi_4^+)(\mu)\\
&\quad +(\xi_4^--\phi_4^-+\psi_4^-)(\mu)(1-2x_3)]\\
P_2(x_i,\mu) &= \frac{3}{2}(x_2-x_1)\Big[\left(\psi_5^0+\psi_5^0-\xi_5^0\right)(\mu)+\left(\xi_5^--\phi_5^-+\psi_5^0\right)(\mu)x_3\\
&\quad +\left(\xi_5^+-\phi_5^+-\psi_5^0\right)(\mu)(1-2x_3)\Big]\,. \qquad \text{(A.1)}
\end{aligned}
$$

the parameters used above are defined in terms of the following eight independent parameters f_N, λ_1, λ_2, V_1^d, A_1^u, f_d^1, f_d^2 and f_u^1 as

$$
\begin{aligned}
\phi_3^0 &= \phi_6^0 = f_N\\
\phi_4^0 &= \phi_5^0 = \frac{1}{2}(\lambda_1+f_N)\\
\xi_4^0 &= \xi_5^0 = \frac{1}{6}\lambda_2\\
\psi_4^0 &= \psi_5^0 = \frac{1}{2}(f_N-\lambda_1)
\end{aligned}
$$

$$
\begin{aligned}
\phi_3^- &= \frac{21}{2}A_1^u, \\
\phi_3^+ &= \frac{7}{2}(1-3V_1^d), \\
\phi_4^- &= \frac{5}{4}\left(\lambda_1(1-2f_1^d-4f_1^u)+f_N(2A_1^u-1)\right), \\
\phi_4^+ &= \frac{1}{4}\left(\lambda_1(3-10f_1^d)-f_N(10V_1^d-3)\right), \\
\psi_4^- &= -\frac{5}{4}\left(\lambda_1(2-7f_1^d+f_1^u)+f_N(A_1^u+3V_1^d-2)\right), \\
\psi_4^+ &= -\frac{1}{4}\left(\lambda_1(-2+5f_1^d+5f_1^u)+f_N(2+5A_1^u-5V_1^d)\right), \\
\xi_4^- &= \frac{5}{16}\lambda_2(4-15f_2^d), \\
\xi_4^+ &= \frac{1}{16}\lambda_2(4-15f_2^d), \\
\phi_5^- &= \frac{5}{3}\left(\lambda_1(f_1^d-f_1^u)+f_N(2A_1^u-1)\right), \\
\phi_5^+ &= -\frac{5}{6}\left(\lambda_1(4f_1^d-1)+f_N(3+4V_1^d)\right), \\
\psi_5^- &= \frac{5}{3}\left(\lambda_1(f_1^d-f_1^u)+f_N(2-A_1^u-3V_1^d)\right), \\
\psi_5^+ &= -\frac{5}{6}\left(\lambda_1(-1+2f_1^d+2f_1^u)+f_N(5+2A_1^u-2V_1^d)\right), \\
\xi_5^- &= -\frac{5}{4}\lambda_2 f_2^d, \\
\xi_5^+ &= \frac{5}{36}\lambda_2(2-9f_2^d), \\
\phi_6^- &= \frac{1}{2}\left(\lambda_1(1-4f_1^d-2f_1^u)+f_N(1+4A_1^u)\right), \\
\phi_6^+ &= -\frac{1}{2}\left(\lambda_1(1-2f_1^d)+f_N(4V_1^d-1)\right).
\end{aligned} \tag{A.2}
$$

The numerical values are obtained using:

$$
\begin{aligned}
f_N &= (5.0\pm0.5)\times10^{-3}\ GeV^2, \\
\lambda_1 &= -(2.7\pm0.9)\times10^{-2}\ GeV^2, \\
\lambda_2 &= (5.4\pm1.9)\times10^{-2}\ GeV^2.
\end{aligned} \tag{A.3}
$$

For the other five independent parameters, we have used three sets as:

$$
\begin{aligned}
\text{Set 1}\ : A_1^u &= 0.38\pm0.15,\ \ V_1^d=0.23\pm0.03,\ \ f_1^d=0.40\pm0.05, \\
f_2^d &= 0.22\pm0.05,\ \ f_1^u=0.07\pm0.05,
\end{aligned} \tag{A.4}
$$

$$\begin{aligned} \text{Set 2} \ : A_1^u &= \frac{1}{14}, \ V_1^d = \frac{13}{42}, \ f_1^d = 0.40 \pm 0.05, \\ f_2^d &= 0.22 \pm 0.05, \ f_1^u = 0.07 \pm 0.05, \end{aligned} \tag{A.5}$$

$$\begin{aligned} \text{Set 3 (asymptotic)} : A_1^u &= 0, \ V_1^d = \frac{1}{3}, \ f_1^d = \frac{3}{10}, \ f_2^d = \frac{4}{15}, \\ f_1^u &= \frac{1}{10} \end{aligned} \tag{A.6}$$

Note that the asymptotic forms of DA's can be obtained from Eqs. (A.1) using the values given in the 3^{rd} set.

VITA

Kazem Azizi was born in Miyaneh, east Azarbaijan, Iran, in 1973. He received his BS degree in physics at Tabriz university in Tabriz, Iran, in 1996. Having completed the BS program, he started MS studies at physics department of Sharif university of technology, Tehran, Iran and received his MS degree in 1998. He started his Ph.D. studies in high energy physics at middle east technical university, METU, in 2004.